

GEOLOGIC MAP OF THE
WILLIAMSBURG 75-MINUTE QUADRANGLE,
SIERRA COUNTY, NEW MEXICO

By
Andrew P. Jochems and Daniel J. Koning

December 2015
[Revised February 2019]

New Mexico Bureau of Geology and Mineral Resources
Open-file Digital Geologic Map OF-GM 250



Scale 1:24,000

This work was supported by the U.S. Geological Survey, National Cooperative Geologic Mapping Program (STATEMAP) under USGS Cooperative Agreement 06HQPA0003 and the New Mexico Bureau of Geology and Mineral Resources.

New Mexico Bureau of Geology and Mineral Resources, New Mexico Institute of Mining and Technology, 801 Leroy Place, Socorro, New Mexico, 87801-4796

The views and conclusions contained in this document are those of the author and should not be interpreted as necessarily representing the official policies, either expressed or implied, of the U.S. Government or the State of New Mexico.

CONTENTS

EXECUTIVE SUMMARY	3
INTRODUCTION	4
GEOLOGIC SETTING.....	5
STRATIGRAPHY	6
PRECAMBRIAN AND PALEOZOIC ROCKS	6
QUATERNARY-TERTIARY BASIN-FILL.....	8
Western piedmont of the Palomas Formation.....	8
Eastern piedmont of the Palomas Formation.....	14
Axial-fluvial facies of the Palomas Formation	15
Palomas Formation thickness and coarsening trends	17
QUATERNARY HISTORY (POST-PALOMAS FORMATION).....	18
STRUCTURAL GEOLOGY	20
HYDROGEOLOGY	23
ACKNOWLEDGEMENTS.....	25
REFERENCES.....	26
Appendix A: Detailed unit descriptions.....	31
Appendix B: Clast count data	46
Appendix C: Paleocurrent data.....	60
Appendix D: ¹⁴ C age data	132

EXECUTIVE SUMMARY

The Williamsburg quadrangle is located in the eastern part of the Palomas basin, an east-tilted half graben in the southern Rio Grande rift, and includes all of the village of Williamsburg and the western part of the city of Truth or Consequences. The Palomas basin is bounded on the west by the Sierra Cuchillo, Salado Mountains, and Animas Hills. To the east, it is bordered by the Mud Springs Mountains and Caballo Mountains. The oldest rocks are Proterozoic plutonic rocks in the easternmost part of the map area that include granite as well as lesser amounts of amphibolite, gneiss, and schist. Cambrian to Ordovician rocks unconformably overlie plutonic lithologies and include a 200 m package of quartzose sandstone, dolomitic limestone, and dolostone deposited in lower shoreface to shallow marine shelf settings (Seager and Mack, 2003). Proterozoic and Paleozoic rocks are down-dropped along the Hot Springs fault and not exposed in the rest of the quadrangle. Tertiary-Quaternary sediment dominates the quadrangle, which overlies the deepest part of the Palomas basin (Gilmer et al., 1986). Inferred Miocene-age basin fill is observed only in limited exposures along the northern margin of the quadrangle. In the deepest well on the quadrangle, the Barney Iorio Fee #1, Miocene-age strata of the Rincon Valley Formation is interpreted to extend from 175 m to the bottom of the well (640 m). Relatively well-exposed Plio-Pleistocene basin-fill of the Palomas Formation overlies the Rincon Valley Formation. Younger deposits in the quadrangle include a well-defined suite of six middle-late Pleistocene Rio Grande terraces and Holocene valley-floor deposits radiocarbon-dated at ~11 ka, ~2.5 ka, and 0.6-0.3 ka. The Palomas Formation and latest Quaternary valley fills host the most important aquifers in the study area.

The Palomas Formation was deposited by: (1) large hanging-wall distributary fan systems emanating from the eastern foothills of the Black Range (western piedmont facies); (2) small footwall alluvial fans draining the western escarpment of the Caballo Mountains (eastern piedmont facies); and (3) the ancestral Rio Grande. The western piedmont is distinguished from footwall-derived eastern piedmont primarily by clast composition. Volcanic lithologies dominate the western piedmont sediment whereas Paleozoic sedimentary clasts and granite dominate eastern piedmont sediment. Furthermore, there is lesser cementation in the western piedmont sediment (Mack et al., 2000) and a greater proportion of coarse-grained beds in the eastern piedmont sediment. Axial-fluvial facies of the ancestral Rio Grande

consist of well-sorted, quartzose sand with subordinate well-rounded gravel of diverse lithologies that interfinger with both the western and eastern piedmont in a 3-5 km belt centered on the modern Rio Grande. The lower 35 m of the axial deposits contain a horse tooth identified by Gary Morgan (NM Museum of Natural History and Science) as belonging to the species *Neohipparion eurystyle*, which is restricted to 5.3-4.9 Ma strata.

The western piedmont facies of the Palomas Formation can be subdivided into six conformable units. The lowest (QTpwlt) includes 6-51 m of transitional pebbly channel fills and extra-channel deposits observed primarily in lithologic well logs from the northern half of the quadrangle. Above that lies the lower unit (QTpwl), consisting of ~20-80 m of coarse channel fills. The middle unit (QTpwm) is dominated by fine-grained strata (fine sand and silt), whose uppermost part contains a fossil assemblage interpreted as 3.0-2.6 Ma in age (Morgan and Lucas, 2012). This middle unit is separated from an upper package by ≤ 35 m of mud and sand containing 2.5-2.0 Ma vertebrate fossils (QTpwt). The upper package is comprised of a lower unit containing up to 45 m of $\geq 60\%$ clayey-silty fine sand and silt and $\leq 40\%$ coarse channel fills (QTpwu), and an upper coarse unit consisting of 2-45 m of amalgamated channel-fill complexes (QTpwuc). The latter commonly features 1-2 m of pedogenic carbonate (stage III-IV morphology) underlying the gently sloping aggradational surface of the Palomas Formation, the ~0.8 Ma Cuchillo surface, which extends throughout the western part of the quadrangle (McCraw and Love, 2012).

Structures in the Williamsburg quadrangle are mostly limited to the eastern half of the map area near the junction of the Hot Springs and Caballo fault systems. These high-angle, west-down normal fault zones separate the east-tilted Caballo block from the Palomas basin to the west. The Hot Springs fault exposes Proterozoic and Paleozoic rocks in its footwall but also deforms deposits of the Palomas Formation and pre-Palomas Santa Fe Group. This implies Plio-Pleistocene vertical movement along the fault, in agreement with earlier interpretations (Mason, 1976; Lozinsky, 1986).

The west-down Williamsburg fault likely represents a northern extension of the Caballo fault system. It cuts Holocene deposits south of Truth or Consequences (Foley et al., 1988) before bending abruptly to the northwest. We interpret that this fault directly links with the Mud Springs fault at the mouth of Mud Springs

Canyon. Though the fault is buried at that location, this interpretation is supported by the following stratigraphic and age constraints: (1) correlation of lower western piedmont deposits of the Palomas Formation exposed in the footwall to buried hanging-wall strata at 73-183 m depths in Truth or Consequences municipal wells 6, 7, and 8; and (2) paleontologic and radiometric data indicating that exposed footwall strata are 5.3-4.8 Ma whereas topographically lower, exposed hanging-wall strata are 3.0-2.6 Ma in age. Estimated post-4.5-Ma vertical throw along the Mud Springs fault on the quadrangle is 190-200 m. Total throw along the Williamsburg segment is unconstrained; Holocene fault ruptures have produced scarps averaging 2.5-3 m in height perhaps as recently as ~2 ka (Foley et al., 1988).

INTRODUCTION

This report accompanies the Geologic Map of the Williamsburg 7.5-Minute Quadrangle, Sierra County, New Mexico (NMBGMR OF-GM 250). Its purpose is to discuss the geologic setting and history of this area, and to identify and explain significant stratigraphic and structural relationships uncovered during the course of mapping.

The Williamsburg quadrangle is located in the eastern part of the Palomas basin and includes all of the village of Williamsburg and the western part of the city of Truth or Consequences (Fig. 1). The map area is bisected by Interstate 25 (I-25) and the south-flowing Rio Grande. The western part is dominated by a gently sloping surface (the Cuchillo surface; see below) that is cut by numerous arroyos and canyons. From north to south, these western drainages include Mud Springs Canyon, Cañada Honda, Palomas Creek, King Arroyo, and Kelly Canyon (Fig. 1). The eastern part of the map area consists of the Rio Grande floodplain and, to the east, hilly terrain extending eastward to the foot of the Caballo Mountains. The Rio Grande floodplain is broad (3 km, 2 mi) in most of the quadrangle, but narrows to 150-600 m (500-2000 ft) in the northeast corner of the quadrangle and near the middle of the quadrangle between the opposing alluvial fans of Palomas Creek and Red Canyon, the latter draining the Caballo Mountains. The highest location in the quadrangle is 1473 m (~4830 ft) above sea level (asl) along its northern border at 279230 mE/3667631 mN (all locations reported in NAD83 UTM 13S). The lowest point is 1279 m (~4195 ft) asl where the Rio Grande exits the quadrangle. Exposures are readily accessed by county

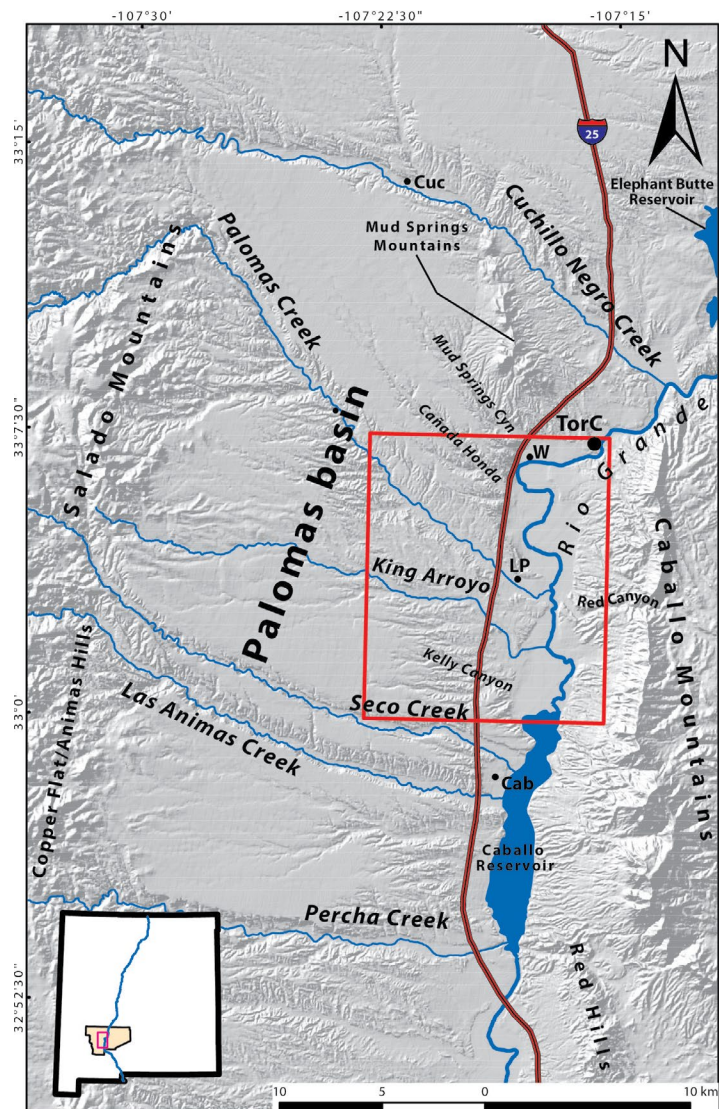


Figure 1. Shaded relief map showing major physiographic features of the Palomas basin and surrounding areas. The basin is bordered on the east by the Caballo Mountains and on the west by the Animas-Salado uplifts and Sierra Cuchillo (not shown). Williamsburg quadrangle is outlined in red on relief map. Inset map shows location in Sierra County, New Mexico; blue line is the Rio Grande. Abbreviations for local communities: Cab = Caballo, Cuc = Cuchillo, LP = Las Palomas, TorC = Truth or Consequences, W = Williamsburg.

roads extending up canyons to the west of I-25, and numerous roadcuts expose strata along I-25 and NM-187. Access to exposures east of the Rio Grande is via unimproved roads that connect with Turtleback Avenue in Truth or Consequences.

The Williamsburg quadrangle (and most of the Palomas basin) has an arid climate. The summer months (June through August) experience average temperature highs of 93-96° F and average lows of 63-67° F. In the winter months (December through February), average temperature highs are 55-63° F and average lows are 27-31° F. Average yearly precipitation is 25.5 cm (10 in), of which 8.4 cm (3.3 in) accumulates as snowfall. Over half

of the mean annual precipitation (13.7 cm) falls during the North American monsoon in the months of July through September. All climate data listed above are from the Truth or Consequences station (ID# 299128) in the NWS Cooperative network and averaged over the years of 1951-2012 (Western Regional Climate Center, 2015).

Early geologic mapping and reconnaissance work in the Palomas basin was done by Gordon and Graton (1907), Gordon (1910), and Harley (1934). Kelley and Silver (1952) produced a benchmark geologic map and report of the Caballo Mountains that included some of the adjacent basin-fill and structures in the Williamsburg quadrangle. Seager and Mack (2003) summarized the geology of the Caballo Mountains, with much discussion on the Palomas Formation and paleogeographic interpretations of the Palomas basin. Geologic maps were prepared at 1:24,000 scale for several of the surrounding quadrangles: Apache Gap and Caballo (Seager and Mack, 2005), Cuchillo (Maxwell and Oakman, 1990), Elephant Butte (Lozinsky, 1986), and Palomas Gap (formerly Caballo Peak; Mason, 1976; Seager, 2015). Foster (2009) mapped the northern ~1 km of the Williamsburg quadrangle at 1:12,000 as part of a thesis on basin-fill stratigraphy surrounding the Mud Springs Mountains north of Williamsburg. The Truth or Consequences-Williamsburg area has also been the focus of several studies on groundwater conditions and/or geothermal resources including those of Murray (1959), Cox and Reeder (1962), and more recently Person et al. (2013).

Numerous studies by Greg Mack and Bill Seager (both of New Mexico State University) and their colleagues shed much light on the Palomas basin and its Plio-Pleistocene basin-fill, the Palomas Formation. These studies range from geochronologic (Seager et al., 1984; Mack et al., 1993; Mack et al., 2009) and sedimentologic and stratigraphic (e.g., Mack et al., 2002, 2008) to investigations of controls on sedimentation (Mack and Seager, 1990; Mack et al., 1994, 2006; Mack and Leeder, 1999) and soils and paleoclimate (Mack and James, 1992; Mack et al., 1994, 2000). These works are cited frequently in the discussion that follows.

This report includes a summary of the geologic setting before describing mapped units and their depositional settings by age, oldest to youngest. The structural geology of the area is discussed, as are hydrogeologic implications for mapped basin-fill. Clast counts, imbrication measurements, radiocarbon data, and detailed unit descriptions are provided as appendices.

GEOLOGIC SETTING

The Williamsburg 7.5-minute quadrangle is located in the southern Rio Grande rift, a series of en echelon basins stretching from northern Colorado to northern Mexico (Chapin and Cather, 1994). The quadrangle includes the eastern part of the Palomas basin, an east-tilted half-graben filled with Miocene through Pleistocene sediment (Figs. 1-2). The western border (i.e. hanging wall) of the Palomas basin is defined by the Animas Hills and Salado Mountains (Fig. 1), east-dipping fault-block

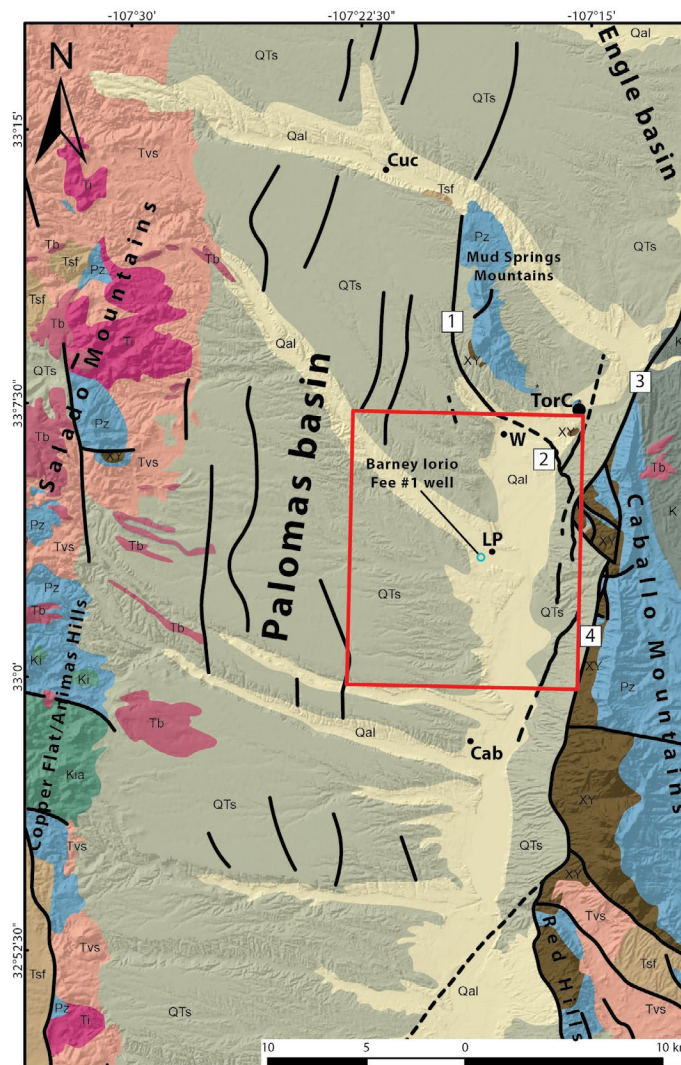


Figure 2. Structure map of the Palomas basin with simplified geology from New Mexico Bureau of Geology and Mineral Resources (2003). Williamsburg quadrangle is outlined in red. Numbers correspond to faults discussed in text: 1 = Mud Springs fault, 2 = Williamsburg fault, 3 = Hot Springs fault, and 4 = Northern Caballo fault. Unit designations are as follows: Qal = Quaternary alluvium, QTs = Tertiary-Quaternary basin-fill, Tsf = Santa Fe Group (pre-dating Palomas Formation), Tb = Pliocene basalt, Tvs = Eocene-Oligocene volcanic and volcanoclastic, undivided, K = Cretaceous sedimentary, undivided, Ki = Cretaceous intrusive, Kia = Cretaceous intrusive/andesite, undivided, Pz = Paleozoic, undivided, and XY = Paleo- to Mesoproterozoic, undivided. Abbreviations for local communities (black dots) as in Figure 1.

uplifts composed primarily of Paleozoic sedimentary and Eocene-Oligocene volcanic bedrock. For simplicity, these ranges are referred to as the Animas-Salado uplifts in this report.

The eastern edge of the Palomas basin coincides with the master fault system of the east-tilted Palomas half-graben. This fault system includes the Caballo, Hot Springs, Williamsburg, and Mud Springs faults (Fig. 2; Seager and Mack, 2003). The footwall uplifts of this master fault system, the Caballo and Mud Springs Mountains, are east-dipping fault blocks cored by Mesoproterozoic plutonic rocks overlain by as much as 1300 m of Paleozoic strata, mostly marine in origin (Seager and Mack, 2003). Maximum displacement along the Caballo fault is estimated at ~6.5 km based on gravity data (Keller and Cordell, 1983; Gilmer et al., 1986) and exposed thicknesses of Precambrian and Phanerozoic packages in the Caballo Mountains (Seager and Mack, 2003). The Caballo fault system merges with the west-down Hot Springs fault near the eastern quadrangle boundary, the latter continuing northward alongside the northern Caballo Mountains (Fig. 2). The Mud Springs fault wraps around the western foot of the Mud Springs Mountains and continues as the Williamsburg fault toward the eastern boundary of the quadrangle.

Plio-Pleistocene basin-fill of the Palomas Formation dominates the Williamsburg quadrangle and is differentiated on the basis of texture and clast lithology. Coarse-grained gravels found east of the Rio Grande were deposited in alluvial fans extending from the western escarpment of the Caballo Mountains (Fig. 3). Consistent with their source area, clasts in these gravels are dominated by limestone, dolostone, and granite. The piedmont deposits in the western two-thirds of the quadrangle contain gravels composed of felsic- to intermediate-composition volcanic rocks. These beds dip toward the east and are capped in many places by a gently inclined ($\leq 1.5^\circ$) plain known as the Cuchillo surface. This surface is constructional in the Williamsburg quadrangle and dates to ~0.8 Ma (Lozinsky, 1986; Lozinsky and Hawley, 1986a, b; Mack et al., 1993; McCraw and Love, 2012). Intertonguing with both the western and eastern piedmont deposits are axial facies of the ancestral Rio Grande, exposed in a 3-5-km-wide belt centered on the modern day river (Fig. 3). The Rio Grande and its tributaries began incising into the Palomas Formation ~0.8 Ma, then alternated with periods of backfilling that resulted in a series of inset terrace deposits distinguished by landscape position, texture, clast lithologies, and soil

development.

STRATIGRAPHY

PRECAMBRIAN AND PALEOZOIC ROCKS

Precambrian rocks are exposed in the footwall of the Hot Springs fault and along the Rio Grande in the northeast corner of the quadrangle. These rocks are primarily granite but include smaller bodies of granitic gneiss, quartzofelspathic schist, metasilstone, and amphibolite. The latter occurs as pods ≤ 20 m across that are either roof pendants or xenoliths in a larger granitic pluton;

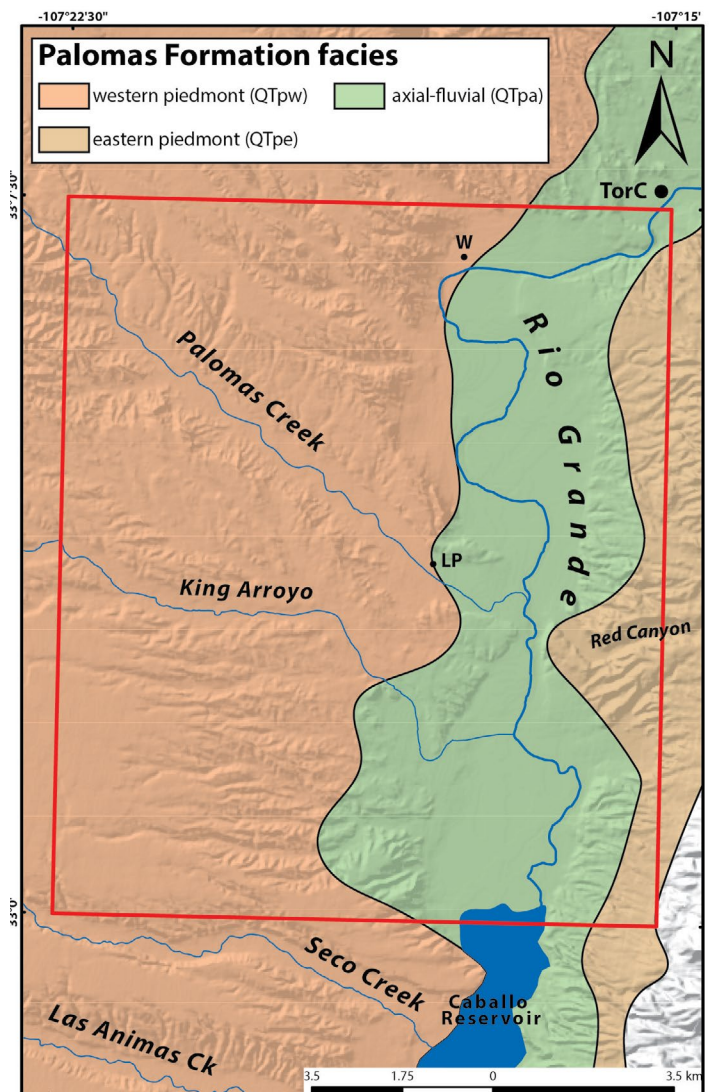


Figure 3. Distribution of Palomas Formation facies in the Williamsburg quadrangle and surrounding areas. Axial-fluvial facies are exposed in a ~3-5 km belt centered on the modern Rio Grande valley. Facies distributions off the quadrangle are modified from Foster (2009) and Mack et al. (2012) to the north, and Seager and Mack (2005) to the south. Abbreviations for local communities (black dots) as in Figure 1.

the protolith for these rocks was likely basalt (Bauer and Lozinsky, 1986). Granitic rocks (**pCg**) exposed in the quadrangle are dominantly pink and hypidiomorphic granular with large phenocrysts of microcline, plagioclase, biotite, and quartz (Fig. 4). The granitic rocks were initially thought to belong to the Caballo granite exposed in the southern half of the Caballo Mountains (Condie and Budding, 1979; Bauer and Lozinsky, 1986). However, Seager and Mack (2003) suggested that this granite may have formed from its own pluton because it lacks pegmatites that are observed in the Caballo granite. Field relationships near Longbottom Canyon south of the quadrangle imply that the northern pluton is somewhat younger than adjacent basement rocks. The latter include granodiorite dated at 1.47 ± 0.21 Ga and gneiss dated at 1.67 ± 0.16 Ga using U-Pb isotopes from zircon (Amato and Becker, 2012). The Caballo granite found in the southern part of the range has been dated at 1.3-1.45 Ga using Rb-Sr and U-Pb isotopes (Muehlberger et al., 1966; Amato and Becker, 2012).



Figure 4. Gneissic granite with well-defined foliation. Located east of the Rio Grande in the footwall of the Hot Springs fault. Hammer is 28 cm long.

Lower to middle Paleozoic rocks in the quadrangle were deposited on a stable, epicratonic shelf with low rates of sedimentation and subsidence. This shelf was subjected to periodic inundation by shallow, tropical seas (Seager and Mack, 2003). The oldest Paleozoic strata exposed throughout southern New Mexico and west Texas is the Cambro-Ordovician Bliss Formation (**EOB**). This unit consists of dark brown to black, cross-stratified, quartzose sandstone containing peloidal glauconite, and is the basal unit of an early eastward to northward transgression (Mack, 2004). The Bliss Formation forms a

prominent dark band visible above pinkish-red granite in the lower slopes of the Caballo Mountains.

The Bliss Formation is gradational with cherty limestone of the overlying El Paso Formation (Oe). The lower ~50 m of the El Paso Formation consists of sparsely fossiliferous packstone with vertical burrows in-filled by dolomite. This package is overlain by 65 m of limestone (cherty wackestone to grainstone) that commonly features stromatolites forming domal structures up to 30 cm in diameter as well as algal mats (Fig. 5). The lower, fossil-poor limestone and upper, stromatolitic limestone are correlative to the Sierrite Limestone and Bat Cave Formation, respectively, of Kelley and Silver (1952). The El Paso Formation was deposited below wave base on a shallow-marine shelf and represents up to five transgressive-regressive cycles (Seager and Mack, 2003;



Figure 5. Algal mats in Bat Cave Member of the El Paso Formation. Located east of Rio Grande in footwall of Hot Springs fault. Pen is 15 cm long.

Mack, 2004).

The middle to upper Ordovician Montoya Formation (Om) disconformably overlies the El Paso Formation. The lower part consists of poorly-sorted quartz arenite underlying cherty dolostone. These beds correspond to the Cable Canyon Sandstone and Upham Dolomite, respectively, of Kelley and Silver (1952), and have a composite thickness of only 37 m. The Cable Canyon Sandstone has been interpreted as representing open-marine sand bars formed by the reworking of sand dunes during a transgressive event (Bruno and Chafetz, 1988; Pope, 2004). Dolostone of the Upham Member was probably deposited on an open-marine carbonate ramp (Pope, 2004).

The upper part of the Montoya Formation consists of cherty dolostone with subordinate amounts of limestone and jasperoid. Although sparsely fossiliferous in the Williamsburg quadrangle, the articulate brachiopods *Rafinesquina* and *Zygospira* were recovered from correlative beds in the Palomas Gap quadrangle to the east (Mason, 1976). Pope (2004) suggests a shallow, open-marine origin for these strata, which may correlate to the Aleman Member of Kelley and Silver (1952).

QUATERNARY-TERTIARY BASIN-FILL

Basins throughout the Rio Grande rift are characterized by thick accumulations of clastic sediment (with subordinate interbedded volcanic deposits) collectively known as the Santa Fe Group (Kelley, 1977; Hawley, 1978; Gile et al., 1981; Chapin and Cather, 1994; Connell, 2008). This sediment was deposited during Rio Grande rift extension. Basin-fill packages vary in age depending on location but generally span the late Oligocene through early Pleistocene. Late Oligocene to early-middle Miocene basin-fill is not exposed in the Williamsburg quadrangle nor penetrated by the 2100-ft-deep Barney Iorio Fee #1 well. Reddish, fine-grained beds of sandstone, pebbly sandstone, and clay (Trvpw, Trvbf) exposed along the northern quadrangle boundary are considered by the authors to be correlative to the upper Miocene Rincon Valley Formation of Seager et al. (1971). These beds are located in the footwall of the Mud Springs-Williamsburg fault and are not observed elsewhere in the quadrangle. Relatively fine-grained strata containing pink to red, sticky clays are correlated to the Rincon Valley Formation in the Barney Iorio Fee #1 well, where they extend from 578 ft to the bottom of the well (2100 ft).

The basin-fill stratigraphy of the Williamsburg quadrangle is dominated by Plio-Pleistocene sediment of the Palomas Formation, the uppermost unit of the Santa Fe Group in the Palomas Basin (Lozinsky and Hawley, 1986a, b). The term “Palomas” was first applied to outcrops of upper Santa Fe Group basin fill by Gordon and Graton (1907), Gordon (1910), and Harley (1934). Lozinsky and Hawley (1986a) formally defined the Palomas Formation. Detailed descriptions of the unit are presented in Lozinsky and Hawley (1986a, b) and Lozinsky (1986). Fossil data (summarized by Morgan and Lucas, 2012), basalt radiometric dates (Bachman and Mehnert, 1978; Seager et al., 1984; Jochems, 2015), and magnetostratigraphic data (Repenning and May, 1986; Mack et al., 1993; Leeder et al., 1996; Mack et al., 1998) indicate an age range of

~5.0-0.8 Ma for the Palomas Formation. Type sections of the Palomas Formation in the Williamsburg quadrangle are found at NW¼ NW¼ sec. 30 and NE¼ SW¼ sec. 33, T. 14 S., R. 4 W (Lozinsky and Hawley, 1986a).

The Palomas Formation exhibits a variety of lithofacies, from gravel-dominated channel fills to clays, silts, and fine sands representing extra-channel or eolian deposition. The Palomas is subdivided into three primary lithofacies in the Williamsburg quadrangle: (1) western-derived piedmont deposited as distributary fan complexes in the hanging wall of the Palomas basin (QTpw units), (2) eastern-derived sand and gravel deposited on much smaller fans emanating from the western escarpment of the Caballo Mountains (QTpe units), and (3) axial-fluvial sandy channel fills and fine floodplain deposits of the ancestral Rio Grande (QTpa units). The distribution of these facies in the Williamsburg quadrangle is shown in Fig. 3. Although broad textural distinctions may apply to each lithofacies, the units are more easily differentiated using lithologic composition of clasts, reflecting the source area of a particular facies. QTpw units are composed of volcanic sand and gravel originating in the Black Range and Animas-Salado uplifts, QTpe sand and gravel are dominated by carbonate and plutonic rocks derived from the western Caballo Mountains, and QTpa channel fills feature exotic clasts such as quartzite. This report describes each facies in the order listed above. Detailed unit descriptions are given in Appendix A, and clast-count and paleocurrent data are given in Appendices B and C, respectively.

Western piedmont of the Palomas Formation

The transitional base of the lower western piedmont facies of the Palomas Formation (QTpwl) consists of interbedded pebbly channel fills and extra-channel deposits dominated by clayey-silty, fine-grained sand (Fig. 6). This unit has a texture intermediate between the overlying and underlying units (QTpwl above, Trvbf and Trvpw below). The apparent lack of aphanitic basalt clasts suggests that the unit pre-dates the mostly 4.8-4.3 Ma basalt flows found in the western Palomas basin (Seager et al., 1984; Jochems, 2015; Koning et al., 2015). It is relatively thin in outcrop (<10 m) and subsumed into the base of the lower western piedmont unit (QTpwl) along the northern quadrangle boundary. Interpretation of well data suggests that the unit thickens southward from a minimum of ~30 m in Truth or Consequences city wells to as much as 51 m in the Barney Iorio Fee #1 well south of Palomas Creek (Tables 1 and 2).

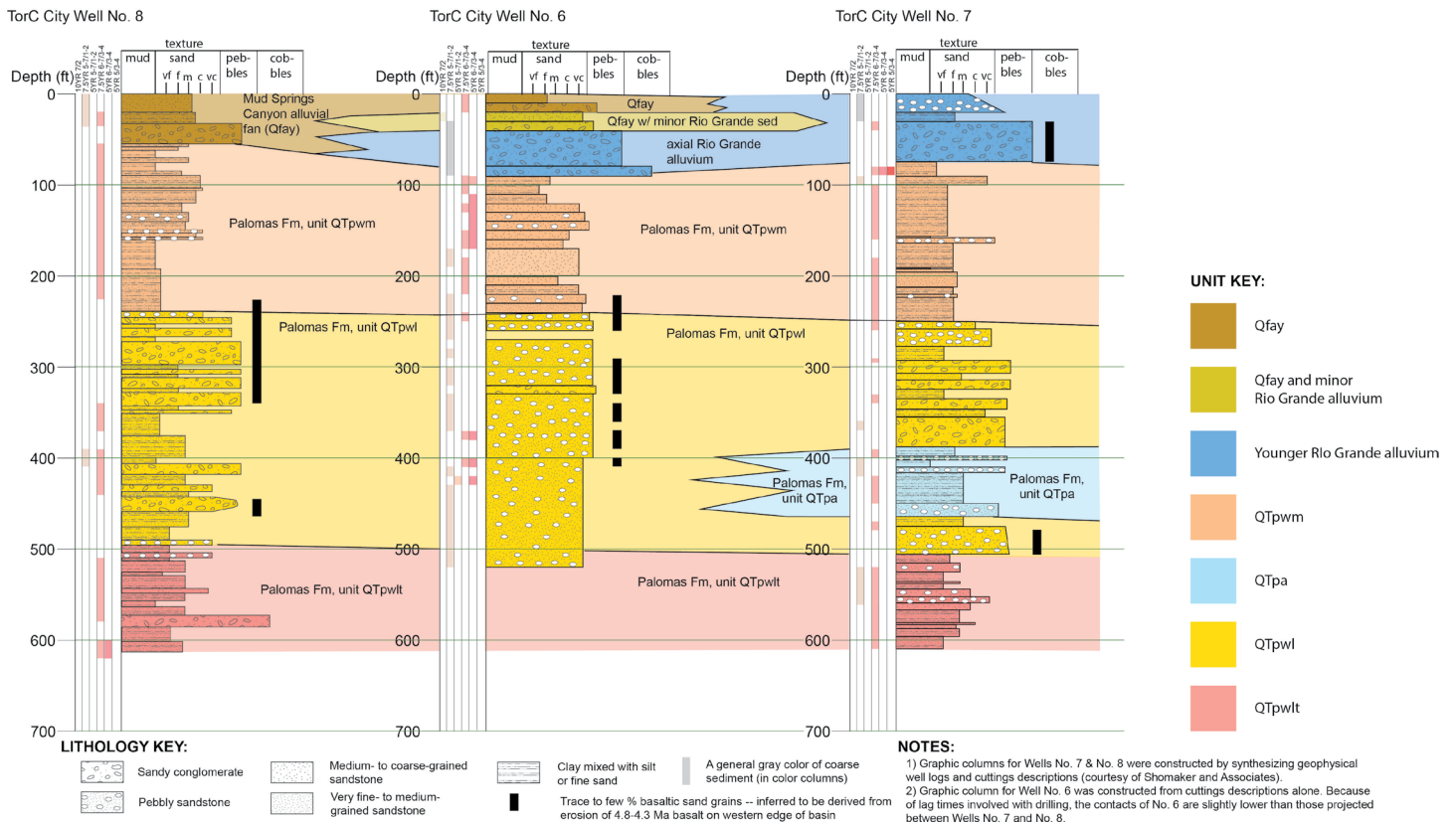


Figure 6. Stratigraphic fence diagram composed from interpretations of lithologic logs for Truth or Consequences city wells 6, 7, and 8. See geologic map for well locations.

Table 1. Location and subsurface stratigraphic data for select wells of the Truth or Consequences city well field.

Well ID	UTM E ^a	UTM N ^a	Location (Township-Range-Sect) ^b	Well head elev. (ft)	Total Depth (ft)	Stratum	Depth from cuttings (ft)	Depth, geophys. logs (ft)	Elevation of base (ft)
Well No. 6	286318	3666768	6.3242-14S-4W	4241	520	Q(f)ayr	0-20		4221
						Qayr/Qtr	20-90		4151
						QTpwm	90-150		4091
						QTpwm-QTpa margin	150-180		4061
						QTpwm	180-220		4021
						QTpwl	220-520		
Well No. 7	286807	3666755	6.423-14S-4W	4238	610	Qayr/Qtr	0-80	0-74	4164
						QTpwm	80-260	74-250	3988
						QTpwl	250-400	250-395	3843
						QTpa	400-470	395-466	3772
						QTpwl	470-520	466-506	3718
						QTpwt	520 to >610	506 to >610	<3628
Well No. 8	286003	3666770	6.32-14S-4W	4239	620	Q(f)ayr	0-62	0-56	4183
						QTpwm	62-225	56-246	3993
						QTpwl	225-510	246-496	3743
						QTpwt	510 to >620	496 to >620	<3623

^aUTM Zone 13S, NAD83.

^bWell locations on subdivision of township and range sections. For example, a location of 1.1234-1S-1W indicates the SE quarter (4) of the SW quarter (3) of the NE quarter (2) of the NW quarter (1) of section 1, Township 1 South, Range 1 West.

Table 2. Location and subsurface stratigraphic data for wells used in Cross-section A-A'

Well ID	UTM E ^a	UTM N ^a	Location (Township- Range-Sect) ^b	Well head elev. (ft)	Total Depth (ft)	Stratum	Depth from cuttings (ft)	Elevation of base (ft)	Groundwater depth (ft)
Barney Iorio Fee #1	284759	3660416	25.41-14S-05W	4303	2100	Qayr	0-17	4286	90, 140, 193, 372, 543, 632, 1160, 1170/1200
						QTpwm	17-70	4233	
						QTpa	70-193	4110	
						QTpwm	193-272	4031	
						QTpa	272-285	4018	
						QTpwm	285-407	3896	
						QTpwl	407-463	3840	
						QTpwl	463-578	3725	
Trv	578 to >2100	<2203							
HS-00146	285052	3660102	25.441-14S-05W	4283	149	Qayr	0-41	4242	70
						QTpwm	41-70	4213	
						QTpa	70 to >149	<4134	
HS-00316	285153	3660003	25.44-14S-05W	4275	100	Qayr	70(?)	4205(?)	62
HS-00773	285456	3659896	30.333-14S-04W	4262	92	Qayr	0-59	4203	37
						QTpwm	59 to >92	<4170	
HS-00033	285556	3659995	30.33-14S-04W	4257	320	Qayr	0-32	4225	NA
						QTpwm	32-100	4157	
						QTpa	100-155	4102	
						QTpwm	155-225	4032	
						QTpa	225-246	4011	
						QTpwm	246 to >320	<3937	
HS-00663	285656	3659896	30.334-14S-04W	4255	55	Qayr	0-42	4213	30
						QTpwm	42-44	4211	
						QTpa	44 to	<4200	
HS-00648 ^c	285671	3659732	31.112-14S-04W	4260	51	QTpwm	0 to >51	4209	20
HS-00737	285848	3659682	31.121-14S-04W	4258	165	Qayr	0-18		70
						QTpa	18 to >165		
HS-00729	286048	3659682	31.122-14S-04W	4252	92	Qayr	0-16	4236	36
						QTpa	16 to >92	<4160	

^aUTM Zone 13S, NAD83.

^bWell locations on subdivision of township and range sections. For example, a location of 1.1234-1S-1W indicates the SE quarter (4) of the SW quarter (3) of the NE quarter (2) of the NW quarter (1) of section 1, Township 1 South, Range 1 West.

^cUTM location moved slightly from what was stated in well log to account for unreasonable position relative to topography

The contact between QTpwl and the overlying lower western piedmont (QTpwl) is sharp to gradational over 4-10 stratigraphic meters. QTpwl is only exposed on the footwall of the Mud Springs-Williamsburg fault, where it consists of stacked, pebbly to cobbly channel fills. In the subsurface on the hanging wall of this fault, these channel fills are interbedded with subordinate, light brown, extra-channel deposits composed of clay, silt, and very fine- to medium-grained sand. Volcanic clasts are dominated by rhyolite with subordinate tuffs and intermediate volcanic varieties. A small amount ($\leq 5\%$) of granite and Paleozoic clasts found in the northern part of the quadrangle suggests mixing of distally derived volcanic sediment with sediment sourced from local bedrock exposed on the western flanks of the east-dipping Mud Springs Mountains. There, QTpwl is correlative with the “sedimentary, granitic, and metamorphic-clast conglomerate facies assemblage” of Foster (2009) and Mack et al. (2012). The presence of trace to 1% vesicular basalt clasts indicates that the unit post-dates 4.8-4.3 Ma basalt flows found in the western Palomas basin (Seager et al., 1984; Jochems, 2015; Koning et al., 2015). The lower western piedmont is 76-78 m thick in Truth or Consequences city wells 7 and 8 (including an intervening tongue of Rio Grande axial sediment in city well #8; Table 1, Fig. 6), and thins southward to 17 m in the Barney Iorio Fee #1 well (Table 2).

Beds of fine-grained sand and silt with subordinate (5-20%) tongues of pebbly sand and sandy pebble gravel comprise the middle western piedmont facies (QTpwm). Its basal contact with QTpwl is not exposed on the quadrangle. This unit is generally light colored (7.5YR 7/3; 6/3-4; 5-7.5YR 6-7/2), and beds are often internally massive (Fig. 7). These beds may contain sparse (3%) pebbles and up to 10% “floating” medium to very coarse sand grains and are interpreted as hyperconcentrated flows (Seager and Mack, 2003). Prominent carbonate ledges may be observed in the upper 10-20 m of the unit. Occasionally, coarse channel fills within this unit are sufficiently extensive to map separately (QTpwmc) in the southern part of the quadrangle. Among many fossils collected by previous workers from QTpwm are *Paramylodon*, a small ground sloth, and the horse *Nannippus* (Tedford, 1981; Morgan and Lucas, 2012). The co-occurrence of these species suggests a late Blancan (~3.0-2.6 Ma) North American Land Mammal age for the upper part of this unit (Fig. 8; Morgan et al., 2008; Morgan and Lucas, 2012). Buried soils with stage II-III carbonate morphology (nodules, tubules) are common

in muddy intervals of QTpwm (Fig. 9). These paleosols typically feature two or more Bt, Bk, and/or K horizons that formed due to vadose zone pedogenesis (Mack et al., 2000). QTpwm interfingers with axial-fluvial facies in wells along Palomas Creek and in Truth or Consequences city well #8, where individual tongues are generally 9-37 m thick (Fig. 6; Tables 1 and 2). The middle western piedmont is approximately 40-60 m thick in Truth or Consequences city wells. In the southern part of the quadrangle, exposed thicknesses coupled with subsurface interpretations of the Barney Iorio Fee #1 well indicate a total thickness of 120-150 m (including tongues of Rio Grande axial fluvial facies).

The middle western piedmont underlies a transitional zone (QTpwt) across the quadrangle. This unit has a maximum thickness of 35 m and thins to the south where it becomes too thin to differentiate. The transitional facies are mostly fine grained (silt and fine sand with subordinate clay), and contain prominent marker beds of pale yellowish pink (7.5YR 9.5/2) to pinkish white (5YR 8/2), massive carbonate (Figs. 7, 10) that envelops pebbles and small cobbles in places. Root mats and laminations are common in these beds, and have been interpreted as spring (ciénega) deposits formed at the medial-distal alluvial-fan interface (Mack et al., 2000). These intervals are common south of King Arroyo. Fossils recovered from QTpwt include gomphothere teeth, limb bones of *Equus* sp., and a tooth of the extinct rabbit *Sylvilagus hibbardi* that indicates a late Blancan (2.5-2.0 Ma) age for the unit (G. Morgan, personal communication, 2014). This age constraint is corroborated by magnetostratigraphic data, which implies that QTpwt lies below the Olduvai subchron (1.95-1.77 Ma) in the Las Palomas Area (Fig. 11; Mack et al., 1993, 1998; Leeder et al., 1996; Seager and Mack, 2003). Transitional beds lie gradationally between QTpwm and the upper western piedmont (QTpwu), both in a vertical and lateral sense, with gradational relationships particularly apparent west of I-25 and south of Palomas Creek.

The upper western piedmont (QTpwu) consists of clay, silt, fine sand, and $\leq 40\%$ pebbly to cobbly coarse channel fills (Fig. 12). This unit forms prominent, cliffy exposures on the south side of Palomas Creek. Clay-rich intervals impart a distinctive reddish color (e.g. 5YR 4/4-6; Fig. 7) and likely represent floodplain depositional settings. Internally massive, clayey to silty sand beds locally contain scattered coarse sand and volcanic pebbles and are interpreted as hyperconcentrated flow deposits (Seager and Mack, 2003). Like QTpwm, fine-grained

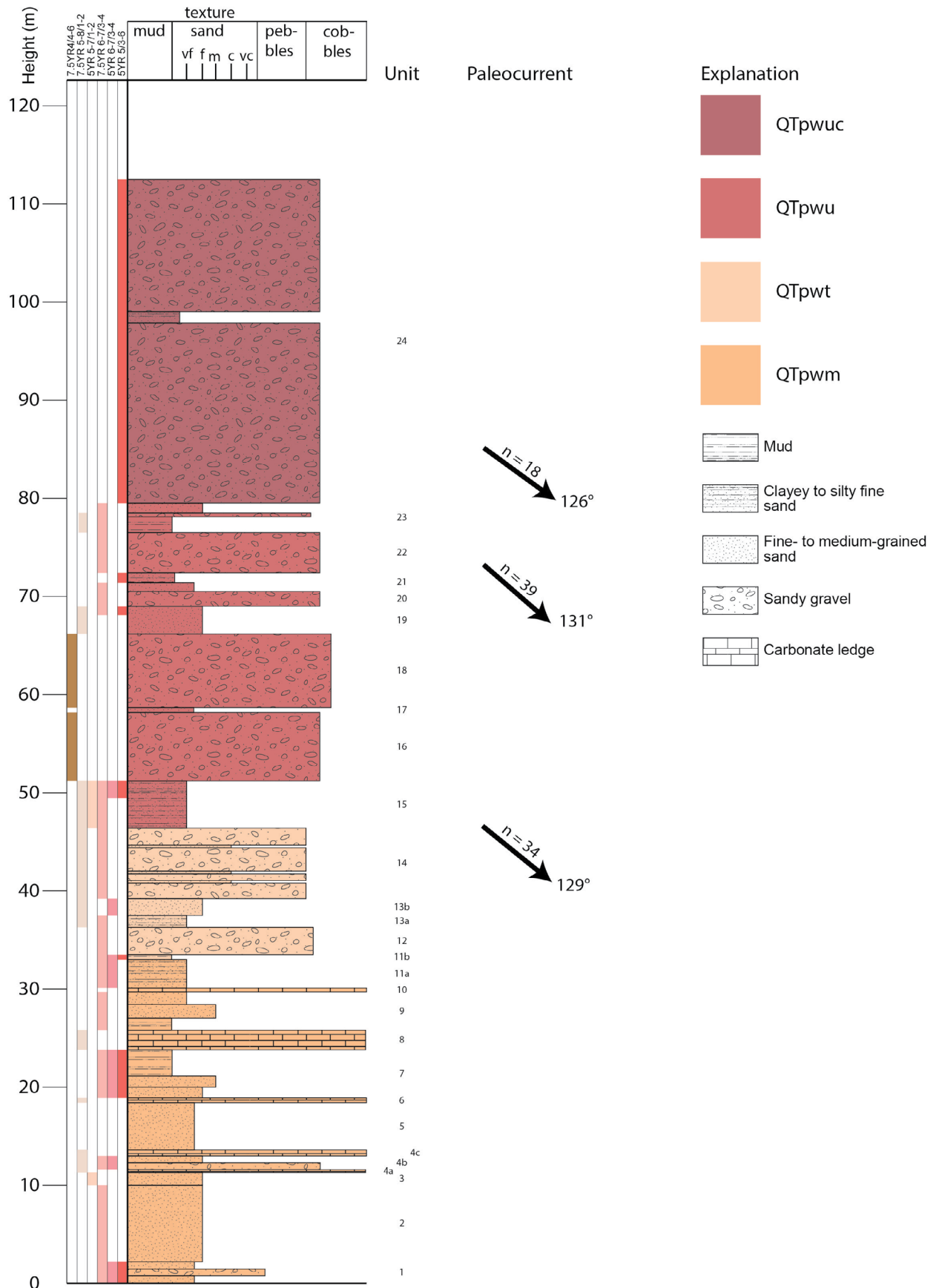


Figure 7. West Williamsburg stratigraphic section. See Appendix A for detailed unit descriptions. Paleocurrent measurements from clast imbrication. Base of section at 285444 mE/3666150 mN.



Figure 8. Contact between transitional (QTpwt) and middle (QTpwm) western piedmont facies of the Palomas Formation along I-25 roadcut just south of Mud Springs Canyon. QTpwt deposit consists of pebble-cobble gravel, silt-clay, very fine- to fine-grained sand, and slightly silty-clayey sand. QTpwm consists of pinkish silty sand with rare, thin gravel stringers. Vertebrate fossils recovered from the top part of QTpwm and described in Morgan and Lucas (2012) suggest a late Blancan age of 2.7-2.5 Ma. Pack is ~0.6 m tall.



Figure 9. Stage II carbonate morphology in middle western piedmont (QTpwm) exposed near the mouth of Kelly Canyon. Vertically elongate carbonate tubules could have formed around roots and/or burrows (P. Mozley, personal communication, 2015). Forms Btk horizon in paleosols that also features slickensides and wedge-shaped peds. Hammer is 28 cm long.

intervals of QTpwu commonly feature paleosols with Bt and Bk horizons. However, select beds with elongate carbonate nodules parallel to bedding may have formed due to a vertically shifting water table rather than vadose zone pedogenesis (Mack et al., 2000). Gravelly channel fills in QTpwu contain up to 7% clasts of vesicular basalt; this proportion decreases to the north. The lower contact of QTpwu lies immediately above the Kelly Canyon Local Fauna site, which features axial-fluvial strata ~2.6-2.0 Ma in age (Morgan et al., 2011; Morgan and Lucas, 2012). Given a similar late Blancan age for the underlying transitional unit as well as magnetostratigraphic data



Figure 10. Carbonate ledge interbedded in transitional western piedmont facies (QTpwt). Prominent ledges form marker beds that are 0.5-1 m thick and are commonly massive and vuggy. Alternatively, beds may be wavy and nonparallel due to lithification of root mats. This bed appears to have collapsed into a small sinkhole. Pack is 0.6 m tall.

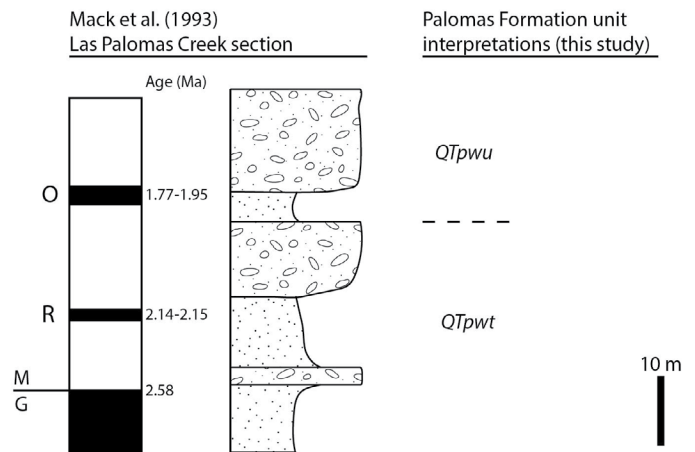


Figure 11. Comparison between paleomagnetostratigraphic section from Las Palomas Creek (Mack et al., 1993) and Palomas Formation unit interpretations from this study. Letters on left correspond to chrons and subchrons: G = Gauss, M = Matuyama (chrons), and R = Reunion, O = Olduvai (subchrons). Modified from figure 9 of Mack et al. (1993) and figure 76 of Seager and Mack (2003).

from the Las Palomas area (Fig. 11; Mack et al., 1993, 1998; Leeder et al., 1996), the age of the upper western piedmont is tentatively estimated at ~2.5-1.8 Ma. This unit is 2-45 m thick.

Lying above QTpwu are coarse, amalgamated, laterally continuous channel-fill complexes (QTpwuc) with 1-15% clasts of vesicular basalt (Fig. 7). The coarse channel fills commonly feature basal scour surfaces with up to 1 m of relief (Fig. 13). Low-angle and trough cross-stratification, lateral accretion cross-stratification, and clast imbrication are common. Paleoflow indicated by clast imbrication is typically east-southeast (Appendix C). QTpwuc underlies the Cuchillo surface, which is marked by a petrocalcic horizon that is 1-2 m thick where not significantly eroded. This surface soil generally exhibits stage III to IV



Figure 12. Contact between upper (QTpwu) and upper coarse (QTpwuc) western piedmont facies of the Palomas Formation in Kelly Canyon west of I-25. QTpwu consists of ~65% pinkish to reddish brown mudstone, silt, and silty sand and ~35% pebbly to cobbly channel-fills. Total relief of exposure is ~20 m.

carbonate morphology (Seager and Mack, 2003; McCraw and Love, 2012), and is correlative to the Jornada I and La Mesa surfaces of the Camp Rice Formation in the Rincon and Mesilla basins to the south (Gile et al., 1981). The age of the youngest coarse upper western piedmont is constrained by magnetostratigraphy at ~0.8 Ma (Mack et al., 1993, 1998; Mack and Leeder, 1999). The upper coarse western piedmont has a maximum thickness of 45 m.

Eastern piedmont of the Palomas Formation

The eastern piedmont facies (QTpe) is differentiated from western-derived piedmont by three criteria: (1) a predominance of coarse-grained beds; (2) common sparry calcite cement; and (3) the presence of Paleozoic carbonate and Proterozoic plutonic clasts. Cementation and sedimentary structures vary according to relative fan position (proximal, medial, and distal) in the eastern piedmont. Proximal deposits consist of poorly sorted, sandy pebble-cobble gravel in tabular beds (Fig. 14). These intervals rarely feature cross-stratification and are cemented by authigenic carbonate precipitated from shallow groundwater or gully-bottom cementation. Both cementation types are non-pedogenic, and the latter forms when bicarbonate-rich runoff evaporates from gravelly stream beds (Mack et al., 2000; Mack and Seager, 2003). Medial deposits consist of massive or imbricated to planar cross-stratified sand and gravel. Occasional paleosols in finer-grained medial facies may feature illuviated clay (Bt) horizons above clay and carbonate-rich horizons (Btk). Distal deposits consist of moderately sorted coarse channel fills (with pebbles or pebble-cobbles) interbedded with matrix-supported

silty or sandy beds. Paleosols with Btk to K horizons are common in distal silt beds. In the northern part of the quadrangle, the eastern piedmont commonly interfingers with axial-fluvial facies. Just south of the quadrangle, the base of the eastern piedmont deposits is interbedded with a basalt dated at 3.1 ± 0.1 Ma (K/Ar; Seager et al., 1984), implying a temporal correlation with western piedmont units QTpwm, QTpwt, QTpwu, and QTpwuc. This unit has a maximum exposed thickness of 110 m.

South of Red Canyon, fine-grained exposures of mostly

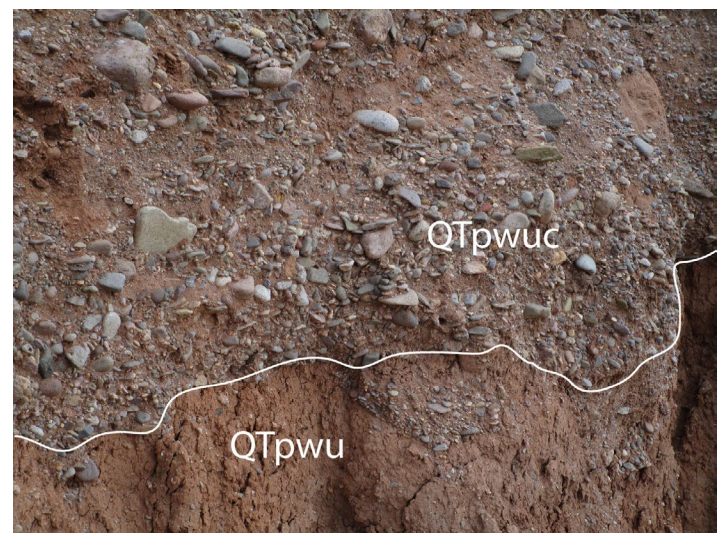


Figure 13. Scoured contact between upper coarse (QTpwuc) and upper (QTpwu) western piedmont facies of the Palomas Formation. Here, local scour relief is less than ~0.5 m. QTpwuc consists of vague, tabular to lenticular beds of clast-supported sandy gravel with minor cross-stratification up to ~0.5 m thick. Upper QTpwu features weakly developed argillic horizon of a paleosol. Largest clasts are 20-30 cm across.



Figure 14. Proximal alluvial fan facies of the eastern piedmont of the Palomas Formation (QTpe). Strongly (sparry) carbonate-cemented pebble gravel forms well-defined erosional surface that may be planar (A) to scoured (B) on more weakly consolidated pebble gravel and silt. Progradational relationships are commonly observed in QTpe exposures. Tape is 2 m tall.

massive clay and silty sand with <40% gravel can be mapped as a subunit of the eastern piedmont (QTpef). Buried soils are common in this unit and include stage I to II+ carbonate morphology with Btk, Bk, and K horizons up to ~1 m thick (Fig. 15). In addition to its obvious textural distinction from the undivided eastern piedmont, QTpef contains no clasts of red Abo Formation siltstone and fine-grained sandstone, distinguishing it from the Red Canyon paleo-fan facies (described below). The unit underlies and/or interfingers with QTpe. It may also interfinger with axial-fluvial facies at depth. Its maximum thickness is estimated at 140 m from cross-section relationships in the Red Canyon area, though it thins northward to ~30 m.

Prominent topographic benches flanking Red Canyon are underlain by strata of the Red Canyon paleo-alluvial fan (QTper). This unit rises above adjoining ridges underlain by QTpe and is clearly delineated in the field and aerial imagery by its reddish hues. Red Canyon paleo-fan facies are characterized by siltstone, sandstone, and sandy pebble-cobble-boulder conglomerate in multi-story beds (Fig. 16). Their red color (5YR 4-5/6 to 5-7/4) is derived from abundant (up to 30%) clasts sourced from the Permian Abo Formation, exposed in the headwaters of Red Canyon. Scoured contacts on underlying sandstone and siltstone beds are common. A stratigraphic section measured by Lozinsky and Hawley (1986a) includes an ash 17 m below the top of the unit correlated with 1.2-1.45 Ma Cerro Toledo tephra units originating from the Jemez volcanic field (Izett et al., 1981; Spell et al., 1996). The top of Red Canyon piedmont features stage III-IV carbonate morphology and correlates to the Cuchillo surface (Lozinsky and Hawley, 1986a; Mack et al., 1993). QTper interfingers with at least two tongues of axial-fluvial strata along the lower 1.7 km of modern Red Canyon (Fig. 17). The Red Canyon paleo-fan facies is 60-

140 (+?) m thick.

Axial-fluvial facies of the Palomas Formation

Most Palomas Formation piedmont units interfinger with axial-fluvial facies of the ancestral Rio Grande (QTpa). This lithofacies is characterized by cross-stratified, well-sorted, well-rounded, quartzose sand containing a heterolithic gravel assemblage of Tertiary volcanics, Cretaceous sandstone, Paleozoic carbonates, and quartzite. Limestone, sandstone, and siltstone constitute a greater proportion (up to 80% total) of clasts in basal beds; volcanics and quartzite increase up-section. This unit was deposited by the ancestral Rio Grande in a 3-5 km belt centered on the modern Rio Grande valley throughout the Palomas basin, and commonly exhibits field relationships suggesting toe-cutting of footwall-derived alluvial fans (Seager et al., 1982; Lozinsky and Hawley, 1986a; Mack and Leeder, 1999; Seager and Mack,



Figure 15. Stage II carbonate morphology observed in fine-grained facies of the eastern piedmont of the Palomas Formation (QTpef). Well-developed carbonate tubules indicate long-lasting stability before the deposit was eroded by younger alluvial fan gravel (upper part of photo). Pack is 0.6 m tall.



Figure 16. Typical exposure of paleo-Red Canyon alluvial fan (QTper) facies. Unit includes thick (up to 30 m) sequences of channel fills and/or conglomerate with abundant clasts of Permian Abo Formation. Subordinate to these facies are tabular silt and sand beds with floating pebbles, representing deposition on floodplains or by hyperconcentrated flows.

2003; this study). One subunit has been differentiated (QTpac).

Pebbly to silty sand with subordinate mudstone floodplain deposits are relatively uncommon in the Williamsburg quadrangle. The presence of reddish to olive, massive mudstones in this unit indicate low-energy floodplain environments (Fig. 18). Scattered concretions of manganese-rich material may be observed in these facies. Fine-grained axial deposits near the mouth of Kelly Canyon have yielded many fossils, including salamanders (*Amystoma* sp.), frogs (*Rana* sp.), and other freshwater

vertebrates that could have inhabited slack-water environments (G. Morgan, personal communication, 2015). A fossil of the extinct muskrat *Ondatra idahoensis* was also recovered from these beds, indicating a late Blancan (~2.6-2.0 Ma) age for axial facies at that location (Morgan and Lucas, 2012).

Coarse-grained axial facies (QTpac) consist of sandy pebble-cobble and pebble-cobble-boulder gravel/conglomerate deposited in laterally extensive channel-fill complexes. Lateral accretion sets are occasionally observed, and strongly indurated exposures sometimes

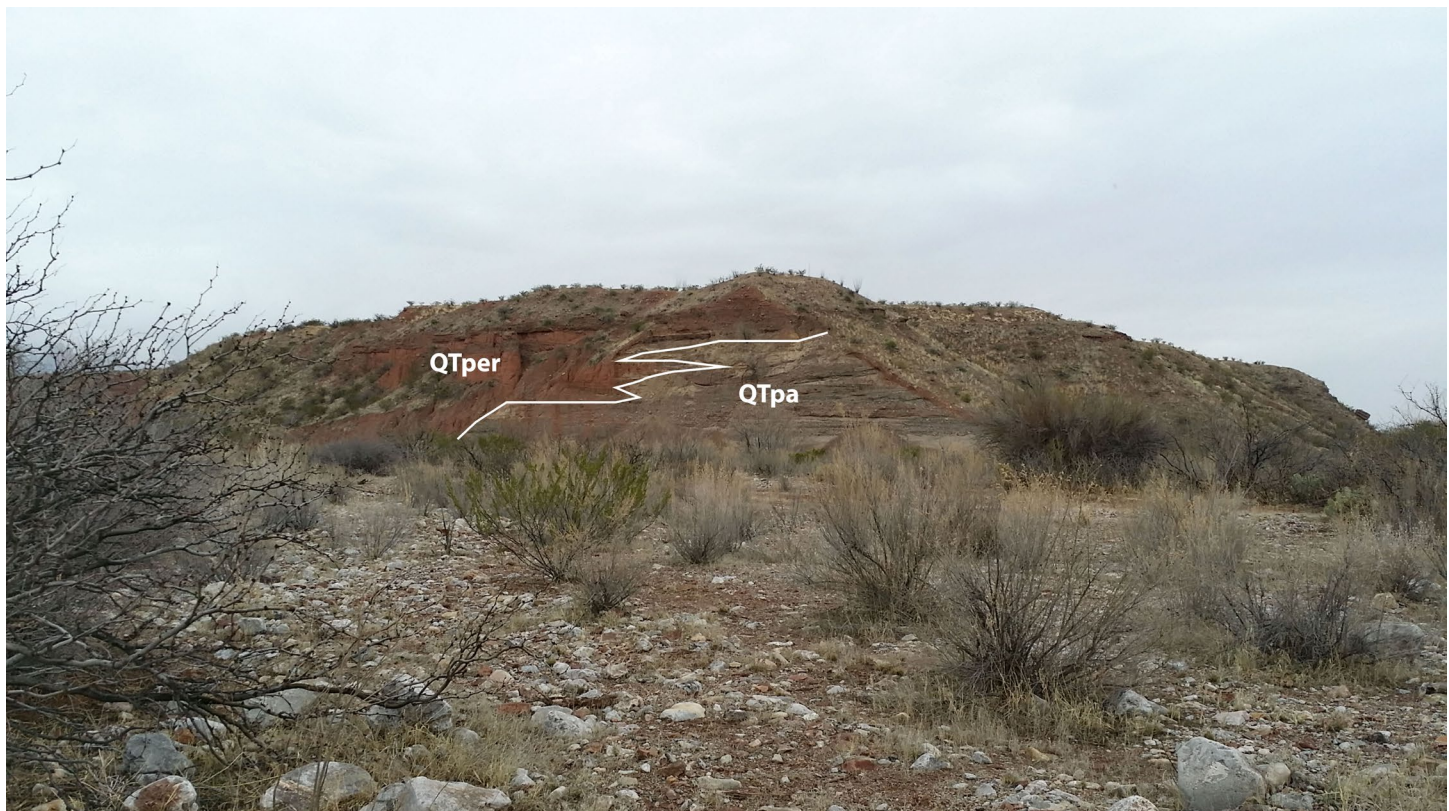


Figure 17. Interfingering between axial-fluvial facies (QTpa) and alluvial fan facies of Red Canyon (QTper), both of the Palomas Formation. Slip along the Caballo fault ~3 km to the west of this exposure (towards the left in photo) likely accounts for onlapping relationships between the two units (e.g, Mack and Leeder, 1999). Total relief of exposure is ~20 m.

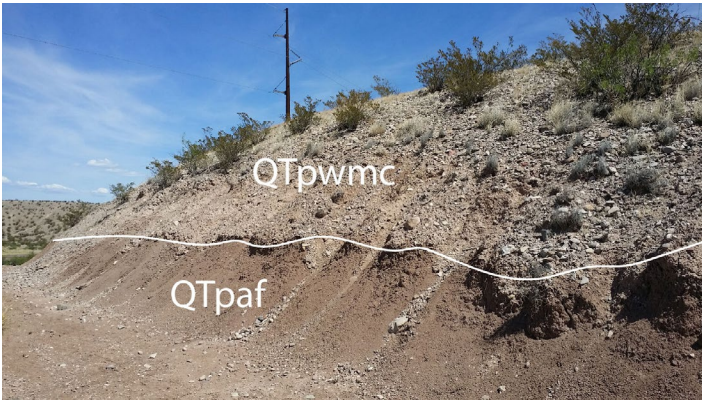


Figure 18. Floodplain axial-fluvial facies (called QTpaf here) overlain by a channel fill of the middle western piedmont facies (QTpwmc). Frequent channel avulsions of the ancestral Rio Grande resulted in overall poor preservation of axial floodplain deposits.

preserve flute casts. Planar to trough cross-stratified sandy beds are interpreted as channel sandbars (Fig. 19). Ellipsoidal concretions are observed where beds are cemented east of the Rio Grande (Fig. 20), and may have formed in the direction of groundwater flow down-gradient of decaying organic matter (Mozley and Davis, 2005). Paleocurrent directions in imbricated gravel beds average south-southeast, though imbricated clasts give south-southwest paleoflow directions in the lower 30 m of the unit along the northern quadrangle boundary. Manganese coats on clasts are common. Coarse axial deposits typically exhibit basal scour contacts on finer-

grained sediment with up to 3 m of relief. A tooth of the late Hemphillian horse *Neobipparion eurystyle*, collected from spoil piles just north of the quadrangle, suggests an age of 5.3-4.9 Ma for the lower 35 m of ancestral Rio Grande gravels (Koning et al., 2016). Thus, the ancestral Rio Grande appears to have entered the Palomas basin at approximately 5 Ma. Inspection of cross-section A-A' indicates a maximum preserved thickness of 250 m for the axial facies in the Williamsburg quadrangle.

Palomas Formation thickness and coarsening trends

Initially thought to be 100-131 m thick (Lozinsky and Hawley, 1986a), our work suggests a total thickness of 150-350 m for the Palomas Formation in the Williamsburg quadrangle. This range is based on the measured thicknesses of QTpw units in the Truth or Consequences city wells and west Williamsburg stratigraphic section (Figs. 6-7), as well as interpreted thickness of QTpe units in the eastern part of the quadrangle. The cumulative thickness, and the thicknesses of most individual units, of the western piedmont facies increases toward the east, where the deepest part of the Palomas basin is located (Fig. 21; Gilmer et al., 1986).

In addition to a pattern of eastward thickening, the Palomas Formation also exhibits an upward-coarsening trend from the QTpwl-QTpwm contact that is observed



Figure 19. Trough cross-stratification in axial-fluvial facies (QTpa) of the Palomas Formation. White lines show apparent (outcrop) direction of individual foresets. Compass for scale (black circle) is 10 cm in diameter.

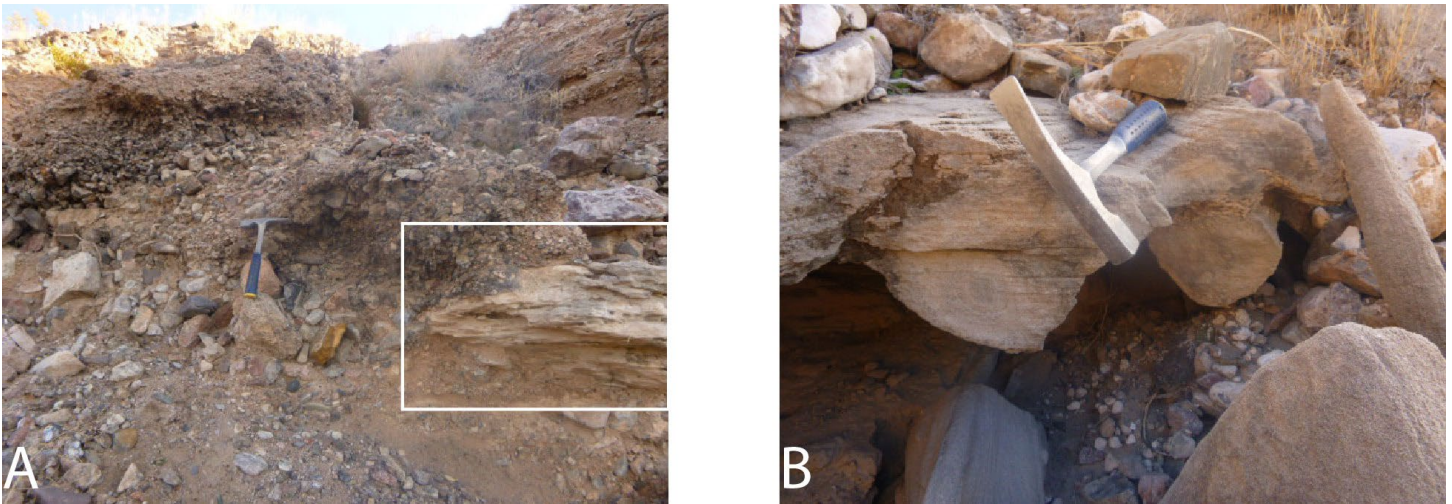


Figure 20. Concretions in axial-fluvial facies (QTpa) of the Palomas Formation. (A) QTpa channel gravel scouring fine- to medium-grained axial sand with concretions (white box). (B) Close-up profile view of concretions. Concretions are commonly ellipsoidal and up to 30 cm across. They typically follow paleocurrent directions and likely form from plumes of groundwater in well-sorted, permeable sand (Mozley and Davis, 2005). Hammer is 28 cm long.

throughout the Palomas basin (Grundwald, 1990; Jochems, 2015; Koning et al., 2015). Though perhaps related in part to tectonic tilting and the large size of hanging-wall catchments, this pattern may be primarily attributed to paleoclimatic drivers in the surrounding mountain ranges that promoted high effective discharge and low sediment/water ratios, conditions favorable for high erosion rates in headwater areas (Mack et al., 2012). Changes in such conditions with climate shifts, such as glacial-interglacial transitions, are well-documented (Bull, 1991), and have been invoked for similar coarsening trends observed in rift-fill packages elsewhere in New Mexico (Koning et al., 2002).

QUATERNARY HISTORY

(POST-PALOMAS FORMATION)

Deposition of the Palomas Formation ceased ~0.8 Ma (Lozinsky and Hawley, 1986a, b; Mack et al., 1993, 1998), after which the Rio Grande and its tributaries began incising and gradually forming the modern network of arroyos and river valleys. Valley-margin deposits are typified by inset stream terraces and, in places, alluvial fans graded to those deposits. Valley-bottom deposits include low-lying terraces adjacent to modern stream courses. Topographically higher deposits are typically middle to late Pleistocene in age. Exposed valley-bottom deposits are considered Holocene on the basis of radiocarbon dates discussed below, but at depth these deposits are likely latest Pleistocene.

In general, Pleistocene and Holocene deposits in the Williamsburg quadrangle formed during periods of

climatic fluctuation related to glacial-interglacial cycles. One model developed for the formation of stream terraces in the southern Rio Grande rift proposes that terrace formation occurred over three stages: (1) the Rio Grande and the lower valleys of its tributaries incised during full glacial conditions; (2) aggradation occurred during the transition to interglacial intervals due to decreased water-to-sediment ratios; and (3) stability ensued for the remainder of interglacial intervals (Gile et al., 1981).

Terrace surfaces underlain by sand and gravel deposited by the Rio Grande represent former base levels of the river, some of which are up to 45+ m above its modern grade. A component of very fine- to fine-grained sand once occupying the terrace surfaces has been deflated by southwesterly winds and deposited on the lee sides of ridges 0.5-3 km east of the modern Rio Grande. The remaining, non-eroded terrace deposits typically comprise thin strath terraces (≤ 5 m thick). However, certain deposits (Qtr1 and Qtr4) approach 10 m in thickness and represent notable periods of river aggradation. Rio Grande deposits are distinguished by an abundance of exotic clasts, particularly quartzite. They also have imbricated clasts that indicate southward paleocurrents (Fig. 22; Appendix C) and contain lenses of well-sorted, quartzose sand. An ash collected from a thin exposure of the Qtr5 Rio Grande terrace deposit along King Arroyo at 284425 mE/3658177 mN is geochemically similar to the 640 ka Lava Creek B ash (N. Dunbar, personal communication, 2015). Located 45 m above modern grade, this deposit provides an approximate mainstem Rio Grande incision rate of 70 m/myr since the mid-Pleistocene. However, this rate does not integrate ages of younger, inset deposits

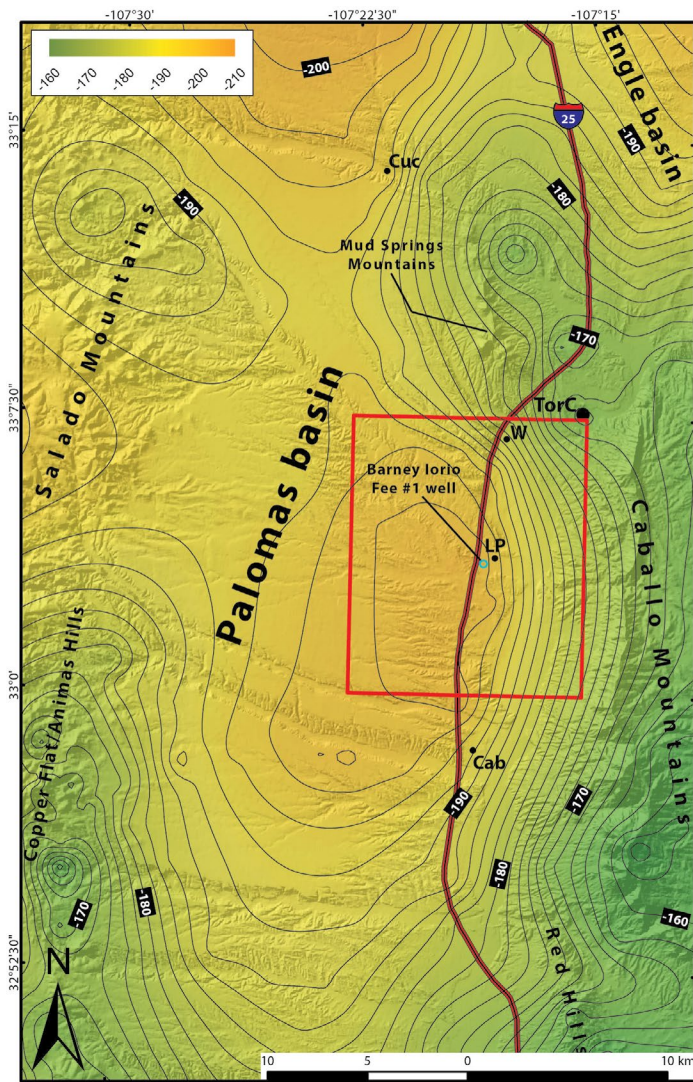


Figure 21. Complete Bouguer-anomaly gravity map of Palomas basin and surrounding uplifts. Williamsburg quadrangle is outlined in red. Note that deepest part of the basin coincides with a low gravity anomaly located southwest of Las Palomas (LP) and the Barney Iorio Fee #1 well (blue circle). Data from Kucks et al. (2001). Reduction density = 2.67 gm/cc; sea level datum. Contour interval = 2 mGal. Abbreviations for local communities (black dots) as in Figure 1.

that currently lack age constraints (i.e. Qtr4-1). Mack et al. (2011) used radiocarbon dates from charcoal, bulk organic matter, and shells to constrain deposition of younger Rio Grande terraces to >12.4 ka (Qtr3), ~8-5.3 ka (Qtr2), and ~0.8-0.3 ka (Qtr1).

Five correlated Palomas Creek terrace deposits (Qtp units) are each 3-5 m thick and can be considered strath terraces. The straths/treads of these terraces lie 7-47 m above modern grade. Older terraces are marked by a greater degree of surface varnish on clasts (up to 80%). Surface erosion hampers the use of soil development to correlate terraces, but where preserved the terrace soils exhibit relatively strong calcium carbonate accumulation (e.g. stage II or greater carbonate morphology), consistent

with long-stable surfaces (Gile et al., 1966; Birkeland, 1999). Terrace deposits flanking Palomas Creek and other Rio Grande tributaries west of the river are distinguished by poor sorting and a high proportion of volcanic clasts. Terrace deposits east of the Rio Grande are likewise poorly sorted but are dominated by clasts of Paleozoic carbonates and Proterozoic granite, and lack cementation observed in Qtp strata. Correlations between tributary and mainstem Rio Grande terraces are confounded by the presence of thin fluvial gravels of the Palomas Formation that have been exhumed in many



Figure 22. Pleistocene Rio Grande terrace deposit (Qtr4). Rio Grande terrace deposits are distinguished from Palomas Formation piedmont gravels by the presence of numerous exotic clasts, particularly quartzite. They also contain a higher proportion of cobbly gravel fills than axial-fluvial facies of the Palomas Formation, and commonly feature clast imbrication (arrows) suggesting paleoflow toward the south. Tape is 2 m tall.

locations (especially in Kelly Canyon). Such intervals were recognized in early mapping of the Palomas basin (Harley, 1934), and resemble younger terrace deposits because they have similar textures and appear topographically inset. Furthermore, soil development could be similar on exhumed Palomas Formation gravels compared to post-0.8-Ma terrace surfaces at the same geomorphic level. Adequate exposure in some localities permits a relatively certain interpretation. However, Qtp1b is clearly inset just beneath Qtr4 at the mouth of Palomas Creek, demonstrating that tributary terraces predate the Holocene.

Younger valley-floor deposits lie well below terrace deposits, flanking arroyos throughout the study area. Like terraces, surface characteristics of these deposits imply relative age, with stage II carbonate morphology observed in soils capping older deposits (Qay) and bar-and-swale topography better preserved in younger deposits that mostly lack well-developed soils (Qah). However, like terrace deposits, surface erosion complicates the use of soil development to infer deposit age. These inset deposits are also associated with alluvial fans (units Qfah, Qfay) that emanate from side gullies and ravines, commonly interfingering with or prograding over deposits associated with the trunk stream (Fig. 23). Modern alluvium (Qam) in ephemeral drainages is marked by sandy pebble to cobble gravel forming pronounced bar-and-swale topography.

Radiocarbon ages acquired in Cañada Honda, a Rio Grande tributary, during the course of mapping demonstrate that valley-bottom deposits span the Holocene and extend into the latest Pleistocene (Table 3; Appendix D). Figure 24 shows radiocarbon sample locations. Based on these ages, younger alluvium (Qay) pre-dating Qah represents backfilling of tributary valleys ~600 cal yr BP (sample WS-204, Table 3). Qfay was aggrading at distal positions in the late Holocene, based on the ~2500 cal yr BP age of sample WS-203 (Table 3). An interval 2.7-3.0 m below the surface (unit D of Figure 23) of a more proximal alluvial fan deposit (Qfay), overlying a paleosol with stage II carbonate morphology, returned an age of ~11000 cal yr BP. The fan sediment below the paleosol, which is finer grained than the Holocene material above, is thus likely latest Pleistocene in age. This fan almost certainly once interfingered with unit Qay, based on similar geomorphic levels in the valley, indicating a general Holocene to latest Pleistocene age for both Qfay and associated Qay deposits. The age of sample WS-204 is broadly similar to radiocarbon ages

obtained from Rio Grande terrace deposit Qtr1 (terrace III dated by Mack et al., 2011). These results are further discussed in Jochems and Koning (2015).

STRUCTURAL GEOLOGY

The Williamsburg quadrangle features four major faults: the Mud Springs, Williamsburg, Hot Springs, and Caballo faults (Fig. 2). Other normal faults are observed in the southwest and southeast corners of the quadrangle.

The northernmost structure in the quadrangle is the west- to southwest-down Mud Springs fault, which wraps around the western foot of the Mud Springs Mountains (Kelley and Silver, 1952; Machette, 1987; Machette et al., 1998). Its exact location has been inconsistently mapped, with previous workers showing a discontinuous structure differing in location by up to ~2 km (Maxwell and Oakman, 1990; Foster, 2009). Although a lack of geomorphic expression complicates mapping of the fault, we have confirmed two definite southwest-down fault strands northeast of the debris dam in lower Mud Springs Canyon (Koning and Jochems, unpublished data). From these exposures, it is evident that the Mud Springs fault continues southeast under Holocene-latest Pleistocene alluvium in lower Mud Springs Canyon. Northeastward roll-over in Palomas Formation bedding, observed adjacent to I-25 (285863 mE/3667325 mN), can be reasonably attributed to deformation along this structure.

The northwest-striking, southwest-down Williamsburg fault is located south of Truth or Consequences and east of the Rio Grande, where it forms fault scarps up to 6.4 m high (Machette et al., 1998). Surface ruptures along a scarp of the Williamsburg fault near 289000 mE/3664626 mN were dated at ~5-2 ka based on charcoal collected from displaced colluvial beds; these ruptures average 2-3 m of vertical offset per event (Foley et al., 1988). The southern segment of the Williamsburg fault juxtaposes eastern piedmont facies of the Palomas Formation in the footwall with younger fan gravel (middle to late Pleistocene age) in the hanging wall. The southern terminus of the Williamsburg fault is not well exposed and thus its location is uncertain. It is possible, however, that the southern end of the fault may swing to the east, truncating the Hot Springs fault and intersecting the Caballo fault just east of the quadrangle, as suggested by previous workers (e.g., Kelley and Silver, 1952; Seager and Mack, 2003). If the latter scenario is true, the fault likely follows the course of one of two arroyos at the southern

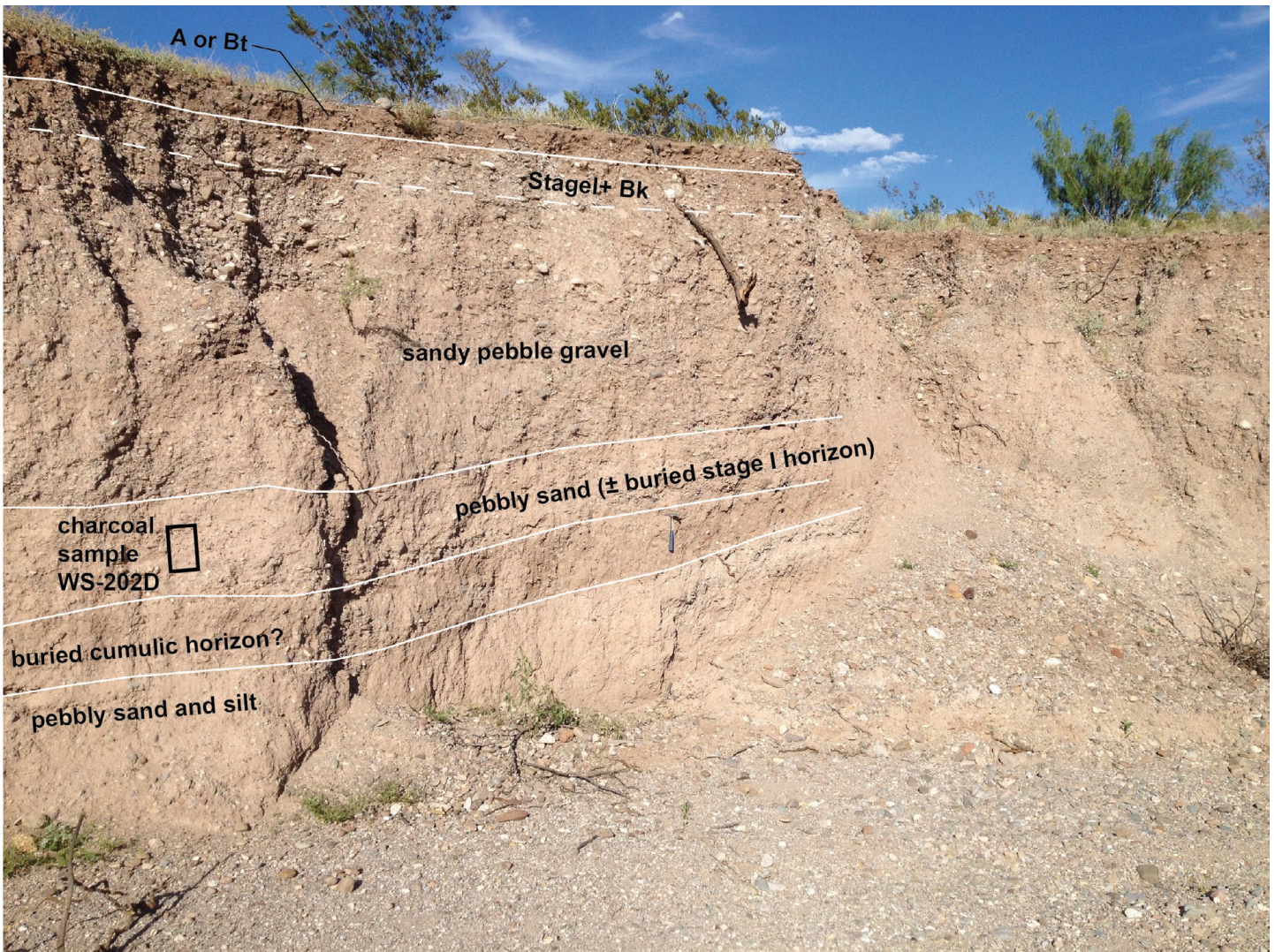


Figure 23. Younger alluvial fan (Q_{fay}) deposit in Cañada Honda. Charcoal sample WS-202D was radiocarbon dated at 11100-10800 cal yr BP (2σ calibration). Unit is characterized by poorly sorted, pebbly sand and gravel with common stage I-II carbonate morphology in both surface and buried soils. Surface soils may also feature illuviated clay (Bt horizons).

Table 3. Summary radiocarbon geochronology for Cañada Honda and Las Animas Creek study areas.

Sample #	Deposit	Material	UTM N ^a	UTM E ^a	Conventional Age (¹⁴ C yr BP ₁₉₅₀) ^b	2σ Calibrated Age Range (cal yr BP ₁₉₅₀) ^c
WS-202-D1	Q _{fay}	charcoal	3665387	284572	9590 ± 30	11106-10763 (1.000)
WS-203	Q _{fay}	charcoal	3665180	284659	2480 ± 30	2390-2385 (0.004), 2723-2432 (0.996)
WS-204	Q _{yai}	charcoal	3665150	284689	540 ± 30	634-596 (0.308), 561-514 (0.692)

^aCoordinates given in UTM Zone 13S, NAD83.

^bConservative error of ±30 ¹⁴C yr BP1950 is given for all samples due to 1σ < ±30 ¹⁴C yr BP1950 in each case.

^c2σ calibrated age ranges calculated as relative probability using Calib 7.1 (Stuiver and Reimer, 1993) and IntCal13 calibration curve of Reimer et al. (2013).

(1976) estimated total displacement across the Hot Springs fault system between 610 and 2740 m in the northern Caballo Mountains, whereas Lozinsky (1986) assigned the fault a minimum displacement of 1220 m at the wing dam of Elephant Butte Reservoir north of the quadrangle. The segment of the Hot Springs fault exposed in the quadrangle is clearly its southern terminus, regardless of whether or not it is truncated by the Williamsburg fault (see above), because exposures of Proterozoic basement step ~800 m east between the quadrangle and the footwall of the Caballo fault.

Together with the Hot Springs fault, the north-striking Caballo fault forms the major range-bounding structure of the Caballo uplift. The 400-m-long section that crosses the extreme southeast corner of the Williamsburg quadrangle has been called the Northern Caballo fault (e.g., Machette, 1987; Foley et al., 1988; Seager and Mack, 2003). Maximum displacement along this west-down structure is estimated at ~6.5 km based on gravity data (Keller and Cordell, 1983; Gilmer et al., 1986) and exposed thicknesses of Precambrian and Phanerozoic packages in the Caballo Mountains (Seager and Mack, 2003). Most of the activity along the Northern Caballo fault appears to predate the Palomas Formation. This inference arises from the observation that the Northern Caballo fault borders the deepest part of the Palomas basin (Fig. 21; Gilmer et al., 1986), yet intervals of the Palomas Formation (particularly units QT_{pwl} and QT_{pwm}) thicken northward away from this structurally deep area.

Even if its slip rate has waned since the Miocene, the Northern Caballo fault is still an active structure. Foley and others (1988) estimated that the most recent surface rupture event of this fault occurred ~4-5 ka based on soil development in faulted and unfaulted colluvium at a trenched scarp south of the quadrangle. They calculated an average of 1.25-2 m of vertical offset per rupture event.

In addition to the major structures described above, several other normal faults are observed in the quadrangle. A series of mostly west-down normal faults were mapped in the southeast corner of the quadrangle east of the Rio Grande and west of the Northern Caballo fault. At least one of these faults offsets deposits that are likely middle-late Pleistocene in age. Apparent vertical throw (i.e. displacement observed in outcrop) is typically <10 m on these faults, yet they may be traced as far as ~4.3 km or more. They are synthetic to the Northern Caballo fault and may or may not be physically linked to it. In the



Figure 25. Brecciated volcanic clasts in strongly silicified Santa Fe Group strata (Tss) forming a sliver between two strands of the Hot Springs fault. Individual clasts may be fractured; reddish matrix likely derived hue from abundant clays. Hammer is 28 cm long.

southwest corner of the quadrangle, a north-striking, west-down fault forms scarps that parallel southerly orientated arroyos transverse to eastward-flowing drainages typical of the Palomas basin. This structure belongs to the “unnamed faults west of Caballo Reservoir” group of Machette et al. (1998), who assigned it a maximum age of <750 ka based on offset of the Cuchillo surface.

HYDROGEOLOGY

Despite the proximity of two of New Mexico’s largest reservoirs, Elephant Butte and Caballo (first and fifth largest, respectively), water for most practical purposes in the Palomas basin is pumped from the ground. Domestic, municipal, and stock wells typically penetrate an artesian aquifer recharged by precipitation in the Animas-Salado uplifts. To a lesser extent, there may be recharge via flash flooding in ephemeral drainages during the summer monsoons (Murray, 1959). Locally, aquifers exist in gravelly pre-Palomas Formation Santa Fe Group beds, medium- to coarse-grained Palomas Formation strata, or Pleistocene to Holocene alluvium (e.g., Murray, 1959; Cox and Reeder, 1962; Davie and Spiegel, 1967). As discussed above and in Appendix A, these units contain lithofacies with varying textures and degrees of cementation that may either facilitate or impede groundwater flow and infiltration. The following discussion examines the aquifer-hosting potential of basin-fill units in the Williamsburg quadrangle and relates these inferences to previous hydrogeologic studies.

Sparsely exposed in the quadrangle, Santa Fe Group

strata predating the Palomas Formation (Trv, correlated to the Rincon Valley Formation of Seager and others, 1971) nevertheless holds important implications for groundwater flow. Piedmont facies of the Rincon Valley Formation (Trvpw) could transmit groundwater where they consist of laterally extensive channel fills with relatively low cementation. Such beds are estimated to comprise $\leq 25\%$ of the unit. In outcrop, Rincon Valley basin-floor facies (Trvbf) consist of very fine- to medium-grained sand and clayey-silty sand with few ($\leq 5\%$) pebbles. This unit includes mud and clay with sparse interbeds of sand and fine gravel in the Barney Iorio Fee #1 well. Only two saturated intervals within Trvbf in the Barney Iorio well were reported in a lithologic log completed in 1941. Although cementation is sparse in this unit, its permeability is likely poor due to the prevalence of fine-grained (especially clayey) beds, which become more abundant to the south as the unit transitions into a playa facies (Seager and Mack, 2003; Koning et al., 2015). Therefore, we infer that Trvbf is probably a poor to moderate aquifer in the northern quadrangle, but becomes increasingly less permeable to the south and transitions to an aquitard under Caballo Reservoir.

Most water-bearing units in the Palomas Formation belong to the western-derived piedmont (QTpw) or axial-fluvial facies (QTpa), as units of the eastern piedmont of the Palomas Formation (QTpe and QTper) are generally too cemented to host extensive aquifers. Additionally, unit QTpef is likely too fine-grained to transmit appreciable amounts of groundwater. The upper western piedmont units (QTpwuc, QTpwu, and QTpwt) lie above the zone of saturation throughout the quadrangle.

The aquifer-hosting potential of the middle and lower western piedmont units may then be distinguished on the basis of texture and continuity of coarser-grained beds (Koning et al., 2015). Although mostly fine-grained, the middle western piedmont (QTpwm) contains up to 20% tongues of pebbly sand and pebble gravel with little to no interstitial clay (Fig. 26). Dense vegetation growing along such beds, observed near the Williamsburg I-25 interchange, suggest that some sand and gravel beds in this unit are saturated. In addition, several wells in Palomas Creek (including the Barney Iorio Fee #1 well) penetrate intervals of QTpwm that host groundwater. Thick, fine-grained strata in this unit likely acts as aquitards, and the degree of connectivity in the coarse channel fills will influence their aquifer potential. A deflection in the otherwise southeast-sloping water table

surface, as interpreted by Murray (1959), near the mouth of Palomas Creek suggests a truncation of QTpwm or QTpwl channel-fill connectivity below the eastern part of Palomas Creek. Seeps on the north side of Palomas Canyon west of I-25 may reflect such a pattern.

The lower western piedmont (QTpwl) consists of relatively abundant, coarse channel fills interbedded with subordinate, light brown, extra-channel deposits composed of clay, silt, and very fine- to medium-grained sand. The channel fills are composed of clast-supported, imbricated, sandy gravel that lacks fine-grained matrix sediment and is not generally cemented (although the lowermost 1-2 m is well-cemented in exposures west of I-25 along the northern quadrangle border). This unit thickens toward the northern edge of the quadrangle and its texture implies that it could be an ideal aquifer in many locations. However, a 1941 lithologic log from the Barney Iorio Fee #1 well did not report any water-bearing intervals from QTpwl. Below this unit lies the transitional base of the western Palomas Formation piedmont facies (QTpwt), observed in cuttings of the Barney Iorio Fee #1 well and Truth or Consequences city wells 7 and 8. There, QTpwt consist of clay, silt, and fine-grained sand with subordinate channel fills. Water was reported from a 1 m interval in this unit in the Barney Iorio well (540-543 ft depth).

In addition to coarse channel fills in QTpwl and in QTpwm, sandy gravel and well-sorted sand of the axial-fluvial facies (QTpa) exhibit strong aquifer-hosting potential, particularly west of the Rio Grande where cementation is not commonly observed. Axial floodplain mudstones and clay facies may locally act as aquitards, as could finer-grained facies in QTpwm tongues. This hydrogeologic relationship is observed in several wells along Palomas Creek (data from NM Office of the State Engineer, 2015).

Finally, Pleistocene and Holocene valley-floor units may also locally host aquifers. Gravelly or sandy channel fills in historical alluvium (Qah) near the northwestern corner of the quadrangle may be saturated in places along Palomas Creek. Elsewhere, coarse valley-floor units can be expected to transmit runoff, mostly during the summer months of the monsoon season, to underlying Palomas Formation aquifers. Alternatively, they may locally receive groundwater discharge from buried Palomas Formation aquifers (Davie and Spiegel, 1967).

ACKNOWLEDGEMENTS

Mapping of the Williamsburg quadrangle was funded by the STATEMAP program, which is jointly supported by the U.S. Geological Survey and the New Mexico Bureau of Geology and Mineral Resources (NMBGMR). We thank Dr. J. Michael Timmons of NMBGMR for logistical support. We are grateful for land access provided by Las Palomas Land & Cattle Company (caretakers Andy Anderson, Jonathan Beaty, and John Walker), Julie Durham, and Twister Smith. Dave Parmelee and Alanna Robison helped with paleocurrent measurements, clast counts, and unit descriptions. Dr. Greg Mack and Dr. Peter Mozley provided valuable field discussions on basin architecture and pedogenic processes. Dr. Nelia Dunbar (NMBGMR) analyzed the ash collected along King Arroyo. Dr. John Hawley, NMBGMR emeritus, gave profound insight into basin-fill stratigraphy and hydrogeology and generously shared his many resources with us. Finally, we are grateful to Dr. William Seager for his thorough review of this map and report.

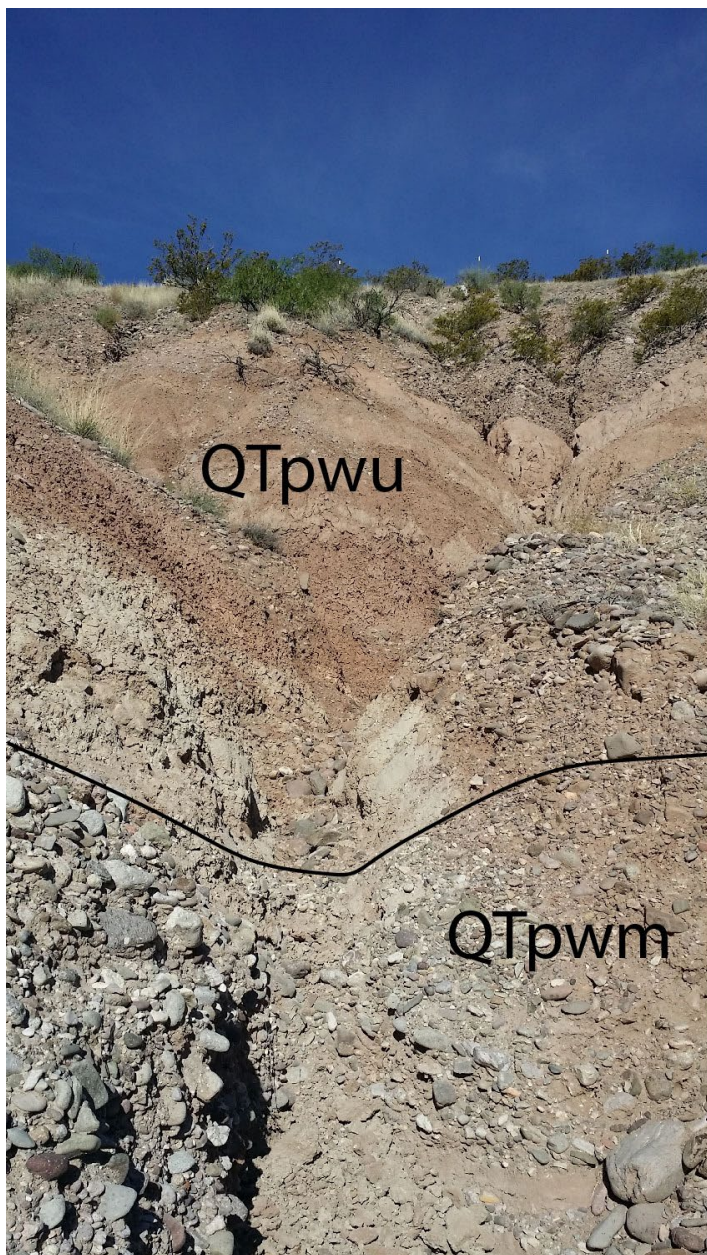


Figure 26. Channel-fill gravel at top of middle western piedmont facies (QTpwm). Though rare, such gravels are commonly extensive over 50+ m and could form important, transmissive units for groundwater because they lack clays and other fine material in their matrices. Exposure in I-25 roadcut north of Las Palomas.

REFERENCES

- Amato, J.M., and Becker, T., 2012, Proterozoic rocks of the Caballo Mountains and Kingston mining district: U-Pb geochronology and correlations within the Mazatzal province of southern New Mexico, *in* Lucas, S.G., McLemore, V.T., Lueth, V.W., Spielmann, J.A., and Krainer, K., eds., *Geology of the Warm Springs Region: New Mexico Geological Society Guidebook 63*, p. 227–234.
- Bachman, G.O., and Mehnert, H.H., 1978, New K-Ar dates and late Pliocene to Holocene geomorphic history of the Rio Grande region, New Mexico: *Geological Society of America Bulletin*, v. 89, no. 2, p. 283–292.
- Bauer, P.W., and Lozinsky, R.P., 1986, Proterozoic geology of supracrustal and granitic rocks in the Caballo Mountains, southern New Mexico, *in* Clemons, R.E., King, W.E., and Mack, G.H., eds., *Truth or Consequences region: New Mexico Geological Society Guidebook 37*, p. 143–149.
- Birkeland, P.W., 1999, *Soils and geomorphology*: Oxford University Press, New York, 448 p.
- Birkeland, P.W., Machette, M.N., and Haller, K.M., 1991, Soils as a tool for applied Quaternary geology: Utah Geological and Mineral Survey Miscellaneous Publication 91-3, 63 p.
- Bruno, L., and Chafetz, H.S., 1988, Depositional environments of the Cable Canyon Sandstone: a mid-Ordovician sandwave complex from southern New Mexico, *in* Mack, G.H., Lawton, T.F., and Lucas, S.G., eds., *Guidebook of Cretaceous and Laramide tectonic evolution of southwestern New Mexico: New Mexico Geological Society Guidebook 39*, p. 127–134.
- Bull, W.B., 1991, *Geomorphic responses to climate change*: Oxford University Press, Oxford, 326 p.
- Chapin, C.E., and Cather, S.M., 1994, Tectonic setting of the axial basins of the northern and central Rio Grande rift, *in* Keller, G.R. and Cather, S.M. eds., *Basins of the Rio Grande Rift: Structure, Stratigraphy, and Tectonic Setting: Geological Society of America Special Paper 291*, p. 5–25.
- Condie, K.C., and Budding, A.J., 1979, Geology and geochemistry of Precambrian rocks, central and south-central New Mexico: New Mexico Bureau of Mines and Mineral Resources Memoir 35, 60 p.
- Connell, S.D., 2008, Refinements to the stratigraphic nomenclature of the Santa Fe Group, northwestern Albuquerque Basin, New Mexico: *New Mexico Geology*, v. 30, p. 14–35.
- Cox, E.R., and Reeder, H.O., 1962, Ground-water conditions in the Rio Grande valley between Truth or Consequences and Las Palomas, Sierra County, New Mexico: New Mexico State Engineer Technical Report 25, 47 p.
- Davie, W., Jr., and Spiegel, Z., 1967, Geology and water resources of Las Animas Creek and vicinity, Sierra County, New Mexico: New Mexico State Engineer Hydrographic Survey Report, 44 p.
- Foley, L.L., LaForge, R.C., and Piety, L.A., 1988, Seismotectonic study for Elephant Butte and Caballo Dams, Rio Grande Project, New Mexico: U.S. Bureau of Reclamation Seismotectonic Report 88-9, 60 p.
- Foster, R., 2009, Basin-fill architecture of the Pliocene-Lower Pleistocene Palomas Formation adjacent to the intrabasinal Mud Springs Mountains, southern Rio Grande rift [Unpublished M.S. thesis]: Las Cruces, New Mexico State University, 81 p.
- Gile, L.H., Peterson, F.F., and Grossman, R.B., 1966, Morphological and genetic sequences of carbonate accumulation in desert soils: *Soil Science*, v. 101, p. 347–360.
- Gile, L.H., Hawley, J.W., and Grossman, R.B., 1981, Soils and geomorphology in the Basin Range area of southern New Mexico—Guidebook to the Desert Project: New Mexico Bureau of Mines and Mineral Resources Memoir 39, 222 p.
- Gilmer, A.L., Mauldin, R.A., and Keller, G.R., 1986, A gravity study of the Jornada del Muerto and Palomas basins, *in* Clemons, R.E., King, W.E., Mack, G.H., and Zidek, J., eds., *Truth or Consequences region: New Mexico Geological Society Guidebook 37*, p. 131–134.
- Gordon, C.H., 1910, Sierra and central Socorro Counties, *in* Lindgren, W., Graton, L.C., and Gordon, C.H., eds., *The Ore Deposits of New Mexico: U.S. Geological Survey Professional Paper 68*, p. 213–285.

- Gordon, C.H., and Graton, L.C., 1907, Lower Paleozoic formations in New Mexico: *Journal of Geology*, v. 15, p. 91–92.
- Grundwald, T.W., 1990, Depositional environments and paleosols of the Palomas Formation (Plio-Pleistocene), Palomas Basin, southern Rio Grande rift [Unpublished M.S. thesis]: Las Cruces, New Mexico State University, 95 p.
- Harley, G.T., 1934, The geology and ore deposits of Sierra County, New Mexico: New Mexico Bureau of Mines and Mineral Resources Bulletin 10, 220 p.
- Hawley, J.W., compiler, 1978, Guidebook to Rio Grande rift in New Mexico and Colorado: New Mexico Bureau of Geology and Mineral Resources Circular 163, 241 p.
- Ingram, R.L., 1954, Terminology for the thickness of stratification and parting units in sedimentary rocks: *Geological Society of America Bulletin*, v. 65, p. 937–938.
- Izett, G.A., Obradovich, J.D., Naeser, C.W., and Cebula, G.T., 1981, Potassium-argon and fission-track zircon of Cerro Toledo rhyolite tephra in the Jemez Mountains, New Mexico: U.S. Geological Survey Professional Paper 1199-D, 37–43 p.
- Jochems, A.P., 2015, Geologic map of the Williamsburg NW 7.5-minute quadrangle, Sierra County, New Mexico: New Mexico Bureau of Geology and Mineral Resources Open-file Geologic Map OF-GM 251, scale 1:24,000.
- Jochems, A.P., and Koning, D.J., 2015, Holocene stratigraphy and a preliminary geomorphic history for the Palomas basin, south-central New Mexico: *New Mexico Geology*, v. 37, p. 77–88.
- Keller, G.R., and Cordell, L., 1983, Bouguer gravity anomaly map of New Mexico: National Oceanic and Atmospheric Administration, Boulder, Colorado, Scientific Map Series.
- Kelley, V.C., 1977, Geology of the Albuquerque Basin, New Mexico: New Mexico Bureau of Mines and Mineral Resources Memoir 33, 60 p.
- Kelley, V.C., and Silver, C., 1952, Geology of the Caballo Mountains: University of New Mexico, Publications in Geology no. 4, 286 p.
- Koning, D.J., Connell, S.D., Pazzaglia, F.J., and McIntosh, W.C., 2002, Redefinition of the Ancha Formation and Pliocene-Pleistocene deposition in the Santa Fe embayment, north-central New Mexico: *New Mexico Geology*, v. 24, no. 3, p. 75–87.
- Koning, D.J., Jochems, A.P., and Cikoski, C.T., 2015, Geologic map of the Skute Stone Arroyo 7.5-minute quadrangle, Sierra County, New Mexico: New Mexico Bureau of Geology and Mineral Resources Open-file Geologic Map OF-GM 252, scale 1:24,000.
- Koning, D.J., Jochems, A.P., Morgan, G.S., Lueth, V., and Peters, L., 2016, Stratigraphy, gravel provenance, and age of early Rio Grande deposits exposed 1-2 km northwest of downtown Truth or Consequences, New Mexico, *in* Frey, B.A., Karlstrom, K.E., Lucas, S.G., Williams, S., Zeigler, K., McLemore, V., and Ulmer-Scholle, D.S., eds., *The Geology of the Belen Area: New Mexico Geological Society Guidebook 67*, p. 459–478.
- Kucks, R.P., Hill, P.L., and Heywood, C.E., 2001, New Mexico aeromagnetic and gravity maps and data: A web site for distribution of data: U.S. Geological Survey Open-File Report 01-0061, <http://pubs.usgs.gov/of/2001/ofr-01-0061/html/newmex.htm>.
- Leeder, M.R., Mack, G.H., and Salyards, S.L., 1996, Axial-transverse fluvial interactions in half-graben—Plio-Pleistocene Palomas Basin, southern Rio Grande rift, New Mexico, USA: *Basin Research*, v. 12, p. 225–241.
- Lozinsky, R.P., 1986, Geology and late Cenozoic history of the Elephant Butte area, Sierra County, New Mexico: New Mexico Bureau of Mines and Mineral Resources Circular 187, 39 p.
- Lozinsky, R.P., and Hawley, J.W., 1986a, The Palomas Formation of south-central New Mexico—A formal definition: *New Mexico Geology*, v. 8, no. 4, p. 73–82.
- Lozinsky, R.P., and Hawley, J.W., 1986b, Upper Cenozoic Palomas Formation of south-central New Mexico, *in* Clemons, R.E., King, W.E., Mack, G.H., and Zidek, J., eds., *Truth or Consequences region: New Mexico Geological Society Guidebook 37*, p. 239–247.
- Machette, M.N., 1987, Preliminary assessment of Quaternary faulting near Truth or Consequences,

- New Mexico: U.S. Geological Survey Open-File Report 87-652, 41 p.
- Machette, M.N., Personius, S.F., Kelson, K.I., Haller, K.M., and Dart, R.L., 1998, Map and data for Quaternary faults and folds in New Mexico: U.S. Geological Survey Open-file Report 98-521, 451 p.
- Mack, G.H., 2004, The Cambro-Ordovician Bliss and lower Ordovician El Paso formations, southwestern New Mexico and west Texas, *in* Mack, G.H. and Giles, K.A., eds., *The Geology of New Mexico: A Geologic History*: New Mexico Geological Society Special Publication 11, p. 35–44.
- Mack, G.H., and James, W.C., 1992, Calcic paleosols of the Plio-Pleistocene Camp Rice and Palomas Formations, southern Rio Grande rift: *Sedimentary Geology*, v. 77, p. 89–109.
- Mack, G.H., and Leeder, M.R., 1999, Climatic and tectonic controls on alluvial-fan and axial-fluvial sedimentation in the Plio-Pleistocene Palomas half graben, southern Rio Grande Rift: *Journal of Sedimentary Research*, v. 69, p. 635–652.
- Mack, G.H., and Seager, W.R., 1990, Tectonic control on facies distribution of the Camp Rice and Palomas Formations (Pliocene-Pleistocene) in the southern Rio Grande rift: *Geological Society of America Bulletin*, v. 102, no. 1, p. 45–53.
- Mack, G.H., Salyards, S.L., and James, W.C., 1993, Magnetostratigraphy of the Plio-Pleistocene Camp Rice and Palomas Formations in the Rio Grande rift of southern New Mexico: *American Journal of Science*, v. 293, p. 49–77.
- Mack, G.H., James, W.C., and Salyards, S.L., 1994, Late Pliocene and early Pleistocene sedimentation as influenced by intrabasinal faulting, southern Rio Grande rift, *in* Keller, G.R. and Cather, S.M., eds., *Basins of the Rio Grande Rift: Structure, Stratigraphy, and Tectonic Setting*: Geological Society of America Special Paper 291, p. 257–264.
- Mack, G.H., Salyards, S.L., McIntosh, W.C., and Leeder, M.R., 1998, Reversal magnetostratigraphy and radioisotopic geochronology of the Plio-Pleistocene Camp Rice and Palomas Formations, southern Rio Grande rift, *in* Mack, G.H., Austin, G.S., and Barker, J.M., eds., *Las Cruces country II: New Mexico Geological Society Guidebook 49*, p. 229–236.
- Mack, G.H., Cole, D.R., and Treviño, L., 2000, The distribution and discrimination of shallow, authigenic carbonate in the Pliocene-Pleistocene Palomas Basin, southern Rio Grande rift: *Geological Society of America Bulletin*, v. 112, no. 5, p. 643–656.
- Mack, G.H., Leeder, M., and Salyards, S.L., 2002, Temporal and spatial variability of alluvial-fan and axial-fluvial sedimentation in the Plio-Pleistocene Palomas half graben, southern Rio Grande rift, New Mexico, USA, *in* Renault, R.W. and Ashley, G.M., eds., *Sedimentation in Continental rifts*: SEPM, Special Publication 73, p. 165–177.
- Mack, G.H., Seager, W.R., Leeder, M.R., Perez-Arlucea, M., and Salyards, S.L., 2006, Pliocene and Quaternary history of the Rio Grande, the axial river of the southern Rio Grande rift, New Mexico, USA: *Earth-Science Reviews*, v. 77, p. 141–162.
- Mack, G.H., Leeder, M.R., and Carothers-Durr, M., 2008, Modern flood deposition, erosion, and fan-channel avulsion on the semiarid Red Canyon and Palomas Canyon alluvial fans in the southern Rio Grande rift, New Mexico, U.S.A.: *Journal of Sedimentary Research*, v. 78, no. 7, p. 432–442, doi: 10.2110/jsr.2008.050.
- Mack, G.H., Dunbar, N., and Foster, R., 2009, New sites of 3.1-Ma Pumice beds in axial-fluvial strata of the Camp Rice and Palomas Formations, southern Rio Grande rift: *New Mexico Geology*, v. 31, p. 31–37.
- Mack, G.H., Leeder, M., Perez-Arlucea, M., and Durr, M., 2011, Tectonic and climatic controls on Holocene channel migration, incision and terrace formation by the Rio Grande in the Palomas half graben, southern Rio Grande rift, USA: *Sedimentology*, v. 58, no. 5, p. 1065–1086, doi: 10.1111/j.1365-3091.2010.01195.x.
- Mack, G.H., Foster, R., and Tabor, N.J., 2012, Basin architecture of Pliocene-lower Pleistocene alluvial-fan and axial-fluvial strata adjacent to the Mud Springs and Caballo Mountains, Palomas half graben, southern Rio Grande rift, *in* Lucas, S.G., McLemore, V.T., Lueth, V.W., Spielmann, J.A., and Krainer, K., eds., *Geology of the Warm Springs Region: New Mexico Geological Society Guidebook 63*, p. 431–446.

- Mason, J.T., 1976, The geology of the Caballo Peak quadrangle, Sierra County, New Mexico [Unpublished M.S. thesis]: Albuquerque, University of New Mexico, 131 p.
- Maxwell, C.H., and Oakman, M.R., 1990, Geologic map of the Cuchillo quadrangle, Sierra County, New Mexico: United State Geological Survey Geologic Quadrangle Map GQ-1686, scale 1:24,000.
- McCraw, D.J., and Love, D.W., 2012, An overview and delineation of the Cuchillo geomorphic surface, Engle and Palomas Basins, New Mexico, *in* Lucas, S.G., McLemore, V.T., Lueth, V.W., Spielmann, J.A., and Krainer, K., eds., *Geology of the Warm Springs Region: New Mexico Geological Society Guidebook 63*, p. 491–498.
- Morgan, G.S., and Lucas, S.G., 2012, Cenozoic vertebrates from Sierra County, southwestern New Mexico, *in* Lucas, S.G., McLemore, V.T., Lueth, V.W., Spielmann, J.A., and Krainer, K., eds., *Geology of the Warm Springs Region: New Mexico Geological Society Guidebook 63*, p. 525–540.
- Morgan, G.S., Sealey, P.L., and Lucas, S.G., 2008, Late Pliocene (late Blancan) vertebrate faunas from Pearson Mesa, Duncan Basin, southwestern New Mexico and southeastern Arizona: *New Mexico Museum of Natural History and Science Bulletin 44*, p. 141–188.
- Morgan, G.S., Sealey, P.L., and Lucas, S.G., 2011, Pliocene and early Pleistocene (Blancan) vertebrates from the Palomas Formation in the vicinity of Elephant Butte Lake and Caballo Lake, Sierra County, southwestern New Mexico: *New Mexico Museum of Natural History and Science Bulletin 53*, p. 664–736.
- Mozley, P.S., and Davis, J.M., 2005, Internal structure and mode of growth of elongate calcite concretions: Evidence for small-scale, microbially induced, chemical heterogeneity in groundwater: *Geological Society of America Bulletin*, v. 117, no. 11-12, p. 1400–1412.
- Muehlberger, W.R., Hedge, C.E., Denison, R.E., and Marvin, R.R., 1966, Geochronology of the mid-continent region, United States, part 3—southern areas: *Journal of Geophysical Research*, v. 71, p. 5409–5426.
- Munsell Color, 2009, Munsell soil color book: X-Rite, Grand Rapids, MI.
- Murray, C.R., 1959, Ground-water conditions in the nonthermal artesian-water basin south of Hot Springs, Sierra County, New Mexico: New Mexico State Engineer Technical Report 10, 33 p.
- New Mexico Bureau of Geology and Mineral Resources, 2003, Geologic map of New Mexico: New Mexico Bureau of Geology and Mineral Resources, scale 1:500,000.
- Person, M., Phillips, F., Kelley, S., Timmons, S., Pepin, J., Blom, L., Haar, K., and Murphy, M., 2013, Assessment of the sustainability of geothermal development within the Truth or Consequences Hot-Springs district, New Mexico: New Mexico Bureau of Geology and Mineral Resources Open-file Report 551, 65 p.
- Pope, M.C., 2004, Upper Ordovician and lower to middle Silurian miogeoclinal rocks, *in* Mack, G.H. and Giles, K.A., eds., *The Geology of New Mexico: A Geologic History: New Mexico Geological Society, Special Publication 11*, p. 45–58.
- Reimer, P.J., et al., 2013, IntCal13 and Marine13 radiocarbon age calibration curves 0-50,000 years cal BP: *Radiocarbon*, v. 55, p. 1869-1887.
- Repenning, C.A., and May, S.R., 1986, New evidence for the age of lower part of the Palomas Formation, *in* Clemons, R.E., King, W.E., Mack, G.H., and Zidek, J., eds., *Truth or Consequences region: New Mexico Geological Society Guidebook 37*, p. 257–260.
- Seager, W.R., 2015, Geologic map of the Palomas Gap 7.5-minute quadrangle, Sierra County, New Mexico: New Mexico Bureau of Geology and Mineral Resources Open-file Geologic Map OF-GM 260, scale 1:24,000.
- Seager, W.R., and Mack, G.H., 2003, Geology of the Caballo Mountains, New Mexico: New Mexico Bureau of Geology and Mineral Resources Memoir 49, 136 p.
- Seager, W.R., and Mack, G.H., 2005, Geology of Caballo and Apache Gap quadrangles, Sierra County, New Mexico: New Mexico Bureau of Geology and Mineral Resources Geologic Map 74, scale 1:24,000.

- Seager, W.R., Hawley, J.W., and Clemons, R.E., 1971, Geology of the San Diego Mountain area, Doña Ana County, New Mexico: New Mexico Bureau of Mines and Mineral Resources Bulletin 97, 38 p., 2 pl.
- Seager, W.R., Clemons, R.E., Hawley, J.W., and Kelley, R.E., 1982, Geology of northwest part of Las Cruces 1° x 2° sheet, New Mexico: New Mexico Bureau of Mines and Mineral Resources Geologic Map 53, scale 1:125,000.
- Seager, W.R., Shafiqullah, M., Hawley, J.W., and Marvin, R.F., 1984, New K-Ar dates from basalts and the evolution of the southern Rio Grande rift: Geological Society of America Bulletin, v. 95, no. 1, p. 87–99.
- Soil Survey Staff, 1992, Keys to soil taxonomy: U.S. Department of Agriculture, 541 p.
- Spell, T.L., Kyle, P.R., and Baker, J., 1996, Geochronology and geochemistry of the Cerro Toledo Rhyolite, *in* Goff, F., Kues, B.S., Rogers, M.A., McFadden, L.D., and Gardner, J.N., eds., Jemez Mountains Region: New Mexico Geological Society Guidebook 47, p. 263–268.
- Stuiver, M., and Reimer, P., 1993, Extended ¹⁴C data base and revised CALIB radiocarbon calibration program: Radiocarbon, v. 35, pp. 215-230.
- Tedford, R.H., 1981, Mammalian biochronology of the Late Cenozoic basins of New Mexico: Geological Society of America Bulletin, v. 92, p. 1008–1022.
- Udden, J.A., 1914, The mechanical composition of clastic sediments: Geological Society of America Bulletin, v. 25, p. 655–744.
- Wentworth, C.K., 1922, A scale of grade and class terms for clastic sediments: Journal of Geology, v. 30, p. 377–392.

APPENDIX A

Detailed descriptions of lithologic units on the
Williamsburg 7.5' quadrangle

UNIT DESCRIPTIONS

The units described below were mapped using aerial photography coupled with field checks, or by examining well cuttings and comparing to existing lithologic descriptions in the case of subsurface units. Stereogrammetry software (Stereo Analyst for ArcGIS 10.1, an ERDAS extension, version 11.0.6) permitted accurate placement of geologic contacts. Grain sizes follow the Udden-Wentworth scale for clastic sediments (Udden, 1914; Wentworth, 1922) and are based on field estimates. The term “clast(s)” refers to the grain size fraction greater than 2 mm in diameter. Descriptions of bedding thickness follow Ingram (1954). Colors of sediment are based on visual comparison of dry samples to Munsell Soil Color Charts (Munsell Color, 2009). Soil horizon designations and descriptive terms follow those of Birkeland et al. (1991), Soil Survey Staff (1992), and Birkeland (1999). Stages of pedogenic calcium carbonate morphology follow those of Gile et al. (1966) and Birkeland (1999). Description of sedimentary, igneous, and metamorphic rocks was based on inspection using a hand lens.

Surface characteristics and relative landscape position were used in mapping middle Pleistocene to Holocene units. Surface processes dependent on age (e.g. desert pavement development, clast varnish, calcium carbonate accumulation, and eradication of original bar-and-swale topography) can be used to differentiate stream terrace, alluvial fan, and valley floor deposits. Younger deposits are generally inset below older deposits. However, erosion may create a young surface on top of an older deposit, so Quaternary deposits were field-checked to identify this relationship.

QUATERNARY

Anthropogenic, eolian, and hillslope units

- daf Disturbed or artificial fill (modern) – Sand and gravel that has been moved by humans to form berms and dams, or has been reworked/remobilized for construction of infrastructure or buildings.
- Qes Eolian sand (Holocene) – Windblown sand occurring in pod-shaped coppice dunes atop flat ridges and on their lee sides. Deposit is unconsolidated and often rippled. Matrix consists of pale to light yellowish brown (10YR 6/3-4), very well sorted, subangular to rounded, very fine- to fine-grained, quartzose sand. Commonly vegetated with little or no soil development. Deposited by southerly to southwesterly winds on the leeward (i.e. north) side of ridges (Kelley and Silver, 1952), with sediment derived from the floodplain of the Rio Grande and deflated Palomas Formation deposits. Higher, non-vegetated dunes may be up to 2.3 m (7.5 ft) thick. Total thickness unknown but probably no more than 2.5 m (8.2 ft) in most locations. Locally mapped as eolian mantle on older units (Qes/unit).
- Qesc Eolian sand, slopewash, and hillslope colluvium, undivided (Holocene) – Mixed windblown sand and pebble-cobble-boulder gravel typically found on lee sides of ridges east of the Rio Grande. Deposit is unconsolidated and massive to rippled where dominated by eolian material. Clasts are poorly sorted and angular to subangular. Commonly vegetated with little or no soil development. Maximum thickness likely no more than 3 m (10 ft). Locally mapped as eolian-colluvial mantle on older units (Qesc/unit).
- Qsc Slopewash and colluvium, undivided (upper Pleistocene to Holocene) – Very pebbly sand found in thick beds on bedrock highs and (less commonly) mantling Quaternary deposits. Deposit is very loosely consolidated and massive. Clasts consist of angular to subrounded granules to pebbles. Matrix consists of light yellowish brown (10YR 6/4), very well sorted silt to fine-grained sand. May be very weakly cemented by carbonate. Commonly bioturbated by fine roots. Likely reworked by sheetflooding in most instances. Total thickness typically 1.5-2 m (4.9-6.6 ft). Locally mapped as slopewash mantle on older units (Qsc/unit).

Valley-floor units dominated by modern and historical sediment (<50-600 yr old)

- Qaarg Active alluvium of the Rio Grande (present) – Sandy pebble-cobble gravel in the axial channel of the

Rio Grande, commonly in longitudinal or transverse bars. Clasts consist of poorly to moderately sorted, subrounded to rounded pebbles and cobbles. Boulders may be present, transported from local tributaries to the active channel during larger flood events. Clast lithologies are diverse, reflecting bedrock exposed throughout Rio Grande catchment. Matrix consists of moderately to very well sorted, subrounded to rounded, fine- to coarse-grained, quartzose sand. Total thickness unknown but likely 1-5 m (3.3-16 ft).

- Qam Modern alluvium (present to ~50 years old) – Sandy pebble to cobble gravel found in ephemeral channels or adjacent low-lying surfaces, fluvially reworked by modern flow events. Unconsolidated and commonly imbricated. Clasts are poorly to very poorly sorted, angular to subrounded, and consist of 65% pebbles, 30% cobbles, and 5% boulders. Clasts are dominated by granite, metamorphic lithologies, and Paleozoic carbonates where streams exit the footwall of the Caballo fault system east of the Rio Grande. To the west, clasts are dominated by volcanic lithologies derived from the Sierra Cuchillo and Black Range (including those reworked from the Palomas Formation). Matrix consists of brown to light brown (7.5YR 5-6/3) to dark yellowish brown or light brownish gray (10YR 4/4-6/2), poorly to moderately sorted, angular to subrounded, fine- to very coarse-grained sand. Pronounced bar-and-swale topography exhibits up to 60 cm (24 in) of relief. Sparsely to non-vegetated with no soil development. Total thickness is unknown but likely 1-3 m (3.3-9.8 ft).
- Qamh Modern and historical alluvium, undivided (present to ~600 years old) – Modern alluvium (Qam) and subordinate historical alluvium (Qah). See detailed descriptions of each individual unit.
- Qamy Modern and younger alluvium, undivided (present to lower Holocene) – Modern alluvium (Qam) and subordinate younger alluvium (Qay). See detailed descriptions of each individual unit.
- Qah Historical alluvium (~50 to ~600 years old) – Pebbly sand and sandy pebble gravel in very thin to thin (less commonly medium to thick), tabular to lenticular beds. Deposit is loosely consolidated, clast- to matrix-supported, and massive to horizontal-planar laminated or imbricated. Clasts are poorly to moderately sorted, angular to rounded, and consist of 80-90% pebbles, 10-20% cobbles, and 0-5% small boulders. Clasts are dominated by granite, metamorphic lithologies, and Paleozoic carbonates where streams exit the footwall of the Caballo fault system east of the Rio Grande. To the west, clasts are dominated by volcanic lithologies derived from the Sierra Cuchillo and Black Range (including those reworked from the Palomas Formation). Matrix consists of brown (7.5YR 6/4) to grayish or yellowish brown (10YR 5/2-4), poorly to well sorted, angular to subrounded, fine- to very coarse-grained sand and silty sand. Very weak carbonate cement may be present. Surface exhibits subdued bar-and-swale topography and channel forms with 10-40 cm (6-8 in) of relief. Moderately vegetated with little or no soil development (marked by weak ped development yet obvious sedimentary fabric) and commonly mantled by 20-30 cm (8-16 in) of silty fine sand related to slopewash or overbank deposition. Bioturbation by fine to very coarse roots or burrows is common. A radiocarbon date from Cañada Honda returned an age of 630-515 cal yr BP. Tread is 0.4-1.3 m (1.3-4.3 ft) above modern grade. Base not observed in thickest deposits; possibly up to 3 m (9.8 ft) maximum thickness.
- Qahm Historical and modern alluvium, undivided (present to ~600 years old) – Historical alluvium (Qah) and subordinate modern alluvium (Qam). See detailed descriptions of each individual unit.
- Qahy Historical and younger alluvium, undivided (~50 years old to lower Holocene) – Historical alluvium (Qah) and subordinate younger alluvium (Qay). See detailed descriptions of each individual unit.
- Qar Recent (historical + modern) alluvium (present to ~600 years old) – Historical alluvium (Qah) and modern alluvium (Qam) in approximately equal proportions. See detailed descriptions of each individual unit.

Valley-floor units dominated by younger sediment (~600-11,000 yr old)

- Qary Recent (historical + modern) and younger alluvium, undivided (present to lower Holocene) – Recent alluvium (Qah + Qam) and subordinate younger alluvium (Qay). See detailed descriptions of each individual unit.
- Qay Younger alluvium (Holocene) – Sand and pebbly sand to sandy pebble-cobble gravel. Finer sediment dominates in low-gradient, low-order drainages and consists of very thin to thick, tabular (minor lenticular) beds of brown to light brown (7.5YR 5/2-4; 6/3-4; 10YR 5/3) to light brownish gray (10YR 6/2), mostly

massive (locally horizontal-planar laminated), very fine- to medium-grained sand or clayey-silty, very fine- to medium-grained sand. This finer sediment generally contains minor coarse- to very coarse-grained sand and 1-20% scattered pebbles, with 1-25% very thin to thin lenses of sandy pebble gravel or pebbly sand (locally 1-10% cobbles). In the finer sediment, cumulic soil development is common and characterized by weakly to strongly developed, medium to coarse, subangular blocky peds as well as local minor clay illuviation and stage I carbonate morphology. Coarser sediment dominates in steep canyons incised relatively deeply in the Palomas Formation. These deposits consist of sandy gravel in very thin, tabular to lenticular beds. In larger, deeply incised drainages this coarse sediment is interbedded with finer sediment like that described above. Gravels are typically clast-supported with minor matrix-supported debris flow beds. Imbrication is common in clast-supported beds and sandy or pebbly beds may be cross-stratified (foresets up to 10 cm thick). Gravel consist of poorly to moderately sorted, subangular to rounded (mostly subrounded) pebbles and subordinate cobbles whose compositions reflect lithologies exposed upstream of the deposit (see descriptions of Qam and Qah clast lithologies). Matrix consists of poorly to moderately well sorted, subangular to subrounded, medium- to very coarse-grained sand. Sand in coarser deposits is brown to light brown (7.5YR 5/2-6/3), dark brown to brown (10YR 3-5/3), or dark yellowish brown to yellowish brown (10YR 4-5/4). Both coarse and fine varieties exhibit little to no pedogenic carbonate development on the surface, but buried calcic horizons are relatively common (stage I to II carbonate morphology). Surfaces locally show signs of erosion. Where erosion is minimal, stage I to II carbonate morphologies in the topsoil are typical, with upper parts locally accompanied by illuviated clay (i.e. Btk horizons overlying a Bk horizon). The calcic or illuviated clay horizons are locally overlain by 10-15 cm (4-6 in) thick, brown (10YR 4-5/3) A horizons marked by accumulation of organic matter and fine sediment deposited by eolian or slopewash processes. A radiocarbon date from Cañada Honda for the lowest part of correlative Qfay deposits returned an age of ~11000 cal yr BP, but upper age is likely middle to late Holocene. Weakly to moderately consolidated and typically 2-5 m (6.6-16.4 ft) thick. Locally divided into an inset deposit:

Qayi Younger inset alluvium (upper Holocene) – Pebbly sand, sandy gravel, and sand in very thin to medium, lenticular to tabular beds. Looser than Qay deposits and lacks buried soils. Gravel are clast-supported, commonly imbricated, and poorly sorted. Sand is grayish brown to pale brown (10YR 5/2-6/3), poorly to moderately sorted, subangular to subrounded, and very fine- to very coarse-grained. Locally silty (1-15% silt). Soil is marked by weak accumulation of calcium carbonate (stage I carbonate morphology), with <30% thin films of calcium carbonate mostly on undersides of clasts. A radiocarbon date from Cañada Honda returned an age of 630-580 cal yr BP. Up to 4.5 m (15 ft) thick.

Qaym Younger and modern alluvium, undivided (present to lower Holocene) – Younger alluvium (Qay) and subordinate modern alluvium (Qam). See detailed descriptions of each individual unit.

Qayh Younger and historical alluvium, undivided (~50 years old to lower Holocene) – Younger alluvium (Qay) and subordinate historical alluvium (Qah). See detailed descriptions of each individual unit.

Qayr Younger and recent (historical + modern) alluvium, undivided (present to lower Holocene) – Younger alluvium (Qay) and subordinate recent alluvium (Qah + Qam). See detailed descriptions of each individual unit.

Terrace deposits of the Rio Grande

Qtr Rio Grande terrace deposits, undivided (middle Pleistocene to Holocene) – Pebble-cobble gravel with sand lenses in mostly thick, tabular to lenticular beds. Mostly unconsolidated, clast-supported, and imbricated to trough cross-stratified. Clasts consist of poorly to moderately sorted, subrounded to well rounded pebbles, cobbles, and small boulders of porphyritic volcanic rocks, Cretaceous sandstone, Paleozoic carbonate and jasperoid, quartzite, and granite. Clast undersides occasionally to commonly coated by carbonate. Matrix consists of silty, fine-to coarse-grained sand containing over 55% rounded quartz grains. Deposit may be capped by pedogenic carbonate or eolian silt to fine-grained sand. Locally subdivided into 6-7 deposits based on landscape position:

Qtr1 First or lowest Rio Grande terrace deposit (~260 to ~800 years old) – Weakly to moderately calcareous and thin- to thick-bedded with occasional ripple cross-stratification (foresets up to 15 cm thick) of sandier layers. Contains very few boulders. Brown to pale brown (10YR 5-6/3) matrix. Commonly

bioturbated by sedges and salt cedar. Locally subdivided into two deposits, Qtr1a and Qtr1b, with tread heights <3 and <5 m (<9.8 and <16.4 ft) above modern grade, respectively. Correlative to terrace deposits IV and III of Mack et al. (2011), respectively. The former was dated at < ~0.3 ka based on air photos and radiocarbon ages for charcoal and bivalve shells, the latter at <0.6-0.8 ka based on radiocarbon ages for microcrystalline calcite filaments in capping soil. Overall, deposits lack strong soil development. Tread height ≤3 m (10 ft) above modern grade. 2.8 to perhaps 7 m (9-23 ft) thick.

- Qtr2 Second or middle-lower Rio Grande terrace deposit (~5,300 to ~8,000 years old) – Pebbly to clayey sand with common calcic horizons. Correlative to terrace deposit II of Mack et al. (2011) that was radiocarbon-dated at <5.3-8 ka. Tread height 3-6 m (10-20 ft) above modern grade. Approximately 2-3 (6.6-10 ft) thick.
- Qtr3 Third or middle Rio Grande terrace deposit (upper Pleistocene to lower Holocene) – Well imbricated with occasional trough cross-stratification. Contains very few boulders. Pale brown (10YR 6/3) matrix. Varnish on 10-12% of clasts at surface. Stage I+ carbonate morphology in upper 80 cm (32 in) indicated by carbonate coats and/or rinds on up to 90% of clasts and common carbonate cement. Capped by up to 40 cm (16 in) of Qes. Perhaps correlative to terrace deposit I of Mack et al. (2011); calcic nodules from a mature soil capping this deposit were radiocarbon-dated at <12.4 ka. Tread height 5-8 m (16-26 ft) above modern grade. 1.5-3 m (5-10 ft) thick.
- Qtr4 Fourth or middle-upper Rio Grande terrace deposit (upper Pleistocene) – Medium- to thick-bedded and well imbricated. Contains up to 15% boulders with ~30% flaggy clasts. Light yellowish brown (10YR 6/4) matrix. Sandy lenses composed of 85-90% pebbles are common and up to 25 cm (10 in) thick. Deposit capped by 35 cm (14 in) thick stage II+ carbonate horizon in which 90% of clasts have carbonate rinds up to 1.5 mm thick. Tread height 18-24 m (59-79 ft) above modern grade. 3.6-9 m (12-30 ft) thick.
- Qtr5 Fifth or upper Rio Grande terrace deposit (middle to upper Pleistocene?) – Mostly unconsolidated, non- to moderately calcareous, broadly lenticular, and well imbricated to vaguely trough cross-stratified. Contains up to 5% boulders. Light brownish gray to pale brown (10YR 6/2-3) matrix. Stage II+ carbonate morphology in upper 70-90 cm (28-35 in) indicated by carbonate coats and/or rinds on all clasts and common carbonate cement. May be mantled by 0.5-2 m (1.6-6.6 ft) of Qes or Qesc. One deposit near King Arroyo contains ash geochemically correlated to 640 ka Lava Creek B tephra (N. Dunbar, personal communication, 2015). Tread height 24-42 m (79-98 ft) above modern grade. 2-6.8 m (6.6-22 ft) thick.
- Qtr6 Oldest or highest Rio Grande terrace deposit (middle Pleistocene) – High exposures of rounded gravel containing exotic clasts such as quartzite. Represents thin remainder of coarse channel load of the ancestral Rio Grande. Tread height >45 m (118-138 ft) above modern grade. Maximum thickness 3 m (10 ft).

Terrace deposits of Palomas Creek

- Qtp Terrace deposits of Palomas Creek, undivided (middle to upper Pleistocene) – Sandy pebble-cobble gravel in thin to very thick, tabular to lenticular beds. Unconsolidated and very weakly to moderately calcareous. Clasts consist of poorly to moderately sorted, subrounded to well rounded pebbles and cobbles of Tertiary volcanic and Paleozoic carbonate lithologies sourced from the Salado Mountains and eastern Black Range. Older terrace deposits may feature more varnished clasts at surface. Deposits underlie inset surfaces along Palomas Creek. Most deposits underlie relatively thin (up to ~5-7 m thick) strath terraces, but thicker fills may be present in places. Locally subdivided into 4-5 deposits based on landscape position:
- Qtp1 First or lowest terrace deposit of Palomas Creek (upper Pleistocene) – Sandy gravel in medium to thick beds. Clasts include subequal proportions of pebbles and cobbles with 10-15% boulders. Locally subdivided into Qtp1a and Qtp1b with tread heights 7-16 m (23-53 ft) and 16-18 m (53-59 ft) above modern grade, respectively. 2-4 m (6.6-13 ft) thick.

- Qtp2 Second or middle-lower terrace deposit of Palomas Creek (upper Pleistocene) – Weakly calcareous and thick- to very thick-bedded. Brown (7.5-10YR 4/3) matrix. Contains no more than 3% boulders. Varnish on 20-30% of clasts at surface. Local Fe-oxidation occurs on clast undersides in ~30 cm (12 in) thick zones. Few preserved soils (likely eroded). Well preserved along most of Palomas Creek in quadrangle. Tread height 24-31 m (80-102 ft) above modern grade. 2-6 m (6.6-20 ft) thick.
- Qtp3 Third or middle terrace deposit of Palomas Creek (middle Pleistocene?) – Very weakly calcareous and thin- to thick-bedded. Brown (10YR 5/3) matrix. Imbricated to weakly planar cross-stratified with fine to medium pebbles concentrated along bases of individual foresets. Clast lithologies include up to 35% Kneeling Nun tuff and aphanitic rhyolite. Varnish on up to 50% of clasts at surface. Contains more feldspar grains (up to 70%) than other terrace deposits. Tread height 33-40 m (108-131 ft) above modern grade. 1.4-3 m (4.6-10 ft) thick.
- Qtp4 Fourth or upper terrace deposit of Palomas Creek (middle Pleistocene) – Sandy pebble-cobble gravel. Brown (7.5YR 4-5/3) matrix. Varnish on up to 80% of clasts at surface. Soil development uncommon (likely eroded). Moderately dissected in places. Tread height 40-47 m (131-154 ft) above modern grade. 5-8 m (16-26 ft) thick.

Terrace deposits of ephemeral drainages

- Qtge Terrace deposits of ephemeral drainages east of the Rio Grande (middle to upper Pleistocene) – Sandy pebble-cobble gravel in medium to thick, tabular to lenticular beds. Unconsolidated, commonly imbricated, and occasionally planar cross-stratified (foresets up to 25 cm thick). Clasts consist of poorly to moderately well sorted, subangular to rounded pebbles (70-90%), cobbles (10-20%), and subordinate boulders (5-10%) derived from the Palomas Gap area. Clasts are composed of Paleozoic sedimentary and Precambrian igneous and metamorphic lithologies. Gravel are better sorted near the top of the deposit and 18-20% of clasts are varnished at the surface. Matrix consists of light grayish brown (10YR 6/2), poorly to moderately sorted, subrounded, very fine- to medium-grained sand that is commonly arkosic (>50% K-spar). May exhibit stage I+ to II carbonate morphology. Tread height up to 19 m (62 ft) above grade. Typically a thin strath terrace deposit that is 1-3 m (3.3-10 ft) thick.
- Qtgw Terrace deposits of ephemeral drainages west of the Rio Grande (middle to upper Pleistocene) – Sandy pebble to pebble-cobble-boulder gravel in thin to thick, tabular to lenticular beds. Local sandy sediment in medium, lenticular to tabular beds. Unconsolidated to very weakly carbonate-cemented and massive to imbricated. Sandy pebble beds may be planar or trough cross-stratified. Clasts are very poorly to poorly sorted, subangular to rounded, and consist of 50-85% pebbles, 15-50% cobbles, and 3-10% boulders of flow-banded rhyolite (≤30%), vesicular or dense basalt (≤20%), andesite or basaltic andesite, and perhaps Paleozoic sedimentary lithologies. Occasional open-framework lenses of pebbles and cobbles are up to 60 cm (24 in) thick. Matrix consists of reddish brown (5YR 4/4) to light brown (7.5YR 6/3), poorly to moderately sorted, angular to rounded, very fine- to coarse-grained sand composed of 30-60% feldspar, 30-50% lithic, and 10-30% quartz grains with up to 15% reddish clay films. Rare sand lenses are under 25 cm (10 in) thick and consist of planar cross-stratified sand with <15% granules. Deposit exhibits stage I-II carbonate morphology and is capped by A and Bw to Bt horizons up to 50 cm (20 in) thick in places. Typically comprises thin strath terrace deposits that underlie treads 6-20 m (20-66 ft) above modern grade. 1-2 m (3.3-6.6 ft) thick.

Alluvial-fan units dominated by modern and historical sediment (<50-600 yr old)

- Qfam Modern alluvial fan deposits (present to ~50 years old) – Unconsolidated pebbly sand and sandy pebble-cobble gravel in channels and low-lying bars of small fans, subjected to fluvial reworking in modern times. Sand consists of light yellowish brown to pale brown (10YR 6/4 to 7/2-3), moderately sorted, subangular to rounded, very fine to medium grains of 50-60% quartz, 30-40% feldspar, and 5-15% lithics. Sand is locally ripple laminated. Gravel clasts are poorly to moderately sorted, subangular to rounded, and consist of 80-90% pebbles and 10-20% cobbles. Both sand and gravel-dominated units form bars, but gravel bars form greater local relief (up to 0.8 m). Maximum thickness approximately 2.5 m (8 ft).

- Qfamh Modern and historical alluvial fan deposits, undivided (present to ~600 years old) – Modern alluvium (Qfam) and subordinate historical alluvium (Qfah) deposited on alluvial fans. See detailed descriptions of each individual unit.
- Qfamy Modern and younger alluvial fan deposits, undivided (present to lower Holocene) – Modern alluvium (Qfam) and subordinate younger alluvium (Qfay) deposited on alluvial fans. See detailed descriptions of each individual unit.
- Qfah Historical alluvial fan deposits (~50 to ~600 years old) – Sandy pebble-cobble gravel in very thin to very thick, tabular beds. Unconsolidated, moderately to strongly calcareous, clast- to matrix-supported, and massive/poorly stratified to weakly imbricated. Clasts consist of poorly sorted, subangular to rounded pebbles (60-80%), cobbles (10-40%), and small boulders (0-10%) Matrix consists of very pale brown (10YR 7/3), poorly to moderately sorted, subangular to rounded, fine- to medium-grained sand composed of 40-60% lithic, 20-40% quartz, and 10-20% feldspar grains. Clasts are covered by up to 70% by carbonate coats, indicating stage I carbonate morphology. Moderately bioturbated by medium to coarse roots and burrows up to 6 cm (2.4 in) in diameter. Surface is non-varnished and has 10-20 cm (4-8 in) of bar-and-swale relief. Deposit surface is graded to a surface 1.5 m (5 ft) above modern grade. 1.2-2 m (3.9-6.6 ft) thick.
- Qfamh Historical and modern alluvial fan deposits, undivided (present to ~600 years old) – Historical alluvium (Qfah) and subordinate modern alluvium (Qfam) deposited on alluvial fans. See detailed descriptions of each individual unit.
- Qfahy Historical and younger alluvial fan deposits, undivided (~50 years old to lower Holocene) – Historical alluvium (Qfah) and subordinate younger alluvium (Qfay) deposited on alluvial fans. See detailed descriptions of each individual unit.
- Qfar Recent (historical + modern) alluvial fan deposits (present to ~600 years old) – Historical (Qfah) and modern (Qfam) fan alluvium in approximately equal proportions. See detailed descriptions of each individual unit.
- Qfary Recent (historical + modern) and younger alluvial fan deposits, undivided (present to lower Holocene) – Recent fan alluvium (Qfah + Qfam) and subordinate younger fan alluvium (Qfay). See detailed descriptions of each individual unit.

Alluvial-fan units dominated by younger sediment (~600-11,000 yr old)

- Qfay Younger alluvial fan deposits (Holocene) – Pebbly sand to sandy gravel in very thin to medium, tabular to lenticular beds. Overall, bedding is convex-up transverse to the fan, centered on fan axis. Unconsolidated to weakly carbonate-cemented, mostly clast-supported, and massive to locally planar cross-stratified (up to 15% of a given exposure). Clasts are poorly to moderately sorted, subrounded, and consist of ≤95% pebbles, ≤30% cobbles, and ≤5% boulders. Clasts are dominated by granite, metamorphic lithologies, and Paleozoic carbonates where streams exit the footwall of the Caballo fault system east of the Rio Grande. To the west, clasts are dominated by volcanic lithologies derived from the Sierra Cuchillo and Black Range (including those reworked from the Palomas Formation). Matrix consists of brown to light brown (7.5YR 4-6/3-4; 10YR 4-5/3) to pinkish gray (7.5YR 6/2) to grayish or yellowish brown (10YR 5/2-4), poorly to moderately well sorted, subrounded, very fine- to very coarse-grained sand that is locally silty. Mostly deposited by stream-flow processes, but 5-25% of outcrops are matrix-supported debris flows or hyperconcentrated flows that are in either: 1) pebbly, internally massive beds; or 2) thin to medium, lenticular beds with pebbles and cobbles in a relatively fine matrix. Sandy sediment is typically bioturbated by medium to very coarse roots. Buried soils are common and marked by accumulation of calcium carbonate (stage I to II carbonate morphologies). Lowest strata is redder and finer-grained (i.e., more clay and fewer cobbles), and may be overprinted by a paleosol marked by illuviated clay. Unit fines in distal part, where it interfingers with and grades into units Qay or Qayi. Deposit is commonly capped by 10 cm (4 in) thick A horizons exhibiting ped development, finer textures, and slight accumulation of organic matter. Underlying the A horizon are: 1) Bt horizons where clasts and peds are covered by clay films (only locally observed); and 2) common calcic horizons with stage I to I+ carbonate morphology that are 10-80 cm (4-32 in) thick. Surface commonly shows evidence of erosion, such as gullies up to 2 m (6.6 ft) deep or an erosional lag of coarse pebbles to cobbles, and in these areas lacks notable soil development. On higher, relatively stable surfaces the clasts are weakly varnished and undersides are reddened. Less than 20 cm (8 in) of bar-and-swale topographic relief,

which is imperceptible on many of the higher surfaces. A radiocarbon date from Cañada Honda returned an age of ~11100-10830 cal yr BP. Maximum thickness ~4 m (13.1 ft). Locally subdivided into an inset unit:

Qfayi Younger alluvial fan deposits graded to Qayi (upper Holocene) – Deposit is as described for Qfay, with weak surface clast varnish and soil development. Perhaps less eroded and featuring greater (up to 20 cm) of bar-and-swale topographic relief than Qfay. A radiocarbon date from Cañada Honda returned an age of 2720-2385 cal yr BP.

Qfaym Younger and modern alluvial fan deposits, undivided (present to lower Holocene) – Younger alluvium (Qfay) and subordinate modern alluvium (Qfam) deposited on alluvial fans. See detailed descriptions of each individual unit.

Qfayh Younger and historical alluvial fan deposits, undivided (~50 years old to lower Holocene) – Younger alluvium (Qfay) and subordinate historical alluvium (Qfah) deposited on alluvial fans. See detailed descriptions of each individual unit.

Qfayr Younger and recent (historical + modern) alluvial fan deposits, undivided (present to lower Holocene) – Younger fan alluvium (Qfay) and subordinate recent fan alluvium (Qfah + Qfam). See detailed descriptions of each individual unit.

Alluvial-fan units dominated by older sediment (late to middle Pleistocene)

Qfao Older alluvial fan deposits (middle to upper Pleistocene) – Alluvial fan deposits underlying surfaces graded to higher positions above modern grade than those of Qfay. Deposit consists of sandy pebble-cobble gravel in thin to thick, tabular to lenticular beds. Unconsolidated to somewhat carbonate-cemented and massive to weakly imbricated. Clasts are poorly sorted, subangular to subrounded, and consist of 55-75% pebbles, 30-40% cobbles, and 0-10% boulders of lithologies reflecting local source areas. Generally features moderate to strong varnish on clasts at surface, which have reddened undersides (more varnished than Qfay surface, except where severely eroded). Matrix consists of mostly brown to light brown (7.5YR-10YR 4-6/3-4), poorly to moderately sorted, subangular to subrounded, very fine- to very coarse-grained sand composed of 60-70% lithic (volcanic+carbonate), 30-40% feldspar, and 5-10% quartz grains. Surface generally shows signs of erosion. Maximum thickness approximately 3-4 m (10-13 ft). Subdivided into 4 deposits along Palomas Creek:

Qf1 Deposits of alluvial fans graded to lowest terraces (upper Pleistocene) – Light yellowish brown (10YR 6/4) matrix. Unconsolidated but strongly calcareous, tabular, and massive to weakly imbricated. Features stage I carbonate morphology in upper part. Generally over 2 m (6.6 ft) thick.

Qf2 Deposits of alluvial fans graded to middle-lower terraces (upper Pleistocene) – Brown (7.5YR 5/4) matrix. Unconsolidated, calcareous, tabular to lenticular, and weakly imbricated. Varnish on 60-70% of clasts at surface. Maximum thickness 4 m (13 ft).

Qf3 Deposits of alluvial fans graded to middle terraces (middle Pleistocene?) – Pinkish gray (7.5YR 6/2) matrix. Somewhat calcareous, tabular, and massive to weakly imbricated. Features stage I+ carbonate morphology in upper part, indicated by carbonate coatings on up to 50% of clasts. Fe-oxide staining observed on up to 10% of clasts. 2-3 m (6.6-10 ft) thick.

Qf4 Deposits of alluvial fans graded to upper terraces (middle Pleistocene) – High, poorly preserved deposit observed near western quadrangle boundary, south of Palomas Creek. Not described in detail.

Qtfw Fan terrace deposits graded to terraces in Cañada Honda (middle to upper Pleistocene) – Sandy fan gravel interbedded with Qtgw terrace surfaces in Cañada Honda. Likely correlative with Qf2 or Qf3 deposits. Perhaps up to 3.5 m (11.5 ft) thick.

Qfe Older alluvial fan deposits east of the Rio Grande (middle to upper Pleistocene) – Sandy pebble-cobble gravel in thick, tabular to broadly lenticular beds underlying surfaces graded to or below Qtr deposits east of the Rio Grande. Weakly to moderately consolidated, moderately to strongly calcareous, clast-supported, and

massive to moderately well imbricated. Clasts are very poorly to poorly sorted, subangular to subrounded, and consist of 50-70% pebbles and 30-50% cobbles of Precambrian granite and metamorphic lithologies (50%), Paleozoic carbonates (45%), and exotic volcanic and quartzite clasts reworked from QTpa (5%). Matrix consists of light yellowish brown (10YR 5-6/4), poorly sorted, mostly subrounded, fine- to medium-grained sand composed of 35% quartz, 35% lithic (carbonate+granite), and 30% feldspar (K-spar>plagioclase) grains. Occasional (15%) matrix-supported intervals are massive and composed of material similar to the gravel matrix. Commonly contains gastropods in sandier beds. Correlates to alluvial fan deposits in unit Qvo of Seager and Mack (2005). >18 m (59 ft) thick.

QUATERNARY-TERTIARY BASIN-FILL UNITS

QTp Palomas Formation (lowermost Pliocene to lower Pleistocene) – Sand, silt, gravel, and clay deposited by coalesced fan complexes and the ancestral Rio Grande in the Palomas and Engle basins. Where not significantly eroded, the surface soil capping the youngest Palomas Formation is marked by a petrocalcic horizon that is 1-2 m (3.3-6.6 ft) thick and generally exhibits stage IV carbonate morphology. More information on this horizon and the constructional surface developed on the Palomas Formation, the Cuchillo surface, can be found in McCraw and Love (2012). Type sections of the Palomas Formation in the Williamsburg quadrangle are found at NW¹/₄ NW¹/₄ sec. 30 and NE¹/₄ SW ¹/₄ sec. 33, T. 14 S., R. 4 W. (Lozinsky and Hawley, 1986a). Initially thought to be 100-131 m (328-439 ft) thick, our work suggests a total thickness for the Palomas Formation of 240-275 m (800-900 ft) in this quadrangle. Subdivided into 12 units, including one cross-section-only unit:

QTpa Axial facies of the Palomas Formation – Pebbly to silty sand that is horizontal-planar laminated to planar or trough cross-stratified; also in laminated to very thick, lenticular beds. Subordinate facies are sandy pebble-cobble gravel in medium to thick, tabular to broadly lenticular, cross-stratified beds up to 1 m thick. This coarse facies dominates the lower 20-25 m (66-82 ft) of the unit, as exposed north of Truth or Consequences. Locally reverse graded. Unconsolidated to weakly carbonate- or silica-cemented. Fluting occurs in select beds. Clasts consist of moderately to moderately well sorted, subangular to subrounded pebbles and cobbles of basalt, rhyolitic ash-flow tuff, andesite, dacite, quartzite, granite, chert, and carbonate and clastic sedimentary strata. Matrix consists of light brown (7.5YR 6/4) to pale brown (10YR 6/3) or light gray (10YR 7/2), moderately to very well sorted, subrounded to rounded, very fine- to coarse-grained sand comprised of 65-85% quartz, 10-25% feldspar, and 5-10% lithic grains. Yellowish tan to very pale green clay occurs in thin lenses in sandy deposits. Deposit commonly features nodular or ellipsoidal concretions of iron-oxide minerals. The former may be up to 30 cm (12 in) across, the latter up to 8 cm (2.4 in) across. Sandy beds typically represent channel-margin or sandbar deposits of the ancestral Rio Grande. Silty to clayey beds are floodplain deposits, while gravel beds are intra-channel facies. Fossils recovered from this unit include gastropods and shells less than 1.5 cm (0.6 in) across, as well as freshwater species represented by salamander (*Amystoma* sp.), frog (*Rana* sp.), and a medium-sized rodent (e.g., a packrat). A tooth of the late Hemphillian horse *Neohipparion eurystyle*, collected from spoil piles just north of the quadrangle, suggests an age of 5.3-4.9 Ma for the earliest ancestral Rio Grande gravels (Koning et al., 2016). 40-115 m (130-380 ft) in a 3-5 km (1.9-3.1 mi) belt centered on the modern Rio Grande valley in the Williamsburg quadrangle. Locally divided into 1 subfacies:

QTpac Coarse-grained axial facies of the Palomas Formation – Sandy pebble-cobble and pebble-cobble-boulder gravel/conglomerate in medium to very thick, tabular to lenticular beds deposited in laterally extensive channel-fill complexes. Weakly to strongly consolidated, moderately calcareous, and massive to well imbricated and/or planar cross-stratified (foresets up to 50 cm thick). Lateral accretion sets are occasionally observed. Strongly indurated exposures preserve flute casts in rare instances. Clasts are very poorly to moderately sorted, subangular to rounded, and consist of 40-50% pebbles, 30-50% cobbles, and 0-20% boulders of diverse lithologies including Tertiary volcanics, Cretaceous sandstone, Paleozoic carbonates, and quartzite. Limestone, sandstone, and siltstone constitute a greater proportion (up to 80% total) of clasts in basal beds; volcanics and quartzite increase up-section. Imbricated gravel beds yield paleocurrent directions averaging SSE, but in the lowest part paleoflow is to the SSW. Matrix consists of light yellowish brown to very pale brown (10YR 6/4-7/3), poorly sorted, subrounded to rounded, fine- to coarse-grained sand composed of 40-65% quartz, 25-35% feldspar, and 10-25% lithic grains, with 5-25% clay chips and films. Common mud rip-ups and manganese coats on clasts. Deposit typically exhibits basal

scour contacts on finer-grained sediment with up to 3 m (10 ft) of relief.

- QTpe Eastern piedmont facies of the Palomas Formation – Sandy granule-pebble, pebble-cobble, and pebble-cobble-boulder gravel derived from the Caballo Mountain fault block. Occurs in thin to very thick, tabular to lenticular to wedge-shaped beds. Subordinate facies include silty sand and silty clay in thinly laminated to very thick, tabular to lenticular beds. Cementation and sedimentary structures vary according to relative fan position (proximal, medial, and distal). Proximal deposits consist of massive to imbricated, poorly sorted, subangular to subrounded, sandy pebble-cobble gravel in clast- to matrix-supported, medium to very thick, tabular beds. Proximal beds may feature rare cross-stratification and are weakly to moderately carbonate-cemented. These facies commonly include authigenic carbonate precipitated from shallow groundwater in gravelly gully beds (Mack et al., 2000). Medial deposits consist of massive or imbricated to planar cross-stratified sand and gravel in clast- to matrix-supported, medium to thick, tabular to lenticular beds. Sandy beds may be thickly laminated. Occasional paleosols in finer-grained medial facies may feature Btk horizons and illuviated clay (Bt) horizons above them. Distal deposits consist of poorly to moderately sorted, subangular to rounded pebble or pebble-cobble gravel interbedded with silty to sandy facies in mostly matrix-supported, medium to very thick, tabular to lenticular beds. Well-defined imbrication of gravel clasts is more common in distal facies than in proximal and medial gravels. Paleosols with Btk to K horizons are common in distal silt beds. In general, eastern piedmont facies matrix consists of poorly to moderately sorted, subangular to subrounded, fine- to coarse-grained sand comprised of 15-80% feldspar, 10-65% quartz, and 5-30% lithic grains. Matrix is typically reddish brown (5YR 4-5/4) to strong brown (7.5YR 4-5/4) in proximal facies, and brown (7.5YR 5/4) to light gray (10YR 7/1-2) in distal facies. Maximum thickness 110 m (361 ft).
- QTper Paleo-Red Canyon alluvial fan deposits of the eastern piedmont facies of the Palomas Formation – Siltstone, sandstone, and sandy pebble-cobble-boulder conglomerate in multi-story, thin to thick, tabular to lenticular beds. Moderately to strongly consolidated, commonly carbonate-cemented, mostly clast-supported, and massive to imbricated to planar cross-stratified. Scoured contacts on underlying sandstone and siltstone beds are common. Clasts are very poorly to moderately sorted, angular to subrounded, and consist of 45-100% pebbles, 35-45% cobbles, and 0-20% boulders of 50-60% Paleozoic carbonates and chert, 20-30% Abo Formation siltstone and sandstone, and 10-20% granite and metamorphics. Matrix consists of yellowish red to reddish brown (5YR 4-5/6 to 5-7/4), poorly to moderately sorted, subrounded, very fine- to coarse-grained sand composed of 40-80% lithic (carbonate+chert+mica), 40-45% feldspar, and 10-20% quartz grains. Rare stage IV carbonate morphology with carbonate laminae and rinds on all clasts. Interfingers with QTpa along lower 1.7 km (1.1 mi) of modern Red Canyon. 60-140 m (200-460 ft) thick.
- QTpef Fine-grained eastern piedmont facies of the Palomas Formation – Clayey to silty sand with less than 40% gravel in thin to medium, tabular to lenticular beds. Reddish yellow (5YR 6/6) to pink (7.5YR 6-8/3-4) to very pale brown (10YR 8/2). Mostly unconsolidated and typically massive. Less commonly, unit is horizontal-planar to ripple laminated or planar cross-stratified. Gravel beds are clast- to matrix-supported and may be imbricated with poorly sorted, subangular to subrounded pebbles (>60%) and cobbles (<40%). Sand consists of moderately to well sorted, subangular to subrounded, very fine to fine grains dominated by feldspar (50-80%). Buried soils are common and include stage I to II+ carbonate morphology with Btk, Bk, or K horizons up to 0.8 m (2.6 ft) thick. Perhaps as much as 140 m (460 ft) thick near Red Canyon, thinning northwards to approximately 30 m (100 ft).
- QTpwuc Upper coarse unit of the western piedmont facies of the Palomas Formation – Uppermost unit of western piedmont facies, consisting of sandy pebble-cobble gravel in amalgamated, laterally continuous channel-fill complexes that are generally 2-6 m (6.6-20 ft) thick. Unit defined where coarse channel-fills occupy more than 65% of sediment volume, the remainder being fine-grained, extra-channel sediment. Basal contact is transitional with unit QTpwu and may vary in elevation by as much as 20 m (66 ft) due to lateral terminations of lower gravelly channel-fills. These coarse channel-fill complexes exhibit scoured lower contacts, with up to 1 m (3.3 ft) of relief, and typically abrupt upper contacts (consistent with channel avulsion). Within coarse channel-fills, bedding is very thin to thick (mostly thin to thick), commonly vague, and lenticular to tabular; 0-7% cross-stratification includes lateral accretion sets up to 1.5 m (5 ft) thick, low-angle cross-stratification, trough cross-stratification, and bar-related cross-stratification with planar foresets (up to 60 cm thick). Gravel is generally clast-supported and imbricated, consistent with being deposited predominately by stream-

flow. Gravel fraction consists of 50-80% pebbles with 25-50% cobbles and 1-20% boulders. Clasts are poorly sorted (lesser moderately sorted), subrounded (lesser rounded), and composed of crystal-poor rhyolites, 5-25% andesite-dacite (dark-colored to north, where plagioclase- and/or pyroxene-phyric types dominate; lighter-colored to south, where feldspar-phyric types dominate), 10-20% tuffs, 1-5% basaltic andesite, 0-10% Paleozoic sedimentary types (mostly <3%), 1-3% hornblende-biotite intrusive found only to the north, and trace to 1% (less commonly up to 15%, particularly near the top of unit) vesicular basalt. Color of sandy matrix ranges from reddish brown (5YR 5/3-4) to light reddish brown (5YR 6/4) to pink or light brown (7.5YR 6-7/4). Fine- to very coarse-grained sand is poorly to moderately sorted, subangular to subrounded, and composed of 55-80% lithic (volcanic), 15-30% feldspar, and 5-15% quartz grains. Sandy matrix contains notable orange clay as chips or coatings/films (1-20%). Extra-channel sediment consists of very fine- to medium-grained sand (mostly very fine- to fine-grained) and clayey-silty fine sand with minor (5-20%), scattered medium to very coarse sand grains and pebbles. Color of extra-channel sediment ranges from reddish yellow to light brown (7.5YR 6/4-6) to strong brown or reddish yellow or yellowish red (5YR 4-5/6; 7.5YR 5-6/6). Commonly capped by a 1-1.5 m (3.3-5 ft) thick stage III-IV carbonate horizon. Moderately to well consolidated, weakly cemented by clay. Preserved top of unit is typically moderately to strongly cemented by soil carbonate. Maximum thickness 1.5-45 m (5-145 ft).

QTpwu Upper western piedmont facies of the Palomas Formation – Interbedded fine-grained sediment and subordinate to subequal, laterally continuous, coarse channel-fill complexes. Upper and lower contacts are transitional with QTpwuc and QTpwm, respectively. Base is placed at the bottom of predominately reddish sediment, locally coinciding with a thick clayey bed. Fine-grained, extra-channel sediment consists of clayey-silty fine sand, very fine- to fine-grained sand, and clay-silt that are in thin to thick, tabular beds that are commonly internally massive; <1-20% very thin to medium, lenticular (lesser tabular to trough-shaped) interbeds of coarse sand ± pebbles. Locally present in the clayey-silty fine sand and very fine- to fine-grained sand is minor (trace-25%), scattered medium to very coarse sand ± volcanic pebbles, consistent with deposition by hyperconcentrated flows. Clayey sediment is reddish brown to light brown to brown to light reddish brown (5-7.5YR 5-6/3-4; 5YR 5/4), clayey fine sand and silt is pinkish gray to pink to light brown (7.5YR 7/2 to 6-7/3-4; 5YR 6-7/2) to brown (7.5YR 5/4) to light reddish brown (5YR 6/3). Clay-silt floodplain deposits appear most abundant along Palomas Creek. Coarse channel-fill complexes are 2-5 m (6.6-16 ft) thick and generally laterally continuous (extending 10s to 100s of meters transverse to paleoflow direction), with scoured bases and typically abrupt tops. These coarse channel-fills consist of clast-supported sandy gravel in vague, thin to thick (mostly thin to medium), lenticular (lesser tabular) beds with minor (1-15%) cross-stratification up to 1 m (3.3 ft) thick and very thin to thin foresets that are tangential, planar, or trough-cross-stratified; sandy sediment is commonly horizontal-planar laminated to low-angle cross-stratified. Gravel is comprised of pebbles with 15-40% cobbles and 0-10% boulders. Within a bed, gravel are generally clast-supported, commonly imbricated, poorly sorted (minor moderate sorting), and subrounded to rounded. Gravel are composed of rhyolite and lesser felsic tuffs, together with 10-30% andesite and dacite (with plagioclase ± pyroxene phenocrysts), 0-7% basaltic andesites, 0-1% intermediate intrusive lithologies, and trace to 7% vesicular basalt (basalt decreases near the northern quadrangle boundary). Sand that is associated with the gravels is fine- to very coarse-grained (mostly medium- to very coarse-grained), moderately to poorly sorted, subrounded to subangular, and composed of volcanic grains, slightly lesser feldspar grains, and minor quartz grains. Sand color ranges from reddish brown to brown to light brown (2.5-7.5YR 4-5/4; 7.5YR 5/2-4/3; 7.5YR 5-6/3-4) to yellowish red (5YR 4/4-6) to light reddish brown (5YR 6/3) to pinkish gray (7.5YR 6/2). 0.5-15% clay argillans that coat clasts and sand grains or occur as interstitial particles. Sand and gravel is weakly to well consolidated and non- to weakly cemented by clay. Clayey-silty sediment is moderately to well consolidated. 10-40 m (30-120 ft) thick.

QTpwv Transitional zone below the upper western piedmont facies of the Palomas Formation – Predominately fine-grained sediment that is redder than QTpwm and slightly less red than QTpwu. Lies gradationally between these two units, both in a vertical and lateral sense (the latter mapped south of Palomas Creek). Fine sediment consists of silt-clay (silt>clay), very fine- to medium-grained (mostly very fine- to fine-grained) sand, and slightly silty-clayey sand in thin to thick (mostly medium to thick), tabular beds. Locally within these fine beds are 1-10% thin to medium, sandy pebble-cobble beds and 1-15% scattered, medium to very coarse-grained sand. Fine beds range in color from light reddish brown to pink to light brown to pinkish gray (5YR-7.5YR 6/3-4; 7.5YR 7/3; 5YR 6/2); 0-5% reduced (yellowish-light greenish) beds. Subordinate coarse channel-fill complexes are lenticular to laterally continuous and up to 3 m (10 ft) thick. Bedding within these

complexes is relatively thin and mostly tabular to lenticular. Gravel is comprised of pebbles with subordinate cobbles that are poorly to moderately sorted and mostly subrounded (minor rounded). Gravel is composed of rhyolite, lesser felsic tuffs, and 5-25% andesite-basaltic andesite. Channel-fill sand is brown to gray (7.5YR 5/2-6/1), mostly medium- to very coarse-grained, moderately sorted, subrounded, and composed of volcanic grains, lesser feldspar, and 10-25% quartz. Fining-upward trends observed in individual beds or channel-fills. Interbedded carbonate ledges are observed south of King Arroyo and are pale yellowish pink (7.5YR 9.5/2) to pinkish white (5YR 8/2), weakly to moderately indurated, medium-bedded, and massive. These beds contain rare, randomly dispersed pebbles up to 3.5 cm (1.4 in) across and common root mats, and likely represent spring deposits (Mack et al., 2000). Fossils of turtles, rodents, rabbits, *Equus* sp., and *Gomphotheriidae* recovered south of Palomas Creek. A tooth from the extinct rabbit species *Sylvilagus hubbardi* indicates a late Blancan (2.5-2.0 Ma) North American Land Mammal age for this deposit (G. Morgan, personal communication, 2014). Moderately to well consolidated; mostly non-cemented but with localized strong cement (1-5%). Up to 35 m (115 ft) thick.

QTpwm Middle western piedmont facies of the Palomas Formation – Very fine- to fine-grained sand, silty fine sand, and silt in thin to thick (mostly medium to thick), tabular beds that are internally massive to horizontal-planar laminated. Intertongues with QTpa. Colors are generally pink to light brown to pinkish gray (7.5YR 7/3; 6/ 3-4; 5-7.5YR 6-7/2); clayey sediment may be light reddish brown (5YR 6/3). Locally within the fine sediment are minor (1-10%), scattered medium to very coarse sand grains (\pm trace to 5% very fine to medium pebbles) or relatively thin, coarse-grained interbeds. <15% clayey beds. Minor (5-20%) tongues of pebbly sand and sandy pebbles are tabular to lenticular and up to 3 m (10 ft) thick. Unit gradationally underlies QTpwt or QTpwu (in the latter situation, the vertical gradation is generally <10 m thick). Coarser intervals consist of amalgamated channel-fills with laminated to medium, lenticular to tabular, cross-stratified bedding. Occasional fining-upward trends observed in channel-fills. Gravel consists of very fine to very coarse pebbles and 0-20% cobbles; clasts are poorly to moderately sorted, subrounded to rounded, and composed of rhyolite, 10-20% tuff, 5-30% intermediate volcanics, and 1% andesitic to dioritic intrusives. Sand in gravelly beds is fine- to very coarse-grained, poorly to moderately sorted, subrounded to subangular, and composed of volcanic and feldspar grains with 10-30% quartz; colors range from brown (7.5YR 5/2-4) to pinkish gray-white (7.5YR 6-8/2) to pink (7.5YR 7/3). Sand in finer strata are well sorted, subangular, and composed of quartz, 5-25% feldspar, and 15% volcanic lithic grains and subequal mafic grains. 3-15% strongly cemented beds are mostly medium- to thick-bedded and composed of dense calcium carbonate impregnating sand and pebbles. The basal contacts of these beds are commonly sharp and likely represent shallow groundwater cementation features. Cemented beds that are predominately calcium carbonate (<30% sand grains), imparting a white color, and exhibiting laminations or vugs are inferred to be precipitated from surface water (seeps or spring mounds; Mack et al., 2000). 1-5% localized calcium carbonate nodules and local paleo-burrows. Poorly sorted and internally massive, fine sand beds (medium- to thick-bedded with 1-5% clay-silt, 10% “floating” medium to very coarse sand grains, and 3% very fine to fine pebbles) are common and interpreted as hyperconcentrated flows (Seager and Mack, 2003). Moderately to well consolidated and weakly to moderately cemented by calcium carbonate. Approximately 100 m (300 ft) thick in northern quadrangle based on comparison of top of exposed unit near the town of Williamsburg with the interpreted base of the unit in City Well 8. About 75-85 m (250-280 ft) thick in the southern quadrangle, where interpretations of lithologic descriptions from the Barney Iorio Fee #1 well suggest that it is underlain by 45 m (150 ft) of ancestral Rio Grande sediment.

QTpwmc Coarse sediment in the middle western piedmont facies of the Palomas Formation – Strata dominated by coarse channel-fills, as described in unit QTpwm that are thick enough to be mappable. 10-20 m (30-60 ft) thick.

QTpwl Lower western piedmont facies of the Palomas Formation – Sediment dominated by stacked, coarse channel-fills composed of clast-supported, imbricated sandy gravel. On footwall of Mud Springs fault, lower contact locally is gradational, coarsening upward over 4-10 m (13-33 ft) as observed immediately east of Interstate 25 along the northern quadrangle boundary. In other exposures, the basal contact is sharp and has >1 m (3.3 ft) of scour relief. In the subsurface south of the Mud Springs fault, the base is transitional over ~30 m (100 ft). Sediment is in thin to medium, lenticular to tabular beds. Gravel includes pebbles, 5-40% cobbles, and 1% boulders. Clasts are poorly sorted, subrounded (lesser rounded), and composed of pinkish to gray rhyolite, 10-25% tuff, 10-15% plagioclase- or pyroxene-phyric andesite to basaltic andesite, 0-5% granite, trace to

1% vesicular basalt, and trace to 1% Paleozoic clasts (quartzose sandstone and limestone). About 5% of sediment is pebbly sand in thin to medium, lenticular beds. Sand is brown to reddish brown (5-7.5YR 5/4), poorly to moderately sorted, subangular to subrounded, and fine- to very coarse-grained. Basal 1-2 m (3.3-6.6 ft) is locally strongly cemented; otherwise, generally non-cemented and moderately consolidated. >87-91 m (285-300 ft) to north based on subsurface data in City Wells 6 and 8, appearing to thin to 17 m (56 ft) near Palomas Creek at the Barney Iorio Fee #1 well.

TERTIARY SANTA FE GROUP UNITS (PRE-PALOMAS FORMATION)

Trvpw Rincon Valley Formation, western piedmont facies (upper Miocene) – Exposed in the bluffs north of lower Mud Springs Canyon along the northern quadrangle boundary. Here, strata are light reddish brown (5YR 6/3-4), in medium to thick, tabular beds, and composed of: 1) siltstone and very fine- to fine-grained sandstone (about 50-70%); and 2) fine- to medium-grained sandstone (~20%), and coarse channel-fills (increasing up-section from 10 to 25%) Locally in the finer sand are scattered, coarse sand grains. Coarse channel-fills are as much as 2 m (6.6 ft) thick and consist of thin to medium, tabular beds composed of pebbly sand or sandy pebbles (with as much as 10% cobbles). Pebbles are very fine to medium, subangular to subrounded, and composed predominately of volcanic clasts (mostly rhyolite with 10% tuffs, 10% intermediate volcanics, 1% basaltic andesite, and perhaps trace basalt) together with 1-5% chert and 0-1% granite (both from the Mud Springs Mountains). Sub- or superjacent to large channel-fills may lie floodplain deposits of mudstone, siltstone, and very fine- to fine-grained sandstone (commonly horizontal-planar to ripple-laminated). Proportion of cemented beds increases up-section from 5 to 50%. Cementation is often nodular (5-10 cm across) and probably controlled by bioturbation or burrowing. At top of exposure lies a 1-2 m (3.3-6.6 ft) thick, laterally extensive, calcium carbonate bed mixed with 20-40% sand and gravel. Well consolidated. Unit is >20 m (60 ft) thick in exposures in northernmost quadrangle; perhaps up to 400 m (1300 ft) thick in the Barney Iorio Fee #1 well.

Trvbf Rincon Valley Formation, basin-floor facies (upper Miocene) – Thin to thick, tabular beds of light reddish brown to yellowish red (5YR 6/4-5/6), very fine- to medium-grained sand and clayey-silty sand. Sand is moderately sorted and subangular to subrounded. Minor (~5%) beds composed of very fine- to very coarse-grained sand with 5% pebbles. Pebbles are mostly very fine to fine, poorly to moderately sorted, angular to rounded (mostly subangular), and composed largely of aphanitic (likely felsic) volcanic rocks, ~25% chert, trace to 10% greenish sandstone (Mesozoic?), ~5% granite, and ~5% gneissic (Proterozoic) clasts. Moderately to well consolidated, with 5% well-cemented, medium to thick layers. 165-180 m (550-600 ft) thick based on interpretations of the Barney Iorio Fee #1 well log.

Tss Santa Fe Group, silicified (upper Miocene) – Strongly silicified Santa Fe Group conglomerate found in a sliver of the Hot Springs fault zone in the eastern part of the quadrangle. Clasts consist of poorly sorted, angular to subangular pebbles and cobbles of aphanitic volcanic lithologies, chert, granite, and metamorphic rocks. Matrix is replaced by silica cement that is weak red (10R 4-5/) to reddish brown (2.5YR 4-5/). Total thickness >15 m (50 ft).

PALEOZOIC BEDROCK UNITS

Pu Pennsylvanian rocks, undivided – Isolated blocks of limestone and subordinate sandstone in hanging wall of main Hot Springs fault trace. Sandstone may be strongly silicified. Thickness unknown.

Om Montoya Formation (middle to upper Ordovician) – Dolostone, limestone, and sandstone. Dolostone is dark to brownish gray, massive to occasionally laminated, and non- to sparsely fossiliferous. It occurs in thin to medium beds in upper part of unit and thick to very thick beds in lower part where it interfingers with pebbly conglomerate. Subordinate limestone contains lacy networks of dark brown chert. Base of unit consists of white to medium gray, medium-bedded, fine- to medium-grained, quartzose sandstone with a dolomitic matrix. Carbonate beds are correlative to the Upham and perhaps Aleman Members of Kelley and Silver (1952). Basal sandstone is the Cable Canyon Sandstone. Unit is strongly brecciated and/or altered to jasperoid adjacent to Hot Springs fault. Jasperoids may contain relict nodules of carbonate and secondary hydrothermal alteration products of quartz and barite. Disconformably overlies the El Paso Formation.

Maximum thickness 64 m (210 ft).

- Oe El Paso Formation (lower Ordovician) – Limestone and minor dolostone. Upper part of unit consists of medium to dark or pinkish gray, ledge-forming, thin- to thick-bedded, massive or wavy-bedded to occasionally ripple-laminated, fossiliferous, cherty limestone. At least two beds of light or brownish gray, matrix-supported, medium-bedded, angular limestone breccia occur in the upper half of this interval. Fossils in upper part of unit include brachiopods, crinoid columnals, and stromatolites. This interval is correlative to the Bat Cave Formation of Kelley and Silver (1952). Lower part of unit consists of medium to dark brownish gray or occasionally reddish, thin- to medium-bedded, tabular, mostly massive, sparsely fossiliferous, cherty, dolomitic limestone. Occasional dark gray dolomite beds up to 15 cm (6 in) thick occur in lower part, which is correlative to the Sierrite Limestone of Kelley and Silver (1952). Basal contact with Bliss Formation is mostly gradational. Maximum thickness 119 m (390 ft).
- €Ob Bliss Formation (upper Cambrian to lower Ordovician) – Very dark brown to nearly black, well indurated, thin- to medium-bedded, occasionally wavy-bedded, tabular, massive to broadly cross-stratified sandstone. Well sorted, subangular to subrounded, quartzose, and very fine- to fine-grained with subordinate, non-calcareous siltstone. Common peloidal glauconite. Generally forms slopes beneath ledges of Oe. Total thickness 12 m (39 ft).

PROTEROZOIC BEDROCK UNITS

- pCu Plutonic and metamorphic rocks, undivided (Paleo- to Mesoproterozoic) – Granitic gneiss, quartzofeldspathic schist, amphibolite, metasiltstone, and granite in unknown proportions. See individual descriptions for Proterozoic granite and metamorphic rocks. Total thickness unknown.
- pCg Granite (Paleo- to Mesoproterozoic) – Pink to pinkish gray to red, hypidiomorphic granular, phaneritic, fine- to very coarse-grained, locally gneissic granite exposed in footwall of Hot Springs fault. Phenocrysts include plagioclase, microcline, quartz, and biotite. Exsolution lamellae of plagioclase are commonly found in microcline crystals and define a perthitic texture. Groundmass is composed of feldspar, quartz, and minor chlorite. Quartz veins are common and range from mm to m-scale thickness. Pink granite is poorly to moderately foliated; gneissic granite is well foliated. Total thickness of plutonic rocks unknown.
- pCm Metamorphic rocks (Paleo- to Mesoproterozoic) – Unit mapped where metamorphic rocks constitute over 60% of exposure. Dark gray gneiss is commonly intruded by granitic to quartzose pegmatite veins up to 25 cm (10 in) wide. Quartzofeldspathic schist is dark to tannish gray and micaceous (biotite+muscovite). Both gneiss and schist are strongly foliated. Metamorphic units often exhibit low amplitude (less than 30 cm) folding and may be boudinaged. Occasional amphibolite pods (roof pendants) contain phenocrysts of plagioclase, biotite, and hornblende, and are <10 m (33 ft) in diameter. Minor reddish brown metasiltstone is observed in places. Total thickness unknown.

SUBSURFACE UNITS

- QTpwl Transitional base of the lower western piedmont facies of the Palomas Formation (lower Pliocene) – Pinkish gray to light brown to pink (7.5YR 7/2-3; 6/3) clay, silt, and fine sand interbedded with minor channel-fills of coarse sand and felsic-intermediate volcanic pebbles (with trace dark, aphanitic clasts that could be basalt). Interpreted to be 51 m (169 ft) thick in the Barney Iorio Fee #1 well. Unit is only ~6 m (20 ft) thick where QTpwl/Trvpw contact is exposed and is accordingly subsumed into QTpwl. Cross-section only.
- Trv Rincon Valley Formation (middle to upper Miocene) – Units Trvpw and Trvbf, undivided. As described in the Barney Iorio Fee #1 well log, the unit consists of interbedded clay and sandstone. Clays are sticky and mostly pink at 632-802 ft, gray at 802-975 ft, and pink to red at 975-1165 ft. At 1170-2100 ft, the unit is harder (better cemented), exhibits gypsum laminations, and may contain ash and/or carbonate beds. ~600 m (1970 ft) thick. Cross-section only.
- Tsl Lower Santa Fe Group (Oligocene to middle Miocene) – Relatively well-cemented Santa Fe Group consisting

of volcaniclastic sandstone and conglomerates. Correlative to the Hayner Ranch Formation and possibly to the Thurman Formation (Seager et al., 1971; Seager et al., 1982). Described using exposures on the Skute Stone Arroyo quadrangle (Koning et al., 2015). Estimated to be 1100 m (360 ft) thick using cross-section on Skute Stone Arroyo quadrangle. Cross-section only.

APPENDIX B

Clast-count data from the Williamsburg 7.5' quadrangle

This appendix contains tabulated clast-count data (lithology type and mean diameter, except where noted) from a variety of geologic units exposed in the Williamsburg quadrangle. These units include Pleistocene terrace and alluvial fan deposits, Palomas Formation units, and one count from piedmont facies of the Rincon Valley Formation. Location coordinates for all counts are given in NAD83 UTM zone 13S, except where noted. Lithology abbreviations include the following: Tb = basalt (typically Pliocene basalt flows, although a single basalt clast in Table A.15 likely represents an older, now-eroded flow), Tba = basaltic andesite, Tvp = Vicks Peak tuff, Thm = Hells Mesa tuff, Tkn = Kneeling Nun tuff, Trrl = Luna Park trachyandesite of the Red Rock Ranch Formation, Tad = intrusive andesite-diorite, Pa = Abo Formation, **Ob** = Bliss Formation, and Pz = Paleozoic.

TABLE B.1 CLAST TYPE AND DIAMETER (cm) FOR UNIT Qtp3

		July 1, 2014											n = 25
		UTM Location 3661879N, 284672E											
Tkn	aphanitic rhyolite	intermediate intrusive	Tb	Tba	flow-banded rhyolite	Pa	dacite	Pz limestone	lithic tuff	plagioclase-phyric andesite	volcaniclastic sandstone	aphanitic tuff	
2.5	6	4	2.5	2	3	3.5	6	3	2.5	2	3	4	
4	4	4	2	4.5	2	5							
2	3												
5.5	2												
2.5													
mean diameter (cm)	3.8	4.0	2.3	3.3	2.5	4.3	6.0	3.0	2.5	2.0	3.0	4.0	
n	4	2	2	2	2	2	1	1	1	1	1	1	
% total	16	8	8	8	8	8	4	4	4	4	4	4	

TABLE B.2 CLAST TYPE AND DIAMETER (cm) FOR UNIT Qtr4

		August 20, 2014											n = 25		
		UTM Location 3659174N, 286970E													
dacite	lithic tuff	aphanitic rhyolite	Pa	aphanitic andesite	Tba	amphibolite	Tb	COB	flow-banded rhyolite	green siltstone	jasperoid	Pz limestone	granite	Tkn	intermediate intrusive
15.5	5	4	7	2	9	2	3.5	10	12	5	18	9.5	2.5	15	7.5
2.5	6	2	6	2.5	4.5										
10	8														
4.5															
mean diameter (cm)	6.3	3.0	6.5	2.3	6.8	2.0	3.5	10.0	12.0	5.0	18.0	9.5	2.5	15.0	7.5
n	4	2	2	2	2	1	1	1	1	1	1	1	1	1	1
% total	16	8	8	8	8	4	4	4	4	4	4	4	4	4	4

TABLE B.3 CLAST TYPE AND DIAMETER (cm) FOR UNIT Qtr5

Date	October 6, 2014											n = 30			
UTM Location	3655626N, 285250E														
	aphanitic rhyolite	quartz-phyric tuff	quartzite	Tb	Thm/Tkn	Pa	granite	plagioclase-phyric andesite	Tba	COB	dacite	lithic tuff	trachyte	plagioclase-quartz-phyric tuff	Tvp
	2.5	5	2.5	3	8	5	3.5	5	5	3	7.5	8	6.5	7.5	7.5
	2	3	2	2.5	3	3	3	5.5	5						
	4	8	2.5	3	8										
	7														
mean diameter (cm)	3.9	5.3	2.3	2.8	6.3	4.0	3.3	5.3	5.0	3.0	7.5	8.0	6.5	7.5	7.5
n	4	3	3	3	3	2	2	2	2	1	1	1	1	1	1
% total	13	10	10	10	10	7	7	7	7	3	3	3	3	3	3

TABLE B.4 CLAST TYPE AND DIAMETER (cm) FOR UNIT Qtr6

Date	February 12, 2014											n = 50		
UTM Location	3664278N, 288842E													
	brown packstone	medium gray limestone with fusulinids	dark packstone or grainstone	gray wackestone	black fossiliferous carbonate	medium gray grainstone	reddish wackestone	tan siltstone	altered limestone	pink nodular siltstone	calcareous siltstone	chert	COB	dark gray dolostone
	2.5	2	5.5	2	1	2	3	1.5	1	2.5	4.5	1.5	3	4
	2.5	2	2.5	2.5	1	3	4	1.5	4	2				
	1	2.5	2.5	2	2	2	4.5	1.5						
	2.5	4	1	1	2									
	5.5	3	3.5	3										
	1	4.5	1											
	3	4	4											
	5.5	3												
mean diameter (cm)	2.9	3.1	2.9	2.1	1.5	2.3	3.8	1.5	2.5	2.3	4.5	1.5	3.0	4.0
n	8	8	7	5	4	4	3	3	2	2	1	1	1	1
% total	16	16	14	10	8	8	6	6	4	4	2	2	2	2

TABLE B.5 CLAST TYPE AND DIAMETER (cm) FOR UNIT QTpwuc

n = 47

Date July 20, 2015

UTM Location 3666426N, 285122E

Tba	plagioclase-phyric andesite	Tkn	aph. rhy. ^b	flow-banded rhyolite	lithic tuff	aph. and. ^b	basalt	chert / jasperoid	dac. ^b	Pa	plagioclase-biotite-quartz-phyric tuff	plagioclase-phyroxene-phyric andesite	quartz-sandstone-phyric tuff	Tad	Typ	volcaniclastic sandstone
1	1	1	1	1	1	1	1	1	1	1	1	1	1	1	1	1
1	1	1	1	1	1	1	1									
1	1	1	1	1	1											
1	1	1	1													
1	1	1	1													
1	1	1														
1	1	1														
1	1	1														
1	1	1														
1	1	1														
NA	NA	NA	NA	NA	NA	NA	NA	NA	NA	NA	NA	NA	NA	NA	NA	NA
n	5	5	4	3	3	2	2	1	1	1	1	1	1	1	1	1
% total	11	11	9	6	6	4	4	2	2	2	2	2	2	2	2	2

^aClast dimensions not measured.

^bLithology abbreviations: aph. = aphanitic, rhy. = rhyolite, and. = andesite, dac. = dacite.

TABLE B.6 CLAST TYPE AND DIAMETER (cm) FOR UNIT QTpwuc

Date May 1, 2015 *n* = 30

UTM Location 3663131N, 284396E

	Tkn	flow-banded rhyolite	Tba	Tb	horn-blende-phyric andesite	plagioclase-phyric andesite	Pz carbonate	jasperoid
	5	3	6.5	9	10	5	7.5	5
	2	3	7	7.5	3	2		
	4	12.5	11	10				
	6.5	8.5	11	4.5				
	9	5	3.5					
	2							
	5							
	5							
	12							
	13							
mean diameter (cm)	6.4	6.4	7.8	7.8	6.5	3.5	7.5	5.0
n	10	5	5	4	2	2	1	1
% total	33	17	17	13	7	7	3	3

TABLE B.7 CLAST TYPE AND DIAMETER (cm) FOR UNIT QTpwuc

Date		September 26, 2013										n = 25
UTM Location ^a		3664141N, 284198E										
	plagioclase-phyric andesite	Tba	basalt	chert	gray siltstone	quartz-biotite-plagioclase-phyric tuff	volcaniclastic sandstone	Tkn	dacite	Pa		
	4	2.5	4.5	2.5	1.5	4.5	3.5	4	3.5	3		
	5	3.5	4.5	2.5	3	3.5	2					
	5	2	4	2	1.5							
	2.5	1										
	7											
mean diameter (cm)	4.7	2.3	4.3	2.3	2.0	4.0	2.8	4.0	3.5	3.0		
n	5	4	3	3	3	2	2	1	1	1		
% total	20	16	12	12	12	8	8	4	4	4		

^aUTM coordinates in NAD27, zone 13S.

TABLE B.9 CLAST TYPE AND DIAMETER (cm) FOR UNIT QTpwu

Date May 1, 2015 n = 30

UTM Location 3667511N, 286410E

	Tkn	Tba	flow-banded rhyolite	Tb	dacite	Pa	pla- gioclase-phyric andesite	lithic tuff
	2	3.5	3	3.5	4.5	8.5	10	4
	3	4	3	3	3	1.5	4.5	
	4.5	3.5	3.5	2.5				
	2	4.5	3					
	6	4.5	6					
	6	3.5						
	2							
	9							
	4							
mean diameter (cm)	4.3	3.9	3.7	3.0	3.8	5.0	7.3	4.0
n	8	6	5	3	2	2	2	1
% total	27	20	17	10	7	7	7	3

TABLE B.10 CLAST TYPE AND DIAMETER (cm) FOR UNIT QTpwt

Date		July 20, 2015		UTM Location		3666279N, 285225E		n = 43			
Tba	Tkn	aphanitic rhyolite	plagioclase-phyric andesite	chert/jasperoid	flow-banded rhyolite	Typ	lithic tuff	aphanitic andesite	sanidine-phyric tuff	Tad	Tb
1	1	1	1	1	1	1	1	1	1	1	1
1	1	1	1	1	1	1	1	1	1	1	1
1	1	1	1	1	1	1	1	1	1	1	1
1	1	1	1	1	1	1	1	1	1	1	1
1	1	1	1	1	1	1	1	1	1	1	1
1	1	1	1	1	1	1	1	1	1	1	1
1	1	1	1	1	1	1	1	1	1	1	1
1	1	1	1	1	1	1	1	1	1	1	1
1	1	1	1	1	1	1	1	1	1	1	1
mean diameter (cm) ^a	NA	NA	NA	NA	NA	NA	NA	NA	NA	NA	NA
n	8	5	5	4	3	3	1	1	1	1	1
% total	23	19	12	9	7	7	2	2	2	2	2

^aClast dimensions not measured.

TABLE B.11 CLAST TYPE AND DIAMETER (cm) FOR UNIT QTpwm

Date May 1, 2015 n = 30

UTM Location 3662874N, 284569E

	Tkn	flow-banded rhyolite	Tba	plagioclase-phyric andesite	Tb	Pa	chert	dacite
	4	3	4.5	4	3.5	2	1.5	6
	3	4	7.5	4.5	1.5	2		
	3	1	4	2.5	5			
	2.5	2	2.5	3				
	2	3	3.5					
	3	3	4					
	5							
mean diameter (cm)	3.2	2.7	4.3	3.5	3.3	2.0	1.5	6.0
n	7	6	6	4	3	2	1	1
% total	23	20	20	13	10	7	3	3

TABLE B.12 CLAST TYPE AND DIAMETER (cm) FOR UNIT QTpwm

Date		September 3, 2014		n = 50					
UTM Location		3658315N, 283940E							
Tkn	Tba	flow-banded rhyolite	plagioclase-py- roxene-phyric andesite	dacite	volcaniclastic sandstone	aphanitic rhyolite	Tb	chert	plagioclase-phyric andesite
2.5	2.5	4.5	1.5	2	1	1	5	2.5	8.5
0.5	7	2	3	2.5	2	2	4		
1	3.5	1.5	5	8	4				
4	1.5	0.5	1						
3.5	0.5	2	2.5						
1	1	2	4						
2	3.5								
8.5	5								
3									
1.5									
4									
1.5									
1.5									
4.5									
3									
1.5									
4									
9									
mean diameter (cm)	3.1	2.1	2.8	4.2	2.3	1.5	4.5	2.5	8.5
n	18	8	6	3	3	2	2	1	1
% total	36	16	12	6	6	4	4	2	2

TABLE B.13 CLAST TYPE AND DIAMETER (cm) FOR UNIT QTper

Date		January 31, 2014										n = 50
UTM Location		3660038N, 289206E										
Pa	phospatic limestone	non-fossiliferous limestone	dark dolostone	gray fossiliferous limestone	green packstone	chert	dark fossiliferous limestone	quartzose sandstone	granite			
2.5	2.5	2.5	3	2	1	2	7	2	4.5			
4	3	2.5	5	11	3.5	3	1	2	4			
1	1	2	6.5	1.5	2	3.5						
2	5	3.5	4	1.5								
4	1	1	4	4.5								
2.5	4	2.5										
9.5	7.5	4										
1.5	2	1										
2	8.5											
2.5												
1												
mean diameter (cm)	3.0	2.4	4.5	4.1	2.2	2.8	4.0	2.0	4.3			
n	11	8	5	5	3	3	2	2	2			
% total	22	16	10	10	6	6	4	4	4			

TABLE B.14 CLAST TYPE AND DIAMETER (cm) FOR UNIT QTpa

Date		May 1, 2015		UTM Location		3655493N, 283871E		n = 30		
quartzite	Tkn	red-tan, very fine to fine sandstone	flow-banded rhyolite	Trri	chert/jasperoid	granite	Tba	laminated lime-stone	plagioclase-phyric andesite	petrified wood
4.5	6.5	8	7.5	5.5	9	1.5	8	11	7	0.5
3	7	2	3	5	7.5	3.5	6.5			
1	10	2	5.5	4.5	3					
3.5	12	6.5								
3.5	4									
mean diameter (cm)	3.1	4.6	5.3	5.0	6.5	2.5	7.3	11.0	7.0	0.5
n	5	4	3	3	3	2	2	1	1	1
% total	14	11	9	9	9	6	6	3	3	3

TABLE B.15 CLAST TYPE AND DIAMETER (cm) FOR UNIT Trvpw

Date May 1, 2015 n = 35

UTM Location 3667511N, 286410E

	Tba	flow-banded rhyolite	granite	plagioclase-phyric andesite	chert/jasperoid	Pa	Tkn	Pz limestone	Tb	dacite
	1	2.5	2	2	3	2.5	2	1	4	2.5
	1	3	2	1	1.5	2	0.5			
	4	1	1.5	6						
	3	3	1.5							
	3.5	2.5	1							
	3	1	2.5							
	4	0.5	0.5							
	1									
	2.5									
mean diameter (cm)	2.6	1.9	1.6	3.0	2.3	2.3	1.3	1.0	4.0	2.5
n	9	7	7	3	2	2	2	1	1	1
% total	26	20	20	9	6	6	6	3	3	3

APPENDIX C

Paleocurrent data from the Williamsburg 7.5' quadrangle

This appendix contains tabulated paleocurrent direction data (azimuthal) measured from imbrication of gravels from a variety of geologic units exposed in the Williamsburg quadrangle. These units include Pleistocene terrace and alluvial fan deposits as well as Palomas Formation units. Location coordinates for all measurements are given in NAD83 UTM zone 13S. Mean paleocurrent directions from imbrication are shown on the geologic map.

TABLE C.1 IMBRICATION PALEOCURRENT MEASUREMENTS AT WAYPOINT W-58		
		Flow direction measurements
Northing	3662317	130
Easting	279340	140
Unit	QTpwu	125
Mean	145	125
Median	145	147
n	9	168
		145
		145
		181

TABLE C.2 IMBRICATION PALEOCURRENT MEASUREMENTS AT WAYPOINT W-66						
		Flow direction measurements				
Northing	3662681	161	184	196	128	127
Easting	280698	152	152	150	142	127
Unit	QTpwu	187	159	212	187	
Mean	177	200	220	142	185	
Median	182	198	228	147	146	
n	42	216	228	147	132	
		216	228	125	156	
		191	204	179	156	
		191	204	168	152	
		191	198	143	277	

TABLE C.3 IMBRICATION PALEOCURRENT MEASUREMENTS AT WAYPOINT W-70				
		Flow direction measurements		
Northing	3662587	175	212	207
Easting	281026	165	215	197
Unit	QTpwu	120	195	215
Mean	195	232	193	187
Median	197	224	193	220
n	26	209	237	220
		196	154	
		209	172	
		180	172	
		165	217	

TABLE C.4 IMBRICATION PALEOCURRENT MEASUREMENTS AT WAYPOINT W-71a					
		Flow direction measurements			
Northing	3662517	98	151	107	128
Easting	281262	128	192	100	135
Unit	QTpwu	116	166	200	148
Mean	132	162	157	130	152
Median	132	100	145	122	152
n	38	107	141	126	155
		110	97	121	147
		115	77	113	156
		152	113	134	
		146	85	134	

TABLE C.5 IMBRICATION PALEOCURRENT MEASUREMENTS AT WAYPOINT W-71b					
		Flow direction measurements			
Northing	3662520	273	282	293	320
Easting	281268	273	308	293	291
Unit	QTpwu	273	308	284	291
Mean	282	273	243	271	323
Median	279	273	250	271	238
n	35	273	250	271	
		273	279	289	
		260	279	324	
		260	278	317	
		282	293	317	

TABLE C.6 IMBRICATION PALEOCURRENT MEASUREMENTS AT WAYPOINT W-79						
		Flow direction measurements				
Northing	3666658	160	172	163	144	120
Easting	283466	160	167	131	161	133
Unit	QTpwuc	153	167	140	161	149
Mean	159	153	175	140	163	114
Median	161	158	175	135	163	162
n	59	156	160	172	163	154
		145	160	156	163	196
		148	165	156	132	170
		148	154	152	165	185
		155	150	152	162	154
		173	178	164	162	170
		173	168	164	162	170
		180	198	162	122	136
		150	168	177	179	

TABLE C.7 IMBRICATION PALEOCURRENT MEASUREMENTS AT WAYPOINT W-85

		Flow direction measurements				
Northing	3667172	136	68	97	123	168
Easting	282824	136	62	78	82	87
Unit	QTpwuc	127	70	124	95	87
Mean	105	125	86	133	116	83
Median	103	74	91	91	110	83
n	70	85	108	103	110	83
		103	130	103	94	91
		121	88	103	118	103
		101	88	93	89	100
		101	115	80	107	100
		101	113	105	107	100
		103	136	106	136	85
		138	136	128	113	113
		126	100	123	113	87

TABLE C.8 IMBRICATION PALEOCURRENT MEASUREMENTS AT WAYPOINT W-88

		Flow direction measurements				
Northing	3666719	150	110	140	60	76
Easting	282956	150	98	130	108	100
Unit	QTpwu	150	120	130	108	100
Mean	113	92	111	130	108	85
Median	111	92	111	130	108	
n	44	145	111	95	95	
		145	111	70	88	
		148	111	88	100	
		148	116	95	91	
		148	116	111	160	

TABLE C.9 IMBRICATION PALEOCURRENT MEASUREMENTS AT WAYPOINT W-94

		Flow direction measurements				
Northing	3666301	194	184	259	236	223
Easting	283650	208	232	238	252	247
Unit	QTpwu	196	211	258	222	265
Mean	234	204	171	258	224	265
Median	239	204	220	265	225	215
n	50	204	239	265	216	268
		210	276	265	243	277
		201	276	239	244	272
		199	258	239	244	272
		166	259	244	221	250

TABLE C.10 IMBRICATION PALEOCURRENT MEASUREMENTS AT WAYPOINT WS-115						
		Flow direction measurements				
Northing	3662706	220	82	212	272	308
Easting	281709	220	105	226	275	332
Unit	QTpwm	221	197	226	252	
Mean	241	221	237	317	310	
Median	239	226	238	225	304	
n	42	217	257	272	360	
		239	220	239	360	
		239	126	321	248	
		137	254	241	280	
		115	197	272	286	

TABLE C.11 IMBRICATION PALEOCURRENT MEASUREMENTS AT WAYPOINT WS-116b						
		Flow direction measurements				
Northing	3662651	198	107	100	189	
Easting	281652	209	156	51	147	
Unit	QTpwm	55	149	110	183	
Mean	127	73	135	108	140	
Median	118	93	112	108	147	
n	35	127	104	128		
		106	115	152		
		117	248	117		
		66	118	115		
		124	118	131		

TABLE C.12 IMBRICATION PALEOCURRENT MEASUREMENTS AT WAYPOINT WS-119						
		Flow direction measurements				
Northing	3662216	172	195	176	133	160
Easting	281780	172	173	162	133	160
Unit	QTpwu	130	182	166	133	177
Mean	151	157	182	166	111	177
Median	155	147	202	155	111	122
n	57	145	165	155	110	162
		152	165	155	90	113
		143	136	152	90	129
		175	169	158	90	132
		165	155	201	85	
		153	172	118	176	
		153	176	118	174	

TABLE C.13 IMBRICATION PALEOCURRENT MEASUREMENTS AT WAYPOINT WS-120_1		Flow direction measurements	
Northing	3662480		176
Easting	281596		165
Unit	QTpwu		165
Mean	157		166
Median	165		195
n	9		162
			132
			150
			101

TABLE C.14 IMBRICATION PALEOCURRENT MEASUREMENTS AT WAYPOINT WS-120_2		Flow direction measurements		
Northing	3662480	60	56	36
Easting	281596	88	15	47
Unit	QTpwu	40	67	
Mean	48	40	67	
Median	40	60	67	
n	22	60	35	
		92	40	
		20	40	
		28	35	
		34	35	

TABLE C.15 IMBRICATION PALEOCURRENT MEASUREMENTS AT WAYPOINT WS-120_3		Flow direction measurements		
Northing	3662479	124	74	117
Easting	281600	124	84	128
Unit	QTpwu	124	96	127
Mean	122	124	122	121
Median	124	124	122	130
n	27	140	122	178
		140	122	155
		140	122	
		101	119	
		74	140	

TABLE C.16 IMBRICATION PALEOCURRENT MEASUREMENTS AT WAYPOINT WS-120_4

		Flow direction measurements				
Northing	3662480	202	188	150	166	146
Easting	281599	229	202	150	166	146
Unit	QTpwu	204	225	181	166	146
Mean	186	162	208	207	167	147
Median	186	180	208	209	176	192
n	62	202	215	207	216	192
		186	215	205	227	182
		186	159	205	227	179
		186	159	106	218	184
		225	209	215	163	200
		225	177	208	163	
		202	177	172	135	
		185	150	196	135	

TABLE C.17 IMBRICATION PALEOCURRENT MEASUREMENTS AT WAYPOINT WS-120b

		Flow direction measurements			
Northing	3662474	199	170	160	164
Easting	281598	150	170	160	
Unit	QTpwu	166	163	177	
Mean	174	187	163	177	
Median	170	187	166	179	
n	31	192	166	180	
		198	159	180	
		198	159	168	
		170	192	168	
		170	192	175	

TABLE C.18 IMBRICATION PALEOCURRENT MEASUREMENTS AT WAYPOINT WS-127b

		Flow direction measurements				
Northing	3661898	287	171	135	122	100
Easting	282453	269	98	135	122	140
Unit	QTpwu	269	98	135	163	108
Mean	178	292	98	158	93	289
Median	145	268	93	135	93	289
n	71	268	95	140	93	289
		250	95	140	99	296
		246	167	151	110	296
		246	167	151	110	341
		244	99	145	110	307
		295	162	150	129	324
		295	162	153	129	
		295	114	137	171	
		282	111	137	103	
		348	123	113	104	

TABLE C.19 IMBRICATION PALEOCURRENT MEASUREMENTS AT WAYPOINT WS-130_1					
		Flow direction measurements			
Northing	3661576	167	76	151	126
Easting	282802	197	95	168	126
Unit	QTpwu	187	100	168	103
Mean	146	147	100	185	103
Median	153	126	181	155	117
n	36	127	181	155	83
		124	225	156	
		124	180	159	
		166	127	168	
		166	151	168	

TABLE C.20 IMBRICATION PALEOCURRENT MEASUREMENTS AT WAYPOINT WS-130_2					
		Flow direction measurements			
Northing	3661576	42	124	106	
Easting	282802	70	129	101	
Unit	QTpwu	70	129	101	
Mean	96	117	96	101	
Median	102	103	40	124	
n	28	103	40	112	
		92	40	112	
		92	114	94	
		92	114		
		124	106		

TABLE C.21 IMBRICATION PALEOCURRENT MEASUREMENTS AT WAYPOINT WS-143b						
		Flow direction measurements				
Northing	3665547	85	122	114	126	99
Easting	284807	108	116	92	95	99
Unit	QTpwu	108	106	104	114	87
Mean	108	104	111	104	108	87
Median	108	104	103	143	114	97
n	53	104	98	143	114	105
		96	98	143	114	105
		118	98	108	119	116
		110	109	113	92	116
		112	109	106	92	
		112	99	126	92	

TABLE C.22 IMBRICATION PALEOCURRENT MEASUREMENTS AT WAYPOINT WS-143b-upper

		Flow direction measurements		
Northing	3665547	157	133	225
Easting	284807	143	90	137
Unit	QTpwu	135	127	125
Mean	138	113	138	99
Median	134	92	169	108
n	28	167	218	65
		132	122	98
		169	122	112
		165	150	
		138	207	

TABLE C.23 IMBRICATION PALEOCURRENT MEASUREMENTS AT WAYPOINT WS-144b

		Flow direction measurements	
Northing	3665537	182	125
Easting	284967	168	183
Unit	QTpwm	176	173
Mean	181	210	224
Median	183	188	157
n	19	183	195
		185	199
		167	203
		182	190
		150	

TABLE C.24 IMBRICATION PALEOCURRENT MEASUREMENTS AT WAYPOINT WS-145

		Flow direction measurements				
Northing	3665463	166	164	172	112	116
Easting	284954	166	105	187	132	116
Unit	QTpwm	172	150	177	103	112
Mean	130	172	156	142	228	68
Median	132	163	154	160	97	156
n	57	215	151	185	15	107
		143	151	148	54	110
		143	214	93	98	110
		143	108	93	198	75
		86	95	132	91	
		100	94	49	49	
		160	160	131	77	

TABLE C.25 IMBRICATION PALEOCURRENT MEASUREMENTS AT WAYPOINT WS-148_1

		Flow direction measurements		
Northing	3665693	88	124	77
Easting	284941	88	183	108
Unit	QTpwuc	88	54	120
Mean	106	73	64	125
Median	108	125	68	156
n	25	125	82	
		103	127	
		114	133	
		118	89	
		128	89	

TABLE C.26 IMBRICATION PALEOCURRENT MEASUREMENTS AT WAYPOINT WS-148_2

		Flow direction measurements	
Northing	3665693	256	250
Easting	284941	270	
Unit	QTpwuc	277	
Mean	274	224	
Median	270	327	
n	11	311	
		294	
		289	
		265	
		250	

TABLE C.27 IMBRICATION PALEOCURRENT MEASUREMENTS AT WAYPOINT WS-148_3

		Flow direction measurements	
Northing	3665693	116	93
Easting	284941	116	110
Unit	QTpwuc	97	110
Mean	106	97	116
Median	110	97	116
n	15	103	
		103	
		110	
		110	
		93	

TABLE C.28 IMBRICATION PALEOCURRENT MEASUREMENTS AT WAYPOINT WS-149						
		Flow direction measurements				
Northing	3665704	92	115	140	168	109
Easting	284910	112	86	137	168	116
Unit	QTpwuc	101	87	137	168	143
Mean	103	98	85	137	168	104
Median	107	123	77	137	162	104
n	128	123	134	130	163	98
		180	128	130	158	103
		180	45	90	188	106
		186	45	111	140	46
		180	58	127	43	46
		180	62	118	55	46
		180	109	118	55	108
		32	109	99	60	108
		32	108	99	58	23
		171	123	68	118	0
		57	123	68	117	108
		59	148	68	136	99
		59	148	44	105	99
		85	94	44	120	107
		73	94	44	113	138
		73	112	0	147	144
		68	107	23	146	86
		81	107	31	138	90
		83	61	112	128	90
		96	122	37	91	
		115	122	22	171	

TABLE C.29 IMBRICATION PALEOCURRENT MEASUREMENTS AT WAYPOINT WS-152_1						
		Flow direction measurements				
Northing	3665783	87	98	89	97	
Easting	284662	134	105	89	97	
Unit	QTpwuc	134	94	98	122	
Mean	97	165	94	162	126	
Median	94	100	92	162		
n	34	100	78	166		
		85	78	91		
		62	99	91		
		29	26	62		
		46	67	65		

TABLE C.30 IMBRICATION PALEOCURRENT MEASUREMENTS AT WAYPOINT WS-152_2

		Flow direction measurements				
Northing	3665783	295	276	225	190	275
Easting	284662	318	276	221	169	186
Unit	QTpwuc	318	308	221	307	237
Mean	251	318	253	232	307	243
Median	250	265	253	233	315	243
n	47	287	244	196	259	189
		255	236	183	250	189
		255	228	183	250	
		292	228	256	275	
		292	225	243	275	

TABLE C.31 IMBRICATION PALEOCURRENT MEASUREMENTS AT WAYPOINT WS-159b_1

		Flow direction measurements				
Northing	3664586				170	
Easting	284835				128	
Unit	QTpwt				128	
Mean	124				126	
Median	125				124	
n	8				124	
					97	
					97	

TABLE C.32 IMBRICATION PALEOCURRENT MEASUREMENTS AT WAYPOINT WS-159b_2

		Flow direction measurements				
Northing	3664589	164	128	195	177	198
Easting	284831	145	122	195	177	252
Unit	QTpwt	145	168	163	199	252
Mean	183	183	144	177	199	269
Median	177	169	144	192	103	179
n	71	165	148	192	103	242
		165	148	125	184	250
		140	148	202	202	246
		152	190	198	264	264
		123	138	215	264	264
		124	194	215	268	258
		122	155	190	268	
		133	185	170	259	
		110	152	234	140	
		101	152	234	140	

TABLE C.33 IMBRICATION PALEOCURRENT MEASUREMENTS AT WAYPOINT WS-159b_3

		Flow direction measurements	
Northing	3664591	119	122
Easting	284826	110	122
Unit	QTpwt	122	
Mean	104	119	
Median	119	82	
n	12	38	
		91	
		121	
		129	
		71	

TABLE C.34 IMBRICATION PALEOCURRENT MEASUREMENTS AT WAYPOINT WS-159b_4

		Flow direction measurements	
Northing	3664595	170	164
Easting	284823	110	
Unit	QTpwt	130	
Mean	104	180	
Median	119	176	
n	12	184	
		173	
		173	
		167	
		164	

TABLE C.35 IMBRICATION PALEOCURRENT MEASUREMENTS AT WAYPOINT WS-159c_1

		Flow direction measurements	
Northing	3664592		119
Easting	284789		119
Unit	QTpwu		110
Mean	122		133
Median	126		133
n	10		85
			133
			133
			154
			103

TABLE C.36 IMBRICATION PALEOCURRENT MEASUREMENTS AT WAYPOINT WS-159c_2

		Flow direction measurements	
Northing	3664592	17	344
Easting	284786	17	10
Unit	QTpwu	34	10
Mean	9	22	
Median	10	18	
n	13	18	
		0	
		0	
		353	
		353	

TABLE C.37 IMBRICATION PALEOCURRENT MEASUREMENTS AT WAYPOINT WS-159c_3

		Flow direction measurements	
Northing	3664596		185
Easting	284778		185
Unit	QTpwu		200
Mean	194		204
Median	193		
n	4		

TABLE C.38 IMBRICATION PALEOCURRENT MEASUREMENTS AT WAYPOINT WS-160_1

		Flow direction measurements				
Northing	3664751	97	50	112	96	122
Easting	284508	97	89	112	117	122
Unit	QTpwu	99	72	104	82	147
Mean	99	99	60	141	85	118
Median	97	76	138	150	170	118
n	62	91	67	101	175	138
		93	64	110	143	138
		63	64	139	47	129
		88	88	51	27	104
		88	53	72	70	75
		85	134	72	136	
		85	59	103	103	
		95	52	138	122	

TABLE C.39 IMBRICATION PALEOCURRENT MEASUREMENTS AT WAYPOINT WS-160_2			
		Flow direction measurements	
Northing	3664752	68	75
Easting	284501	78	116
Unit	QTpwu	110	116
Mean	91	110	74
Median	99	109	74
n	17	109	63
		56	105
		85	
		103	
		99	

TABLE C.40 IMBRICATION PALEOCURRENT MEASUREMENTS AT WAYPOINT WS-160_3				
		Flow direction measurements		
Northing	3664758	84	131	235
Easting	284494	68	64	
Unit	QTpwu	68	107	
Mean	141	182	68	
Median	131	116	68	
n	21	131	216	
		137	216	
		137	196	
		135	237	
		131	235	

TABLE C.41 IMBRICATION PALEOCURRENT MEASUREMENTS AT WAYPOINT WS-160_4			
		Flow direction measurements	
Northing	3664753		134
Easting	284502		166
Unit	QTpwu		153
Mean	178		165
Median	171		220
n	10		175
			201
			195
			217
			153

TABLE C.42 IMBRICATION PALEOCURRENT MEASUREMENTS AT WAYPOINT WS-168_1

		Flow direction measurements				
Northing	3664105	118	140	118	135	120
Easting	284629	171	87	118	135	120
Unit	QTpwu	171	80	117	135	103
Mean	130	145	158	117	135	114
Median	130	145	154	117	135	
n	44	157	136	124	135	
		162	133	122	115	
		162	135	122	105	
		171	135	123	126	
		140	123	123	102	

TABLE C.43 IMBRICATION PALEOCURRENT MEASUREMENTS AT WAYPOINT WS-168_2

		Flow direction measurements	
Northing	3664111	178	101
Easting	284628	178	101
Unit	QTpwu	110	98
Mean	112	123	116
Median	105	123	
n	14	78	
		78	
		78	
		95	
		108	

TABLE C.44 IMBRICATION PALEOCURRENT MEASUREMENTS AT WAYPOINT WS-170_1

		Flow direction measurements	
Northing	3664010	108	66
Easting	284506	108	72
Unit	QTpwuc	110	72
Mean	114	105	61
Median	90	110	215
n	17	90	215
		90	265
		90	
		78	
		77	

TABLE C.45 IMBRICATION PALEOCURRENT MEASUREMENTS AT WAYPOINT WS-170_2						
		Flow direction measurements				
Northing	3664007	206	227	148	144	125
Easting	284501	210	223	179	102	99
Unit	QTpwuc	252	204	142	108	68
Mean	141	268	222	174	113	81
Median	131	223	128	174	113	118
n	54	151	128	208	113	105
		143	157	208	113	8
		144	146	110	106	352
		133	167	110	106	6
		133	123	110	106	47
		280	148	121	125	

TABLE C.46 IMBRICATION PALEOCURRENT MEASUREMENTS AT WAYPOINT WS-175_1						
		Flow direction measurements				
Northing	3664266	113	138	93		
Easting	284116	113	138	121		
Unit	QTpwuc	180	138	90		
Mean	131	110	157	88		
Median	126	110	175	151		
n	26	91	168	151		
		130	168			
		140	119			
		116	119			
		158	119			

TABLE C.47 IMBRICATION PALEOCURRENT MEASUREMENTS AT WAYPOINT WS-175_2						
		Flow direction measurements				
Northing	3664270	126	22			
Easting	284115	126	9			
Unit	QTpwuc	156	9			
Mean	36	358	33			
Median	24	358	6			
n	18	320	32			
		32	0			
		32	25			
		64				
		22				

TABLE C.48 IMBRICATION PALEOCURRENT MEASUREMENTS AT WAYPOINT WS-175_3		Flow direction measurements			
Northing	3664270	18	10	12	31
Easting	284113	27	24	20	
Unit	QTpwuc	30	17	49	
Mean	18	30	17	51	
Median	12	0	2	42	
n	31	0	2	57	
		11	12	38	
		11	12	38	
		0	12	15	
		0	12	345	

TABLE C.49 IMBRICATION PALEOCURRENT MEASUREMENTS AT WAYPOINT WS-181_1		Flow direction measurements				
Northing	3667208	141	127	118	159	150
Easting	285600	141	133	102	159	138
Unit	QTpwu	151	141	162	135	138
Mean	127	117	141	160	135	113
Median	122	116	82	173	104	111
n	58	117	108	173	96	111
		148	108	107	76	123
		148	100	105	105	99
		148	100	122	123	99
		122	109	112	123	110
		122	118	112	168	
		127	118	157	176	

TABLE C.50 IMBRICATION PALEOCURRENT MEASUREMENTS AT WAYPOINT WS-181_2		Flow direction measurements			
Northing	3667206	152	147	150	73
Easting	285604	163	147	147	
Unit	QTpwu	163	143	147	
Mean	145	171	154	178	
Median	147	171	154	178	
n	31	139	145	126	
		139	145	139	
		145	159	150	
		147	133	150	
		145	131	73	

TABLE C.51 IMBRICATION PALEOCURRENT MEASUREMENTS AT WAYPOINT WS-197a_1

		Flow direction measurements	
Northing	3667269	90	0
Easting	284197	90	4
Unit	QTpwuc	88	122
Mean	77	91	
Median	90	125	
n	13	95	
		109	
		0	
		100	
		81	

TABLE C.52 IMBRICATION PALEOCURRENT MEASUREMENTS AT WAYPOINT WS-197a_2

		Flow direction measurements	
Northing	3667274	265	224
Easting	284197	265	233
Unit	QTpwuc	237	207
Mean	237	237	221
Median	235	237	232
n	16	225	222
		256	
		252	
		254	
		231	

TABLE C.53 IMBRICATION PALEOCURRENT MEASUREMENTS AT WAYPOINT WS-197a_3

		Flow direction measurements	
Northing	3667265	73	10
Easting	284195	73	
Unit	QTpwuc	52	
Mean	31	13	
Median	24	13	
n	11	6	
		24	
		24	
		40	
		10	

TABLE C.54 IMBRICATION PALEOCURRENT MEASUREMENTS AT WAYPOINT WS-197a_4

		Flow direction measurements	
Northing	3667277	11	61
Easting	284200	11	
Unit	QTpwuc	8	
Mean	13	350	
Median	8	3	
n	11	3	
		352	
		13	
		0	
		47	

TABLE C.55 IMBRICATION PALEOCURRENT MEASUREMENTS AT WAYPOINT WS-197b_1

		Flow direction measurements	
Northing	3667278	290	258
Easting	284205	290	242
Unit	QTpwuc	240	259
Mean	256	250	262
Median	250	250	
n	14	262	
		244	
		250	
		235	
		247	

TABLE C.56 IMBRICATION PALEOCURRENT MEASUREMENTS AT WAYPOINT WS-197b_1

		Flow direction measurements	
Northing	3667281		60
Easting	284207		61
Unit	QTpwuc		71
Mean	61		72
Median	61		50
n	8		43
			43
			85

TABLE C.57 IMBRICATION PALEOCURRENT MEASUREMENTS AT WAYPOINT WS-199_1		
		Flow direction measurements
Northing	3666785	328
Easting	284348	328
Unit	QTpwuc	328
Mean	314	294
Median	318	294
n	10	318
		318
		318
		318
		298

TABLE C.58 IMBRICATION PALEOCURRENT MEASUREMENTS AT WAYPOINT WS-199_2		
		Flow direction measurements
Northing	3666784	103
Easting	284342	108
Unit	QTpwuc	61
Mean	98	61
Median	103	61
n	7	147
		147

TABLE C.59 IMBRICATION PALEOCURRENT MEASUREMENTS AT WAYPOINT WS-199_3				
		Flow direction measurements		
Northing	3666781	73	15	22
Easting	284343	73	92	22
Unit	QTpwuc	80	96	85
Mean	70	80	77	85
Median	74	80	77	128
n	25	74	66	
		74	66	
		52	99	
		52	97	
		71	15	

TABLE C.60 IMBRICATION PALEOCURRENT MEASUREMENTS AT WAYPOINT WS-199_4

		Flow direction measurements	
Northing	3666779	140	153
Easting	284343	129	157
Unit	QTpwuc	124	179
Mean	138	119	188
Median	131	119	138
n	17	131	113
		129	113
		116	
		148	
		148	

TABLE C.61 IMBRICATION PALEOCURRENT MEASUREMENTS AT WAYPOINT WS-199_5

		Flow direction measurements	
Northing	3666786	147	116
Easting	284354	147	116
Unit	QTpwuc	125	
Mean	122	125	
Median	121	117	
n	12	111	
		102	
		93	
		125	
		143	

TABLE C.62 IMBRICATION PALEOCURRENT MEASUREMENTS AT WAYPOINT WS-199_6

		Flow direction measurements	
Northing	3666788	147	128
Easting	284353	167	128
Unit	QTpwuc	170	100
Mean	136	185	93
Median	137	160	164
n	20	152	108
		150	107
		140	107
		143	107
		125	133

TABLE C.63 IMBRICATION PALEOCURRENT MEASUREMENTS AT WAYPOINT WS-236_1

		Flow direction measurements			
Northing	3655382	204	220	242	198
Easting	283565	204	210	235	196
Unit	QTpa	203	209	235	194
Mean	212	203	209	228	200
Median	210	203	185	228	200
n	38	200	210	215	212
		234	182	215	212
		198	260	215	215
		192	231	211	
		192	219	240	

TABLE C.64 IMBRICATION PALEOCURRENT MEASUREMENTS AT WAYPOINT WS-236_2

		Flow direction measurements	
Northing	3655372	117	162
Easting	283566	117	102
Unit	QTpa	135	208
Mean	138	112	131
Median	133	100	176
n	20	148	110
		118	113
		146	141
		207	142
		162	108

TABLE C.65 IMBRICATION PALEOCURRENT MEASUREMENTS AT WAYPOINT WS-242

		Flow direction measurements				
Northing	3655535	200	170	171	190	223
Easting	283125	200	160	171	168	180
Unit	QTpwu	159	160	190	172	120
Mean	170	159	175	160	135	228
Median	173	159	161	160	137	190
n	72	175	205	171	137	190
		175	178	140	185	190
		162	176	140	192	189
		162	181	140	155	178
		162	181	173	180	0
		162	185	177	179	178
		152	200	177	178	151
		151	203	161	178	
		153	190	160	165	
		170	183	190	165	

TABLE C.66 IMBRICATION PALEOCURRENT MEASUREMENTS AT WAYPOINT WS-245b						
		Flow direction measurements				
Northing	3656110	157	187	180	187	162
Easting	283155	150	173	185	187	162
Unit	QTpwu	167	172	186	161	167
Mean	173	167	172	168	133	185
Median	172	142	172	173	151	187
n	97	142	171	169	151	170
		144	171	170	180	170
		157	167	157	194	189
		157	161	187	167	172
		147	148	192	165	198
		147	143	180	161	198
		173	169	180	166	189
		173	197	172	177	171
		160	204	172	172	178
		176	187	195	172	157
		147	192	195	150	157
		192	172	195	200	157
		182	172	210	210	
		182	158	210	210	
		202	159	195	162	

TABLE C.67 IMBRICATION PALEOCURRENT MEASUREMENTS AT WAYPOINT WS-250b						
		Flow direction measurements				
Northing	3654396	173	180	168	143	
Easting	283542	187	180	192	143	
Unit	QTpwuc	190	187	192	143	
Mean	175	190	187	192	165	
Median	178	198	158	172	154	
n	35	174	158	184		
		174	188	184		
		177	172	184		
		173	178	189		
		189	178	137		

TABLE C.68 IMBRICATION PALEOCURRENT MEASUREMENTS AT WAYPOINT WS-252b						
		Flow direction measurements				
Northing	3654368	242	182	275	275	360
Easting	283503	323	208	293	275	282
Unit	QTpwuc	320	190	83	298	282
Mean	234	322	199	56	266	282
Median	244	322	188	210	246	261
n	66	208	188	133	275	360
		277	173	142	288	302
		275	198	212	327	272
		215	167	142	271	278
		217	163	122	271	229
		217	190	110	316	
		284	152	110	297	
		213	313	110	280	
		184	317	201	225	

TABLE C.69 IMBRICATION PALEOCURRENT MEASUREMENTS AT WAYPOINT WS-253						
		Flow direction measurements				
Northing	3654234	59	34	85	67	
Easting	283413	72	74	70	43	
Unit	QTpwuc	68	74	123	34	
Mean	69	62	74	52		
Median	68	77	55	63		
n	33	124	55	92		
		124	53	71		
		47	53	71		
		47	85	106		
		35	72	45		

TABLE C.70 IMBRICATION PALEOCURRENT MEASUREMENTS AT WAYPOINT WS-256-lower						
		Flow direction measurements				
Northing	3654230	146	174	121	110	135
Easting	283215	148	174	111	138	133
Unit	QTpwuc	18	155	120	138	104
Mean	133	172	143	120	136	110
Median	133	194	0	118	128	110
n	59	151	187	116	147	105
		114	284	128	139	91
		124	284	117	136	121
		118	281	110	136	133
		141	0	110	134	133
		138	150	115	134	96
		132	150	110	135	

TABLE C.71 IMBRICATION PALEOCURRENT MEASUREMENTS AT WAYPOINT WS-256-upper

		Flow direction measurements				
Northing	3654230	148	323	69	11	28
Easting	283215	175	6	29	11	26
Unit	QTpwuc	358	25	48	11	5
Mean	36	176	25	48	11	5
Median	26	138	35	30	8	347
n	73	138	35	14	48	342
		178	5	14	48	1
		58	338	6	47	355
		58	5	32	45	3
		114	5	37	32	3
		138	357	37	32	340
		65	3	44	22	15
		42	3	42	22	9
		41	62	357	12	
		58	62	11	28	

TABLE C.72 IMBRICATION PALEOCURRENT MEASUREMENTS AT WAYPOINT WS-256-top

		Flow direction measurements		
Northing	3654227	45	80	150
Easting	283216	45	80	150
Unit	QTpwuc	38	53	
Mean	93	111	72	
Median	82	78	72	
n	22	78	72	
		110	110	
		110	110	
		110	147	
		83	147	

TABLE C.73 IMBRICATION PALEOCURRENT MEASUREMENTS AT WAYPOINT WS-260

		Flow direction measurements				
Northing	3654170	68	65	61	88	114
Easting	282847	40	65	58	88	118
Unit	QTpwuc	54	62	58	82	68
Mean	64	42	50	50	78	68
Median	63	80	61	50	89	33
n	70	48	81	48	74	62
		83	41	48	74	48
		70	53	24	68	75
		70	53	24	80	47
		67	70	59	80	47
		67	40	59	75	48
		63	63	89	68	48
		61	31	89	62	96
		65	28	89	111	62

TABLE C.74 IMBRICATION PALEOCURRENT MEASUREMENTS AT WAYPOINT WS-261b-lower

		Flow direction measurements		
Northing	3654235	42	68	108
Easting	282963	78	75	106
Unit	QTpwu	78	39	104
Mean	83	78	39	118
Median	83	34	95	155
n	26	34	105	146
		33	59	
		103	88	
		103	110	
		40	108	

TABLE C.75 IMBRICATION PALEOCURRENT MEASUREMENTS AT WAYPOINT WS-261b-upper

		Flow direction measurements				
Northing	3654231	167	235	200	163	182
Easting	282968	205	192	200	162	194
Unit	QTpwu	122	12	185	171	194
Mean	173	212	145	180	171	201
Median	178	204	32	180	160	201
n	60	204	32	180	175	222
		208	216	189	170	222
		120	132	189	165	222
		208	124	219	160	172
		249	126	219	156	146
		249	112	170	156	146
		235	168	163	156	129

TABLE C.76 IMBRICATION PALEOCURRENT MEASUREMENTS AT WAYPOINT WS-264-1

		Flow direction measurements		
Northing	3654626	345	345	9
Easting	282628	345	358	346
Unit	QTpwuc	350	9	28
Mean	358	350	359	
Median	358	350	359	
n	23	355	3	
		355	3	
		358	3	
		355	8	
		345	9	

TABLE C.77 IMBRICATION PALEOCURRENT MEASUREMENTS AT WAYPOINT WS-264-2				
		Flow direction measurements		
Northing	3654622	70	38	19
Easting	282624	43	30	19
Unit	QTpwuc	36	30	31
Mean	37	61	30	89
Median	32	61	31	22
n	30	55	10	23
		35	18	5
		58	25	3
		46	32	53
		37	32	53

TABLE C.78 IMBRICATION PALEOCURRENT MEASUREMENTS AT WAYPOINT WS-264-3				
		Flow direction measurements		
Northing	3654617	114	105	
Easting	282627	114	82	
Unit	QTpwuc	105	88	
Mean	102	110	90	
Median	106	110		
n	14	106		
		106		
		110		
		95		
		95		

TABLE C.79 IMBRICATION PALEOCURRENT MEASUREMENTS AT WAYPOINT WS-264-4					
		Flow direction measurements			
Northing	3654626	73	105	55	57
Easting	282623	73	98	55	57
Unit	QTpwuc	56	70	66	6
Mean	61	56	70	78	124
Median	61	72	61	73	125
n	35	72	61	24	
		30	58	24	
		45	60	64	
		56	65	7	
		56	65	7	

TABLE C.80 IMBRICATION PALEOCURRENT MEASUREMENTS AT WAYPOINT WS-273a-1

		Flow direction measurements	
Northing	3655115	250	
Easting	281619	250	
Unit	QTpwu	220	
Mean	222	219	
Median	219	207	
n	7	202	
		209	

TABLE C.81 IMBRICATION PALEOCURRENT MEASUREMENTS AT WAYPOINT WS-273a-2

		Flow direction measurements	
Northing	3655115	346	17
Easting	281619	348	8
Unit	QTpwu	350	8
Mean	0	10	
Median	357	352	
n	13	350	
		357	
		357	
		7	
		7	

TABLE C.82 IMBRICATION PALEOCURRENT MEASUREMENTS AT WAYPOINT WS-273a-3

		Flow direction measurements	
Northing	3655115	132	
Easting	281619	132	
Unit	QTpwu	116	
Mean	135	116	
Median	132	158	
n	6	158	

TABLE C.83 IMBRICATION PALEOCURRENT MEASUREMENTS AT WAYPOINT WS-273a-4

		Flow direction measurements				
Northing	3655115	43	9	42	23	116
Easting	281619	43	9	46	39	125
Unit	QTpwu	82	0	30	63	128
Mean	55	82	3	30	60	57
Median	41	78	3	12	52	121
n	49	38	3	23	41	0
		113	22	32	153	142
		358	22	32	111	125
		25	35	3	180	100
		25	42	23	133	

TABLE C.84 IMBRICATION PALEOCURRENT MEASUREMENTS AT WAYPOINT WS-273a-5

		Flow direction measurements		
Northing	3655115	191	222	182
Easting	281619	191	222	165
Unit	QTpwu	195	214	
Mean	199	204	214	
Median	195	207	220	
n	22	161	222	
		195	190	
		190	190	
		208	175	
		227	182	

TABLE C.85 IMBRICATION PALEOCURRENT MEASUREMENTS AT WAYPOINT WS-273a-6

		Flow direction measurements		
Northing	3655115	30	57	30
Easting	281619	34	10	21
Unit	QTpwu	8	10	86
Mean	30	8	352	86
Median	11	358	0	105
n	29	5	0	81
		7	11	81
		6	359	75
		6	359	75
		34	15	

TABLE C.86 IMBRICATION PALEOCURRENT MEASUREMENTS AT WAYPOINT WS-273a-7

		Flow direction measurements	
Northing	3655115	167	168
Easting	281619	158	182
Unit	QTpwu	152	210
Mean	168	179	
Median	167	179	
n	13	160	
		134	
		162	
		162	
		174	

TABLE C.87 IMBRICATION PALEOCURRENT MEASUREMENTS AT WAYPOINT WS-273b

		Flow direction measurements				
Northing	3655115	141	161	169	203	253
Easting	281613	160	161	170	203	224
Unit	QTpwu	160	147	170	241	216
Mean	191	144	168	171	184	226
Median	173	144	212	165	184	232
n	60	144	212	165	196	248
		152	254	140	242	249
		227	254	136	270	248
		166	158	139	260	227
		162	158	157	260	183
		161	158	157	239	223
		161	164	199	174	228

TABLE C.88 IMBRICATION PALEOCURRENT MEASUREMENTS AT WAYPOINT WS-274

		Flow direction measurements				
Northing	3655070	135	202	162	173	174
Easting	281735	93	146	163	158	174
Unit	QTpwu	148	146	163	158	174
Mean	171	171	168	163	178	228
Median	174	182	168	174	178	212
n	74	182	158	174	185	212
		100	148	174	185	195
		120	180	174	185	205
		160	180	174	202	205
		118	180	173	197	154
		115	180	173	197	194
		119	179	172	197	189
		193	175	162	166	189
		193	154	162	166	175
		193	154	173	155	

TABLE C.89 IMBRICATION PALEOCURRENT MEASUREMENTS AT WAYPOINT WS-285						
		Flow direction measurements				
Northing	3655094	3	47	70	332	50
Easting	281358	3	52	70	330	31
Unit	QTpwu	19	52	70	358	31
Mean	18	25	64	0	320	42
Median	25	25	56	31	320	45
n	54	25	56	31	324	45
		50	16	76	324	318
		50	19	65	337	343
		50	16	335	358	324
		47	16	342	358	324
		47	7	325	44	

TABLE C.90 IMBRICATION PALEOCURRENT MEASUREMENTS AT WAYPOINT WS-289-1						
		Flow direction measurements				
Northing	3655195	157	180	158	136	153
Easting	280408	147	150	158	136	159
Unit	QTpwu	188	169	165	136	168
Mean	160	158	169	138	208	207
Median	158	145	171	138	208	136
n	54	170	180	160	131	136
		180	153	124	157	136
		180	153	124	140	136
		173	175	184	140	136
		204	144	148	195	136
		180	144	182	195	

TABLE C.91 IMBRICATION PALEOCURRENT MEASUREMENTS AT WAYPOINT WS-289-2						
		Flow direction measurements				
Northing	3655181	183	307			
Easting	280418	183	307			
Unit	QTpwu	183	191			
Mean	228	265	191			
Median	223	206	225			
n	19	206	236			
		223	256			
		223	256			
		222	256			
		213				

TABLE C.92 IMBRICATION PALEOCURRENT MEASUREMENTS AT WAYPOINT WS-289-3				
		Flow direction measurements		
Northing	3655181	317	325	259
Easting	280418	310	248	259
Unit	QTpwu	245	190	288
Mean	262	221	190	236
Median	253	221	221	236
n	28	222	276	314
		291	258	314
		290	233	314
		247	233	
		325	242	

TABLE C.93 IMBRICATION PALEOCURRENT MEASUREMENTS AT WAYPOINT WS-289-4						
		Flow direction measurements				
Northing	3655181	182	150	197	123	202
Easting	280418	182	154	197	123	
Unit	QTpwu	209	186	163	254	
Mean	176	172	186	159	254	
Median	182	190	192	162	254	
n	41	190	192	162	129	
		166	205	144	129	
		170	205	124	188	
		170	202	124	188	
		170	202	95	188	

TABLE C.94 IMBRICATION PALEOCURRENT MEASUREMENTS AT WAYPOINT WS-290_1						
		Flow direction measurements				
Northing	3655347	266	181	181	198	207
Easting	280105	266	195	226	198	219
Unit	QTpwu	278	195	226	183	208
Mean	214	262	206	206	183	205
Median	207	262	206	206	183	194
n	53	218	195	207	234	215
		210	195	207	222	195
		192	180	196	222	283
		279	229	196	212	244
		255	220	192	180	
		217	214	192	219	

TABLE C.95 IMBRICATION PALEOCURRENT MEASUREMENTS AT WAYPOINT WS-290_2

		Flow direction measurements			
Northing	3655352	76	155	139	50
Easting	280104	76	151	146	
Unit	QTpwu	77	151	119	
Mean	124	108	129	147	
Median	139	105	129	147	
n	31	105	150	144	
		153	150	118	
		153	143	130	
		105	143	151	
		105	139	50	

TABLE C.96 IMBRICATION PALEOCURRENT MEASUREMENTS AT WAYPOINT WS-290b

		Flow direction measurements				
Northing	3655358	165	70	178	119	178
Easting	280090	165	135	178	131	178
Unit	QTpwu	166	120	153	130	144
Mean	127	164	125	153	130	119
Median	130	168	103	153	101	47
n	114	168	130	142	101	38
		163	173	142	10	108
		167	135	129	55	108
		167	135	169	66	94
		182	125	111	28	74
		182	194	111	78	78
		175	171	97	74	77
		175	123	97	92	59
		177	123	97	92	59
		164	143	117	131	43
		236	148	117	94	42
		236	93	170	85	98
		220	93	172	84	148
		190	109	142	98	83
		185	170	145	89	83
185	212	172	89	83		
70	148	103	152	88		
70	162	117	152			

TABLE C.97 IMBRICATION PALEOCURRENT MEASUREMENTS AT WAYPOINT WS-290c			
		Flow direction measurements	
Northing	3655348	147	
Easting	280078	154	
Unit	QTpwu	146	
Mean	156	151	
Median	152	152	
n	10	152	
		152	
		220	
		141	
		141	

TABLE C.98 IMBRICATION PALEOCURRENT MEASUREMENTS AT WAYPOINT WS-290d-1			
		Flow direction measurements	
Northing	3655358	212	250
Easting	280060	276	250
Unit	QTpwu	238	243
Mean	218	183	243
Median	215	183	
n	14	183	
		183	
		180	
		215	
		215	

TABLE C.99 IMBRICATION PALEOCURRENT MEASUREMENTS AT WAYPOINT WS-290d-2					
		Flow direction measurements			
Northing	3655358	156	165	151	178
Easting	280060	156	165	160	195
Unit	QTpwu	175	207	160	212
Mean	179	175	207	160	
Median	183	138	195	157	
n	33	183	191	157	
		183	192	208	
		183	195	208	
		195	193	175	
		195	151	190	

TABLE C.100 IMBRICATION PALEOCURRENT MEASUREMENTS AT WAYPOINT WS-293				
		Flow direction measurements		
Northing	3655286	17	45	98
Easting	279628	4	45	122
Unit	QTpwuc	60	65	45
Mean	61	53	71	23
Median	59	73	71	38
n	30	43	92	38
		57	92	112
		15	111	114
		15	103	33
		67	102	15

TABLE C.101 IMBRICATION PALEOCURRENT MEASUREMENTS AT WAYPOINT WS-294-1				
		Flow direction measurements		
Northing	3655250	55	127	
Easting	279539	56	98	
Unit	QTpwuc	56	103	
Mean	67	41	88	
Median	56	41	32	
n	19	90	32	
		80	32	
		103	359	
		103	25	
		103		

TABLE C.102 IMBRICATION PALEOCURRENT MEASUREMENTS AT WAYPOINT WS-294-2				
		Flow direction measurements		
Northing	3655245	17	17	
Easting	279536	17	17	
Unit	QTpwuc	17	6	
Mean	14	37	3	
Median	17	37	10	
n	19	5	0	
		5	21	
		5	2	
		15	25	
		17		

TABLE C.103 IMBRICATION PALEOCURRENT MEASUREMENTS AT WAYPOINT WS-300-1

		Flow direction measurements	
Northing	3654044	251	222
Easting	281651	251	170
Unit	QTpwu	268	238
Mean	245	267	253
Median	245	297	
n	14	312	
		229	
		229	
		222	
		222	

TABLE C.104 IMBRICATION PALEOCURRENT MEASUREMENTS AT WAYPOINT WS-300-2

		Flow direction measurements		
Northing	3654045	73	103	102
Easting	281650	70	104	
Unit	QTpwu	72	102	
Mean	90	53	102	
Median	102	53	102	
n	21	53	140	
		41	119	
		53	130	
		63	130	
		103	130	

TABLE C.105 IMBRICATION PALEOCURRENT MEASUREMENTS AT WAYPOINT WS-300-3

		Flow direction measurements		
Northing	3654040	207	140	260
Easting	281648	196	140	213
Unit	QTpwu	196	66	245
Mean	177	129	66	255
Median	196	233	48	252
n	27	215	120	244
		181	200	211
		158	152	
		148	152	
		140	202	

TABLE C.106 IMBRICATION PALEOCURRENT MEASUREMENTS AT WAYPOINT WS-300-4

		Flow direction measurements		
Northing	3654053	68	66	49
Easting	281649	68	49	53
Unit	QTpwu	68	49	38
Mean	52	68	39	38
Median	56	65	33	
n	24	65	78	
		58	26	
		58	26	
		65	23	
		65	28	

TABLE C.107 IMBRICATION PALEOCURRENT MEASUREMENTS AT WAYPOINT WS-300-5

		Flow direction measurements	
Northing	3654049	98	139
Easting	281648	98	139
Unit	QTpwu	62	110
Mean	128	125	142
Median	133	125	183
n	17	105	183
		78	183
		140	
		140	
		133	

TABLE C.108 IMBRICATION PALEOCURRENT MEASUREMENTS AT WAYPOINT WS-301

		Flow direction measurements				
Northing	3660774	141	97	173	143	355
Easting	284031	141	97	100	134	144
Unit	QTpwt	141	141	100	173	144
Mean	145	119	141	107	173	86
Median	141	119	141	107	125	86
n	80	119	116	107	125	125
		154	116	141	125	125
		154	123	141	242	178
		154	186	211	200	138
		125	90	114	200	189
		125	90	114	6	96
		166	90	114	6	96
		166	285	297	163	95
		166	220	115	170	95
		166	220	115	172	220
		164	220	143	172	220

TABLE C.109 IMBRICATION PALEOCURRENT MEASUREMENTS AT WAYPOINT WS-305						
		Flow direction measurements				
Northing	3660773	128	160	322	170	145
Easting	283914	128	153	105	172	145
Unit	QTpa	168	145	130	310	129
Mean	154	135	145	186	115	129
Median	145	155	145	156	118	179
n	47	155	188	156	130	96
		132	140	138	148	96
		132	165	138	152	
		185	155	110	132	
		160	322	110	105	

TABLE C.110 IMBRICATION PALEOCURRENT MEASUREMENTS AT WAYPOINT WS-305a						
		Flow direction measurements				
Northing	3655346	141	0	106	218	
Easting	283568	141	0	26	3	
Unit	QTpa	105	24	131	157	
Mean	92	105	24	131	157	
Median	55	19	24	152	151	
n	39	46	24	129	28	
		46	25	55	324	
		46	25	55	348	
		34	106	55	225	
		34	106	55		

TABLE C.111 IMBRICATION PALEOCURRENT MEASUREMENTS AT WAYPOINT WS-305b						
		Flow direction measurements				
Northing	3655342	358	122	143	34	3
Easting	283567	358	140	85	121	157
Unit	QTpa	56	140	86	223	157
Mean	127	56	65	86	233	151
Median	122	151	65	186	56	28
n	48	151	65	186	56	324
		151	65	105	56	348
		151	44	105	56	225
		122	44	27	56	
		122	143	34	218	

TABLE C.112 IMBRICATION PALEOCURRENT MEASUREMENTS AT WAYPOINT WS-306						
		Flow direction measurements				
Northing	3655745	10	14	53	348	15
Easting	283396	10	357	350	354	18
Unit	QTpwm	6	357	353	24	18
Mean	14	41	308	346	24	310
Median	15	31	3	346	357	310
n	120	116	357	31	17	3
		116	15	26	23	12
		33	15	26	23	54
		33	15	48	23	42
		155	0	48	24	349
		345	307	341	0	349
		27	309	341	349	342
		27	309	144	349	29
		2	330	144	358	357
		2	330	128	336	357
		19	17	128	336	357
		19	17	17	326	35
		21	17	17	26	35
		13	17	29	347	47
		19	17	29	347	47
		19	1	8	347	18
		19	1	8	16	18
		330	1	8	16	329
		14	53	348	16	15

TABLE C.113 IMBRICATION PALEOCURRENT MEASUREMENTS AT WAYPOINT WS-506						
		Flow direction measurements				
Northing	3667194	239	215	137	232	233
Easting	288209	240	206	137	232	233
Unit	QTpa	197	157	199	223	233
Mean	214	219	157	206	223	227
Median	223	208	200	203	239	227
n	73	259	170	203	237	232
		223	170	190	237	232
		208	191	190	225	239
		119	197	224	225	239
		241	239	225	208	228
		222	169	276	230	246
		240	169	276	243	246
		200	197	193	243	230
		217	184	215	243	
		177	193	232	243	

TABLE C.114 IMBRICATION PALEOCURRENT MEASUREMENTS AT WAYPOINT WS-507_1

		Flow direction measurements		
Northing	3667240	263	227	190
Easting	288505	263	229	193
Unit	QTpa	225	229	193
Mean	213	250	227	241
Median	227	227	195	145
n	28	196	216	145
		232	245	157
		232	226	157
		238	205	
		238	190	

TABLE C.115 IMBRICATION PALEOCURRENT MEASUREMENTS AT WAYPOINT WS-507_2

		Flow direction measurements	
Northing	3667237	240	173
Easting	288496	158	155
Unit	QTpa	201	210
Mean	195	190	280
Median	184	190	280
n	16	185	151
		180	
		180	
		182	
		170	

TABLE C.116 IMBRICATION PALEOCURRENT MEASUREMENTS AT WAYPOINT 130926_2

		Flow direction measurements				
Northing	3664345	106	145	65	51	99
Easting	284149	139	119	86	71	99
Unit	QTpwu	110	221	59	104	221
Mean	115	141	87	106	109	58
Median	106	163	84	58	184	121
n	67	96	205	144	95	104
		119	134	106	102	51
		116	90	109	95	71
		178	74	100	96	95
		146	99	121	119	102
		140	163	53	159	102
		159	86	79	221	
		190	109	106	205	
		154	221	104	74	

TABLE C.117 IMBRICATION PALEOCURRENT MEASUREMENTS AT WAYPOINT 131104_1-2a						
		Flow direction measurements				
Northing	3665693	316	260	290	249	251
Easting	289828	273	306	309	321	251
Unit	QTpe	311	299	279	310	284
Mean	289	301	255	285	275	290
Median	290	264	274	341	266	290
n	66	265	298	256	265	341
		291	371	249	346	281
		302	251	281	291	321
		310	313	246	316	265
		301	284	326	273	265
		268	289	321	302	
		276	295	323	260	
		315	284	266	306	
		321	290	269	271	

TABLE C.118 IMBRICATION PALEOCURRENT MEASUREMENTS AT WAYPOINT 131104_2-3d						
		Flow direction measurements				
Northing	3663637	204	248	181	170	170
Easting	288860	156	229	196	141	173
Unit	QTpa	210	170	176	136	150
Mean	190	264	173	202	160	150
Median	185	250	140	151	210	202
n	62	250	150	194	236	151
		206	206	218	131	205
		189	254	156	180	141
		162	239	134	198	236
		166	149	256	170	198
		247	256	209	249	
		174	154	205	210	
		178	138	150	250	

TABLE C.119 IMBRICATION PALEOCURRENT MEASUREMENTS AT WAYPOINT 140130_1-6

		Flow direction measurements				
Northing	3660677	190	189	194	171	224
Easting	288290	171	213	206	189	240
Unit	QTpa	189	190	196	189	205
Mean	208	235	256	197	230	205
Median	203	230	229	206	245	191
n	84	236	234	190	176	192
		245	226	175	184	192
		176	215	196	184	197
		170	224	174	172	190
		184	240	244	173	175
		230	246	216	219	196
		172	198	201	219	196
		250	205	216	219	201
		214	245	184	213	216
		234	191	175	213	184
		173	210	221	256	221
		219	192	190	215	

TABLE C.120 IMBRICATION PALEOCURRENT MEASUREMENTS AT WAYPOINT 140131_2-3

		Flow direction measurements				
Northing	3660038	226	265	237	231	234
Easting	289206	203	176	181	262	234
Unit	QTper	201	252	254	203	171
Mean	224	244	262	299	244	182
Median	220	234	185	216	234	216
n	79	235	197	191	234	216
		234	220	249	204	181
		195	231	244	204	299
		198	234	224	204	191
		221	171	276	201	276
		204	169	190	176	190
		201	209	226	262	184
		280	226	184	262	184
		304	182	243	185	231
		302	216	200	197	262
		244	224	214	197	

TABLE C.121 IMBRICATION PALEOCURRENT MEASUREMENTS AT WAYPOINT 140212_5						
		Flow direction measurements				
Northing	3664312	241	249	273	270	218
Easting	289596	222	230	287	217	221
Unit	QTpe	240	239	253	255	221
Mean	250	241	266	261	230	276
Median	249	236	280	264	251	276
n	75	281	252	274	222	273
		280	218	259	240	259
		226	222	256	236	256
		235	271	235	235	235
		276	230	248	262	229
		262	221	229	262	229
		262	252	235	231	270
		273	277	242	266	217
		236	265	249	280	217
		231	276	235	252	251

TABLE C.122 IMBRICATION PALEOCURRENT MEASUREMENTS AT WAYPOINT 140221_2-5a						
		Flow direction measurements				
Northing	3663141	176	200	180	168	179
Easting	289032	197	138	194	194	189
Unit	Qfe	211	201	181	176	194
Mean	184	191	175	182	197	182
Median	180	219	150	203	191	176
n	77	188	171	176	170	176
		203	170	170	204	170
		221	176	189	228	166
		170	170	166	211	178
		194	141	171	200	166
		184	174	181	138	181
		204	171	178	175	204
		196	193	166	171	168
		218	179	155	176	
		228	189	181	170	
		211	162	204	141	

TABLE C.123 IMBRICATION PALEOCURRENT MEASUREMENTS AT WAYPOINT 140701_2

		Flow direction measurements				
Northing	3661778	126	146	130	105	114
Easting	285273	126	96	130	84	114
Unit	QTpwm	101	96	130	84	84
Mean	113	101	134	130	104	84
Median	116	101	134	130	104	116
n	129	101	123	100	104	116
		101	123	104	66	116
		104	123	124	66	116
		104	65	124	124	70
		104	65	124	124	70
		104	65	140	124	129
		104	96	140	124	90
		123	96	136	124	90
		123	90	136	116	114
		123	97	136	116	114
		123	97	121	116	143
		126	120	125	131	143
		126	111	148	131	89
		126	111	148	134	89
		126	141	148	91	84
		161	141	148	91	84
		161	114	148	91	84
		139	107	118	91	84
		139	107	118	91	84
		139	107	118	104	
		146	107	105	104	

TABLE C.124 IMBRICATION PALEOCURRENT MEASUREMENTS AT WAYPOINT 140701_3

		Flow direction measurements				
Northing	3661879	121	129	115	138	109
Easting	284672	115	81	130	123	109
Unit	Qtp3	130	119	129	129	92
Mean	115	129	87	164	91	134
Median	116	116	71	120	91	144
n	127	164	71	124	156	125
		120	144	140	119	125
		124	94	140	129	125
		140	81	135	129	125
		135	95	135	81	99
		124	109	124	119	95
		136	110	136	87	95
		111	92	111	71	95
		88	134	111	71	121
		131	144	88	71	89
		145	125	88	71	100
		127	99	131	71	100
		96	95	131	144	100
		109	138	145	94	100
		138	121	145	81	105
		123	89	145	81	105
		129	100	127	81	105
		91	105	127	81	109
		156	109	127	95	
		90	121	109	95	
		119	121	109	95	

TABLE C.125 IMBRICATION PALEOCURRENT MEASUREMENTS AT WAYPOINT 140701_4c

		Flow direction measurements				
Northing	3661404	121	74	93	80	106
Easting	285512	98	93	74	130	80
Unit	QTpwu	124	121	74	103	130
Mean	99	91	121	74	70	130
Median	93	80	124	74	66	102
n	62	71	91	93	106	66
		70	71	93	80	66
		66	70	86	99	106
		130	66	101	109	106
		78	78	139	86	99
		132	78	111	139	
		149	149	96	139	
		93	93	106	96	

TABLE C.126 IMBRICATION PALEOCURRENT MEASUREMENTS AT WAYPOINT 140710A_1d						
		Flow direction measurements				
Northing	3658441	174	190	175	164	172
Easting	288821	206	171	199	164	184
Unit	QTpa	164	165	178	164	196
Mean	183	166	155	191	164	196
Median	186	186	169	160	166	200
n	89	194	171	159	186	190
		166	168	196	186	170
		179	199	189	186	190
		201	179	198	186	187
		172	199	203	194	187
		184	155	168	194	190
		196	194	180	194	171
		200	209	183	194	165
		190	201	190	179	155
		170	200	174	179	169
		170	204	206	201	169
		190	146	206	201	171
		187	174	206	201	

TABLE C.127 IMBRICATION PALEOCURRENT MEASUREMENTS AT WAYPOINT 140710B_1d						
		Flow direction measurements				
Northing	3658441	199	201	199	189	180
Easting	288821	199	200	199	189	180
Unit	QTpa	179	200	178	198	183
Mean	187	179	204	178	198	183
Median	190	199	204	191	203	183
n	56	199	204	160	203	183
		155	146	159	203	190
		155	174	159	203	190
		194	174	196	168	
		194	175	196	168	
		209	175	189	180	
		209	199	189	180	

TABLE C.128 IMBRICATION PALEOCURRENT MEASUREMENTS AT WAYPOINT 140729A_1-2a

		Flow direction measurements	
Northing	3660504	139	177
Easting	279820	129	164
Unit	QTpwu	123	182
Mean	142	96	165
Median	147	150	99
n	20	131	144
		153	134
		155	104
		166	150
		131	151

TABLE C.129 IMBRICATION PALEOCURRENT MEASUREMENTS AT WAYPOINT 140729B_1-2a

		Flow direction measurements		
Northing	3660504	140	141	109
Easting	279820	134	151	111
Unit	QTpwu	134	141	119
Mean	127	106	114	108
Median	127	94	125	91
n	30	191	123	96
		155	134	133
		98	120	166
		100	165	135
		136	127	126

TABLE C.130 IMBRICATION PALEOCURRENT MEASUREMENTS AT WAYPOINT 140730_2-1

		Flow direction measurements				
Northing	3659140	166	154	172	136	170
Easting	279474	150	151	154	142	117
Unit	QTpwuc	119	190	144	145	151
Mean	156	160	185	162	154	135
Median	154	184	179	174	170	184
n	49	161	141	201	197	165
		171	164	140	149	146
		165	124	140	152	144
		173	151	130	177	151
		147	161	126	134	

TABLE C.131 IMBRICATION PALEOCURRENT MEASUREMENTS AT WAYPOINT 140730_2-1b

		Flow direction measurements				
Northing	3660074	117	140	155	152	136
Easting	278860	101	188	138	156	184
Unit	QTpwu	155	117	155	138	197
Mean	146	145	151	196	91	165
Median	148	166	135	199	110	153
n	50	153	190	128	103	150
		141	150	139	108	151
		136	128	116	127	156
		120	169	159	132	138
		166	146	124	201	154

TABLE C.132 IMBRICATION PALEOCURRENT MEASUREMENTS AT WAYPOINT 140730_2-1c

		Flow direction measurements				
Northing	3661051	93	106	124	135	149
Easting	278485	120	123	144	156	119
Unit	QTpwuc	89	125	151	137	130
Mean	133	98	126	109	110	164
Median	129	111	129	106	126	166
n	50	125	146	119	160	131
		122	118	125	164	168
		124	128	141	150	159
		135	114	141	175	126
		140	161	150	165	123

TABLE C.133 IMBRICATION PALEOCURRENT MEASUREMENTS AT WAYPOINT 140730_2-3

		Flow direction measurements				
Northing	3659005	158	150	130	161	167
Easting	279834	153	176	105	132	175
Unit	QTpwuc	164	190	82	209	208
Mean	158	184	126	136	191	216
Median	160	137	134	146	171	158
n	50	151	209	118	169	186
		124	105	105	139	166
		196	120	121	190	204
		205	125	122	194	203
		161	136	125	174	202

TABLE C.134 IMBRICATION PALEOCURRENT MEASUREMENTS AT WAYPOINT 140731A_3-3b

		Flow direction measurements	
Northing	3658484	146	96
Easting	283110	101	55
Unit	QTpwt	100	46
Mean	93	98	70
Median	98	65	110
n	19	71	100
		108	78
		110	88
		144	76
		104	

TABLE C.135 IMBRICATION PALEOCURRENT MEASUREMENTS AT WAYPOINT 140731B_3-3b

		Flow direction measurements	
Northing	3658484		259
Easting	283110		291
Unit	QTpwt		269
Mean	262		251
Median	262		241
n	6		264

TABLE C.136 IMBRICATION PALEOCURRENT MEASUREMENTS AT WAYPOINT 140731A_3-4a

		Flow direction measurements	
Northing	3658640	131	90
Easting	281458	96	116
Unit	QTpwu	111	71
Mean	104	125	141
Median	99	85	99
n	15	91	
		95	
		91	
		110	
		108	

TABLE C.137 IMBRICATION PALEOCURRENT MEASUREMENTS AT WAYPOINT 140731B_3-4a

		Flow direction measurements	
Northing	3658640	134	146
Easting	281458	115	120
Unit	QTpwu	135	160
Mean	135	116	159
Median	136	111	136
n	15	115	
		141	
		145	
		142	
		148	

TABLE C.138 IMBRICATION PALEOCURRENT MEASUREMENTS AT WAYPOINT 140820_1a

		Flow direction measurements				
Northing	3659174	231	170	181	185	216
Easting	286970	181	204	196	201	164
Unit	Qtr4	216	242	197	178	160
Mean	171	186	176	205	199	209
Median	199	186	194	235	175	204
n	50	241	212	198	220	208
		207	197	204	172	155
		182	170	202	203	166
		176	214	230	210	228
		190	174	222	230	171

TABLE C.139 IMBRICATION PALEOCURRENT MEASUREMENTS AT WAYPOINT 140820_2a

		Flow direction measurements		
Northing	3658350	70	55	112
Easting	286010	94	104	78
Unit	QTpa	112	107	64
Mean	93	65	80	100
Median	95	95	86	103
n	25	90	83	
		86	99	
		124	121	
		97	82	
		122	103	

TABLE C.140 IMBRICATION PALEOCURRENT MEASUREMENTS AT WAYPOINT 140903_1c

		Flow direction measurements		
Northing	3658188	154	90	166
Easting	284403	129	131	110
Unit	QTpwm	148	129	148
Mean	127	107	86	155
Median	129	98	139	109
n	25	115	128	
		155	175	
		71	172	
		33	180	
		103	112	

TABLE C.141 IMBRICATION PALEOCURRENT MEASUREMENTS AT WAYPOINT 140903A_3

		Flow direction measurements		
Northing	3658315	45	27	44
Easting	283940	41	82	71
Unit	QTpwm	60	56	72
Mean	67	26	24	65
Median	65	45	92	68
n	25	63	69	
		80	133	
		109	101	
		61	101	
		100	53	

TABLE C.142 IMBRICATION PALEOCURRENT MEASUREMENTS AT WAYPOINT 140903B_3

		Flow direction measurements		
Northing	3658315	72	51	39
Easting	283940	107	70	69
Unit	QTpwm	79	98	106
Mean	86	111	114	97
Median	84	51	91	110
n	25	80	84	
		97	83	
		146	92	
		72	81	
		85	56	

TABLE C.143 IMBRICATION PALEOCURRENT MEASUREMENTS AT WAYPOINT 140903_4			
		Flow direction measurements	
Northing	3657970	50	75
Easting	282858	72	103
Unit	QTpwt	52	67
Mean	77	54	98
Median	77	78	105
n	15	77	
		48	
		85	
		81	
		107	

TABLE C.144 IMBRICATION PALEOCURRENT MEASUREMENTS AT WAYPOINT 140910_1-2c				
		Flow direction measurements		
Northing	3657529	161	160	127
Easting	285332	145	183	148
Unit	QTpwm	174	152	198
Mean	159	146	243	124
Median	157	121	134	163
n	25	157	176	
		91	136	
		241	180	
		171	125	
		207	143	

TABLE C.145 IMBRICATION PALEOCURRENT MEASUREMENTS AT WAYPOINT 140930_2				
		Flow direction measurements		
Northing	3661328	126	124	124
Easting	283002	153	197	78
Unit	QTpwu	156	116	119
Mean	129	167	148	139
Median	126	151	123	101
n	27	101	116	175
		108	56	133
		88	146	
		79	134	
		151	266	

TABLE C.146 IMBRICATION PALEOCURRENT MEASUREMENTS AT WAYPOINT 141006A_1-1e

		Flow direction measurements		
Northing	3654831	112	109	236
Easting	284549	104	122	107
Unit	QTpwuc	114	150	153
Mean	97	73	41	78
Median	92	89	57	80
n	25	146	42	
		168	43	
		49	105	
		42	51	
		91	61	

TABLE C.147 IMBRICATION PALEOCURRENT MEASUREMENTS AT WAYPOINT 141006B_1-1e

		Flow direction measurements		
Northing	3654831	291	109	136
Easting	284549	51	101	41
Unit	QTpwuc	111	64	41
Mean	70	51	70	75
Median	68	55	39	226
n	25	26	55	
		52	56	
		81	74	
		50	112	
		119	68	

TABLE C.148 IMBRICATION PALEOCURRENT MEASUREMENTS AT WAYPOINT 141006_1-2b

		Flow direction measurements			
Northing	3655626	228	191	334	29
Easting	285250	72	180	325	18
Unit	Qtr5	41	210	229	179
Mean	214	0	153	226	182
Median	200	353	171	224	232
n	35	207	352	2	
		216	241	198	
		194	190	223	
		228	140	229	
		186	200	226	

TABLE C.149 IMBRICATION PALEOCURRENT MEASUREMENTS AT WAYPOINT 141029_1e

		Flow direction measurements				
Northing	3664454	231	230	217	251	277
Easting	288554	250	258	192	223	240
Unit	QTpe	280	186	267	291	204
Mean	242	250	256	276	260	225
Median	243	228	198	224	274	254
n	52	212	211	255	262	219
		235	220	291	276	235
		222	269	243	253	250
		244	212	271	229	
		216	215	257	206	
		213	242	291	270	

TABLE C.150 IMBRICATION PALEOCURRENT MEASUREMENTS AT WAYPOINT 141029_3

		Flow direction measurements			
Northing	3665004	266	267	281	250
Easting	288726	245	260	289	261
Unit	QTpe	251	240	292	312
Mean	254	250	241	274	
Median	251	256	286	251	
n	33	264	223	247	
		226	199	264	
		218	209	249	
		265	251	284	
		244	218	256	

TABLE C.151 IMBRICATION PALEOCURRENT MEASUREMENTS AT WAYPOINT 141029_4e

		Flow direction measurements				
Northing	3665863	294	2	232	350	312
Easting	289977	331	319	285	316	266
Unit	QTpe	332	286	304	305	320
Mean	306	309	275	333	314	322
Median	307	309	321	320	266	304
n	56	348	291	336	267	266
		310	355	310	281	344
		279	294	270	359	341
		227	335	281	274	
		252	330	294	250	
		348	329	1	244	
		349	297	321	273	

TABLE C.152 IMBRICATION PALEOCURRENT MEASUREMENTS AT WAYPOINT 141107_1c

		Flow direction measurements				
Northing	3658842	199	170	226	190	164
Easting	287595	174	163	167	179	176
Unit	QTper	177	195	235	215	205
Mean	182	160	165	194	152	170
Median	179	161	174	157	181	
n	44	194	159	172	151	
		134	185	149	204	
		180	153	179	184	
		178	206	203	209	
		177	218	215	202	

TABLE C.153 IMBRICATION PALEOCURRENT MEASUREMENTS AT WAYPOINT 141107_3

		Flow direction measurements				
Northing	3658275	190	178	205	153	150
Easting	289680	218	281	220	197	206
Unit	QTper	224	274	195	211	211
Mean	197	214	270	197	208	222
Median	199	188	179	255	148	204
n	52	204	270	161	124	194
		206	184	169	200	225
		226	241	170	181	182
		157	201	129	179	
		154	216	155	146	
		150	231	159	210	

TABLE C.154 IMBRICATION PALEOCURRENT MEASUREMENTS AT WAYPOINT 141107_3b

		Flow direction measurements			
Northing	3657907	226	268	196	181
Easting	289205	256	204	174	200
Unit	QTper	222	199	178	
Mean	217	209	194	158	
Median	218	243	200	219	
n	32	233	250	240	
		225	244	218	
		206	180	237	
		218	216	251	
		249	179	259	

TABLE C.155 IMBRICATION PALEOCURRENT MEASUREMENTS AT WAYPOINT 141107_5b				
		Flow direction measurements		
Northing	3658043	246	162	193
Easting	288894	234	205	169
Unit	QTper	187	213	179
Mean	210	175	217	215
Median	216	233	256	
n	24	249	176	
		190	190	
		236	221	
		230	223	
		220	225	

TABLE C.156 IMBRICATION PALEOCURRENT MEASUREMENTS AT WAYPOINT 141120_1-2b				
		Flow direction measurements		
Northing	3656912	182	194	241
Easting	289696	246	224	201
Unit	QTpef	250	227	209
Mean	228	216	176	254
Median	231	254	264	263
n	26	170	249	251
		284	250	
		222	247	
		234	186	
		219	211	

TABLE C.157 IMBRICATION PALEOCURRENT MEASUREMENTS AT WAYPOINT 141120_1-3a						
		Flow direction measurements				
Northing	3656175	220	203	234	225	177
Easting	289068	180	174	181	255	210
Unit	QTpa	219	186	208	216	209
Mean	212	184	156	193	194	175
Median	212	226	250	228	207	244
n	52	259	263	218	248	214
		181	275	194	212	195
		204	214	223	224	241
		180	244	211	249	
		173	249	241	209	
		191	149	226	189	

TABLE C.158 IMBRICATION PALEOCURRENT MEASUREMENTS AT WAYPOINT 141120_1-3d

		Flow direction measurements		
Northing	3655928	264	236	278
Easting	289499	223	214	236
Unit	QTpe	296	212	268
Mean	244	314	207	272
Median	236	246	268	285
n	25	232	200	
		200	227	
		239	200	
		266	204	
		267	234	

TABLE C.159 IMBRICATION PALEOCURRENT MEASUREMENTS AT WAYPOINT 141120_1-4d

		Flow direction measurements		
Northing	3655667	245	217	241
Easting	288860	238	160	195
Unit	QTpa	245	149	207
Mean	213	203	210	164
Median	211	294	161	265
n	26	249	175	250
		226	212	
		266	252	
		149	174	
		205	173	

TABLE C.160 IMBRICATION PALEOCURRENT MEASUREMENTS AT WAYPOINT 141121_2-1a

		Flow direction measurements		
Northing	3653893	200	179	221
Easting	287664	226	172	246
Unit	Qtr4	222	211	221
Mean	213	210	229	220
Median	219	234	209	184
n	26	187	249	223
		246	198	
		221	191	
		187	217	
		225	212	

TABLE C.161 IMBRICATION PALEOCURRENT MEASUREMENTS AT WAYPOINT 141121_2-3

		Flow direction measurements		
Northing	3653878	291	261	290
Easting	288948	0	294	
Unit	QTpe	281	300	
Mean	298	310	262	
Median	294	332	310	
n	21	325	314	
		279	280	
		294	307	
		268	312	
		318	270	

TABLE C.162 IMBRICATION PALEOCURRENT MEASUREMENTS AT WAYPOINT 141121_2-4b

		Flow direction measurements		
Northing	3654682	218	231	195
Easting	288642	240	249	184
Unit	QTpe	254	265	216
Mean	225	241	258	220
Median	220	246	239	196
n	25	260	206	
		197	217	
		249	208	
		210	194	
		204	230	

TABLE C.163 IMBRICATION PALEOCURRENT MEASUREMENTS AT WAYPOINT 141121_2-5

		Flow direction measurements				
Northing	3656265	174	223	180	205	180
Easting	288458	194	193	195	195	140
Unit	QTpa	202	181	196	187	168
Mean	188	220	205	184	210	186
Median	191	230	179	225	200	174
n	57	205	166	210	194	186
		197	164	141	208	191
		210	199	202	190	155
		203	171	206	136	176
		177	180	161	156	
		194	191	146	181	
		221	143	211	192	

TABLE C.164 IMBRICATION PALEOCURRENT MEASUREMENTS AT WAYPOINT 141126_1c

		Flow direction measurements	
Northing	3657356	146	157
Easting	281208	168	127
Unit	QTpwuc	155	158
Mean	157	115	191
Median	155	179	152
n	15	155	
		180	
		149	
		177	
		150	

TABLE C.165 IMBRICATION PALEOCURRENT MEASUREMENTS AT WAYPOINT 141126_1h

		Flow direction measurements		
Northing	3657938	191	254	180
Easting	281894	174	241	173
Unit	QTpwu	233	211	156
Mean	211	224	246	231
Median	213	187	251	221
n	25	209	195	
		213	220	
		236	181	
		200	221	
		222	206	

TABLE C.166 IMBRICATION PALEOCURRENT MEASUREMENTS AT WAYPOINT 141126_5a

		Flow direction measurements			
Northing	3657195	87	136	154	127
Easting	283808	111	135	98	129
Unit	QTpwm	114	159	61	
Mean	107	96	96	96	
Median	104	85	139	95	
n	32	113	120	84	
		98	97	124	
		102	105	91	
		76	128	111	
		64	104	103	

TABLE C.167 IMBRICATION PALEOCURRENT MEASUREMENTS AT WAYPOINT 150127_1a

		Flow direction measurements	
Northing	3654549	266	
Easting	288313	254	
Unit	Qfe	233	
Mean	250	279	
Median	252	234	
n	10	261	
		271	
		226	
		227	
		249	

TABLE C.168 IMBRICATION PALEOCURRENT MEASUREMENTS AT WAYPOINT 150127_1e

		Flow direction measurements	
Northing	3654223	194	
Easting	287905	224	
Unit	Qfe	240	
Mean	208	210	
Median	202	194	
n	6	185	

TABLE C.169 IMBRICATION PALEOCURRENT MEASUREMENTS AT WAYPOINT 150127A_3a

		Flow direction measurements			
Northing	3655754	137	132	252	255
Easting	283427	182	220	185	218
Unit	QTpa	112	110	252	60
Mean	206	150	140	207	335
Median	214	185	42	212	
n	34	265	216	282	
		350	88	260	
		125	60	350	
		350	240	281	
		118	234	277	

TABLE C.170 IMBRICATION PALEOCURRENT MEASUREMENTS AT WAYPOINT 150127B_3a

		Flow direction measurements	
Northing	3655754	197	270
Easting	283427	207	251
Unit	QTpa	210	245
Mean	231	253	237
Median	239	232	240
n	16	258	247
		270	
		75	
		200	
		140	

TABLE C.171 IMBRICATION PALEOCURRENT MEASUREMENTS AT WAYPOINT 150317A_1-1b

		Flow direction measurements		
Northing	3656535	51	65	51
Easting	280032	17	343	61
Unit	QTpwuc	17	33	25
Mean	35	45	64	25
Median	41	29	40	90
n	25	136	41	
		336	54	
		336	46	
		330	64	
		318	64	

TABLE C.172 IMBRICATION PALEOCURRENT MEASUREMENTS AT WAYPOINT 150317B_1-1b

		Flow direction measurements	
Northing	3656535	59	92
Easting	280032	39	160
Unit	QTpwuc	163	144
Mean	119	163	144
Median	160	163	180
n	19	356	254
		356	126
		356	126
		168	356
		92	

TABLE C.173 IMBRICATION PALEOCURRENT MEASUREMENTS AT WAYPOINT 150317A_1-1d

		Flow direction measurements		
Northing	3656426	154	116	179
Easting	280793	154	153	206
Unit	QTpwuc	203	131	232
Mean	183	203	90	232
Median	188	203	185	120
n	25	148	233	
		194	233	
		194	210	
		143	185	
		188	239	

TABLE C.174 IMBRICATION PALEOCURRENT MEASUREMENTS AT WAYPOINT 150317B_1-1d

		Flow direction measurements		
Northing	3656426	182	119	140
Easting	280793	120	98	109
Unit	QTpwuc	70	103	181
Mean	123	178	136	160
Median	119	125	97	114
n	25	141	97	
		168	97	
		145	196	
		86	64	
		104	64	

TABLE C.175 IMBRICATION PALEOCURRENT MEASUREMENTS AT WAYPOINT 150317C_1-1d

		Flow direction measurements		
Northing	3656426	268	310	269
Easting	280793	254	319	232
Unit	QTpwuc	254	287	232
Mean	266	181	287	224
Median	268	179	249	209
n	27	272	330	172
		327	303	129
		290	295	
		266	295	
		266	324	

TABLE C.176 IMBRICATION PALEOCURRENT MEASUREMENTS AT WAYPOINT 150317_1-1e

		Flow direction measurements				
Northing	3656392	80	324	115	74	5
Easting	280984	80	324	75	60	5
Unit	QTpwuc	95	62	113	28	11
Mean	64	134	36	78	38	30
Median	74	45	65	138	38	30
n	45	120	11	55	110	
		120	11	20	110	
		58	11	20	110	
		106	141	78	44	
		118	129	74	30	

TABLE C.177 IMBRICATION PALEOCURRENT MEASUREMENTS AT WAYPOINT 150317A_1-2a

		Flow direction measurements	
Northing	3657254	31	81
Easting	280863	31	175
Unit	QTpwuc	103	26
Mean	58	123	23
Median	51	123	23
n	20	150	23
		76	339
		92	339
		70	344
		171	12

TABLE C.178 IMBRICATION PALEOCURRENT MEASUREMENTS AT WAYPOINT 150317B_1-2a

		Flow direction measurements	
Northing	3657254	122	150
Easting	280863	104	320
Unit	QTpwuc	86	50
Mean	84	71	50
Median	83	92	120
n	16	92	79
		56	
		56	
		139	
		66	

TABLE C.179 IMBRICATION PALEOCURRENT MEASUREMENTS AT WAYPOINT 150317_1-2d

		Flow direction measurements		
Northing	3656534	121	56	79
Easting	281488	71	189	131
Unit	QTpwuc	71	189	92
Mean	99	59	119	43
Median	96	100	119	87
n	30	15	161	87
		124	197	99
		124	211	33
		101	226	68
		64	79	50

TABLE C.180 IMBRICATION PALEOCURRENT MEASUREMENTS AT WAYPOINT 150317_1-2g

		Flow direction measurements				
Northing	3656882	60	74	71	31	106
Easting	282039	60	81	78	36	96
Unit	QTpwuc	60	28	83	81	110
Mean	74	64	112	83	113	134
Median	76	11	112	116	136	134
n	54	26	112	115	11	106
		26	73	124	8	89
		68	108	100	8	80
		68	86	27	71	64
		17	113	26	14	107
		55	71	26	106	

TABLE C.181 IMBRICATION PALEOCURRENT MEASUREMENTS AT WAYPOINT 150317A_1-3c

		Flow direction measurements			
Northing	3655400	74	54	138	41
Easting	281765	74	14	148	
Unit	QTpwu	36	14	148	
Mean	71	110	14	148	
Median	74	74	80	72	
n	31	74	105	58	
		34	114	18	
		81	123	18	
		81	89	33	
		54	82	49	

TABLE C.182 IMBRICATION PALEOCURRENT MEASUREMENTS AT WAYPOINT 150317B_1-3c

		Flow direction measurements		
Northing	3655400	153	109	161
Easting	281765	125	66	152
Unit	QTpwuc	212	127	139
Mean	140	212	185	139
Median	146	81	119	139
n	25	96	119	
		156	110	
		149	156	
		149	156	
		146	156	

TABLE C.183 IMBRICATION PALEOCURRENT MEASUREMENTS AT WAYPOINT 150317A_1-3e

		Flow direction measurements		
Northing	3655587			124
Easting	281301			69
Unit	QTpwuc			91
Mean	106			81
Median	92			86
n	10			86
				92
				127
				153
				153

TABLE C.184 IMBRICATION PALEOCURRENT MEASUREMENTS AT WAYPOINT 150317B_1-3e

		Flow direction measurements		
Northing	3655587			144
Easting	281301			101
Unit	QTpwuc			76
Mean	129			76
Median	134			156
n	10			201
				173
				99
				134
				134

TABLE C.185 IMBRICATION PALEOCURRENT MEASUREMENTS AT WAYPOINT 150317_1-4g

		Flow direction measurements		
Northing	3654381	53	114	82
Easting	284187	85	132	59
Unit	QTpwu	85	132	107
Mean	100	130	94	74
Median	104	130	70	118
n	30	129	139	118
		129	139	34
		104	78	66
		127	104	86
		139	70	55

TABLE C.186 IMBRICATION PALEOCURRENT MEASUREMENTS AT WAYPOINT 150317_1-4h

		Flow direction measurements				
Northing	3654395	32	24	95	60	79
Easting	284139	78	24	114	60	22
Unit	QTpwu	56	68	34	60	70
Mean	55	41	68	34	29	66
Median	60	6	64	34	29	66
n	45	6	84	48	75	
		46	84	98	34	
		46	84	23	94	
		4	109	61	94	
		35	59	61	14	

TABLE C.187 IMBRICATION PALEOCURRENT MEASUREMENTS AT WAYPOINT 150318A_2-3b

		Flow direction measurements	
Northing	3655058	186	221
Easting	288815	186	192
Unit	QTpa	186	172
Mean	205	204	135
Median	206	231	209
n	20	204	209
		204	207
		204	220
		228	216
		234	246

TABLE C.188 IMBRICATION PALEOCURRENT MEASUREMENTS AT WAYPOINT 150318B_2-3b

		Flow direction measurements	
Northing	3655058	196	
Easting	288815	184	
Unit	QTpa	250	
Mean	185	177	
Median	185	174	
n	10	71	
		71	
		241	
		199	
		185	

TABLE C.189 IMBRICATION PALEOCURRENT MEASUREMENTS AT WAYPOINT 150318_2-4d

		Flow direction measurements	
Northing	3660342	309	267
Easting	288328	331	350
Unit	QTpe	275	282
Mean	308	275	282
Median	311	274	318
n	20	330	318
		330	286
		330	310
		344	286
		344	312

TABLE C.190 IMBRICATION PALEOCURRENT MEASUREMENTS AT WAYPOINT 150318_2-5d

		Flow direction measurements				
Northing	3653934	174	188	266	221	171
Easting	285119	189	165	248	249	189
Unit	QTpa	186	167	240	220	201
Mean	195	189	155	280	220	215
Median	192	158	188	280	161	
n	44	234	195	169	173	
		236	194	169	138	
		218	200	169	116	
		255	200	133	149	
		198	200	221	171	

TABLE C.191 IMBRICATION PALEOCURRENT MEASUREMENTS AT WAYPOINT 150318_2-5h

		Flow direction measurements			
Northing	3654214	81	80	65	95
Easting	284776	81	80	50	
Unit	QTpwuc	60	31	66	
Mean	43	18	31	359	
Median	31	18	33	31	
n	31	73	50	31	
		75	11	12	
		50	11	12	
		5	29	31	
		5	29	95	

TABLE C.192 IMBRICATION PALEOCURRENT MEASUREMENTS AT WAYPOINT 150408_2

		Flow direction measurements			
Northing	3667417			177	
Easting	290218			177	
Unit	Qtr3			196	
Mean	194			187	
Median	193			204	
n	10			172	
				220	
				210	
				210	
				189	

TABLE C.193 IMBRICATION PALEOCURRENT MEASUREMENTS AT WAYPOINT 150501_1

		Flow direction measurements			
Northing	3662874	134	135	184	
Easting	284569	142	151	146	
Unit	QTpwm	142	151	177	
Mean	140	100	182	137	
Median	141	86	182	201	
n	30	71	56	140	
		171	56	140	
		63	170	162	
		134	170	116	
		84	184	106	

TABLE C.194 IMBRICATION PALEOCURRENT MEASUREMENTS AT WAYPOINT 150501_1b

		Flow direction measurements		
Northing	3662873	144	156	151
Easting	284549	111	156	149
Unit	QTpwu	122	151	141
Mean	139	171	167	139
Median	143	171	147	105
n	30	171	113	105
		148	96	112
		195	125	139
		195	131	49
		106	152	130

TABLE C.195 IMBRICATION PALEOCURRENT MEASUREMENTS AT WAYPOINT 150501_1e

		Flow direction measurements		
Northing	3663131	161	153	164
Easting	284396	153	180	164
Unit	QTpwuc	153	126	125
Mean	142	127	136	131
Median	137	152	126	197
n	28	152	121	166
		131	111	167
		131	111	95
		126	137	
		153	137	

TABLE C.196 IMBRICATION PALEOCURRENT MEASUREMENTS AT WAYPOINT 150501_2b

		Flow direction measurements		
Northing	3655824	126	183	188
Easting	283890	118	156	202
Unit	QTpwmc	135	109	131
Mean	144	135	109	99
Median	131	98	228	123
n	27	216	228	123
		204	111	123
		165	111	
		86	115	
		149	188	

TABLE C.197 IMBRICATION PALEOCURRENT MEASUREMENTS AT WAYPOINT 150501_2e

		Flow direction measurements		
Northing	3656039	211	165	182
Easting	283943	211	172	135
Unit	QTpa	140	143	175
Mean	173	190	174	158
Median	174	174	243	158
n	25	176	161	
		167	161	
		182	217	
		182	185	
		134	152	

TABLE C.198 IMBRICATION PALEOCURRENT MEASUREMENTS AT WAYPOINT 150501_2i

		Flow direction measurements		
Northing	3655494	195	142	168
Easting	283871	174	184	191
Unit	QTpa	159	184	199
Mean	181	190	194	215
Median	188	190	166	166
n	30	190	216	195
		190	192	155
		156	186	155
		156	186	201
		142	200	201

TABLE C.199 IMBRICATION PALEOCURRENT MEASUREMENTS AT WAYPOINT 150501_3

		Flow direction measurements		
Northing	3662393	42	216	129
Easting	284860	92	216	169
Unit	QTpwu	92	216	151
Mean	156	211	176	175
Median	161	176	150	188
n	25	144	163	
		141	192	
		161	65	
		176	65	
		156	134	

TABLE C.200 IMBRICATION PALEOCURRENT MEASUREMENTS AT WAYPOINT 150501_4

		Flow direction measurements			
Northing	3667457	140	164	160	180
Easting	286478	151	210	158	170
Unit	QTpwl	139	192	180	210
Mean	173	157	156	180	210
Median	170	157	133	145	118
n	39	145	146	200	158
		203	178	200	203
		205	168	200	203
		175	168	146	203
		175	200	146	

APPENDIX D

Radiocarbon calibration data from the Williamsburg 7.5' quadrangle

This appendix contains radiocarbon age calibration plots from three charcoal samples collected from Holocene deposits along Cañada Honda. All data are from AMS analyses performed by Beta Analytic Inc., Miami, FL. Calibrated 2σ age ranges determined using the Intcal13 calibration curve of Reimer et al. (2013) are given in Table 1.

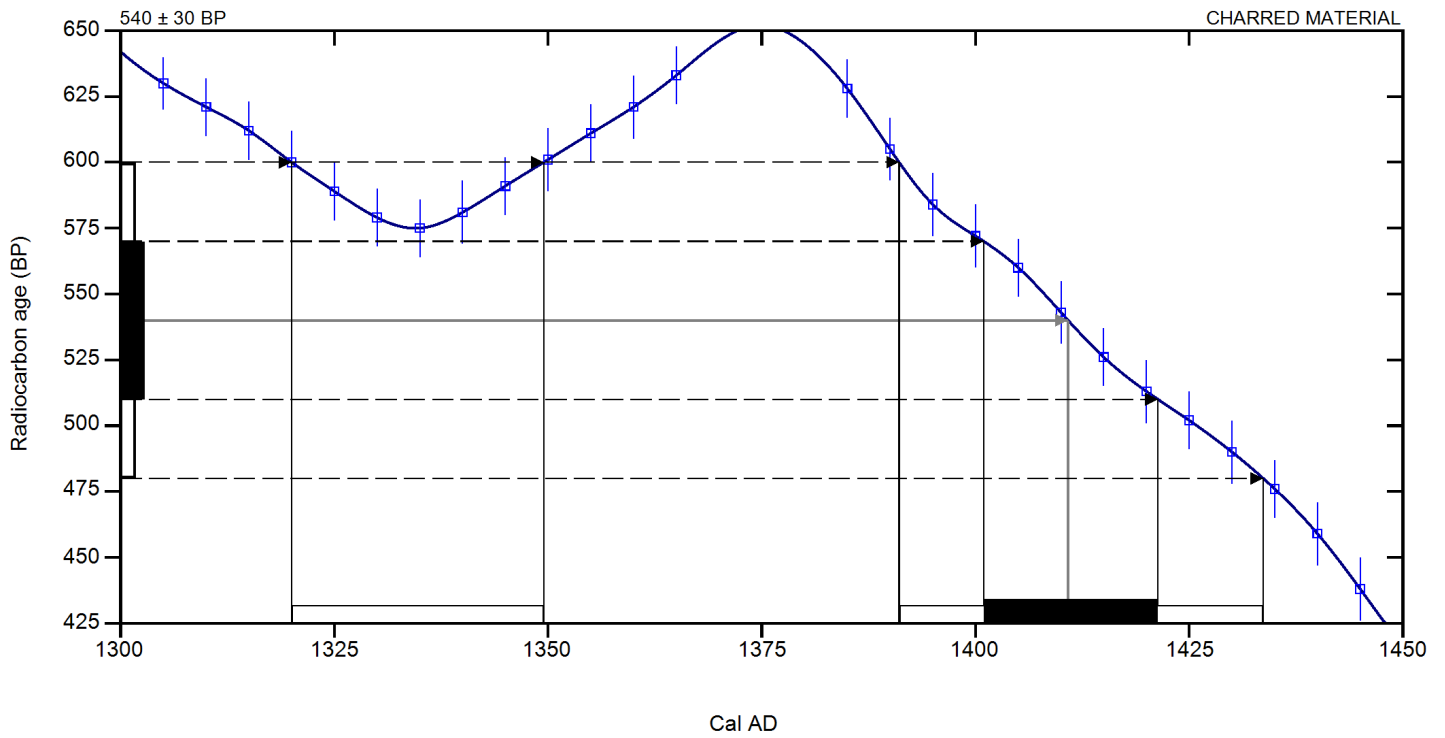


Figure D.1. Calibration curve for sample WS-204 (unit Qayi). Age given in upper left is conventional age (^{14}C yr BP).

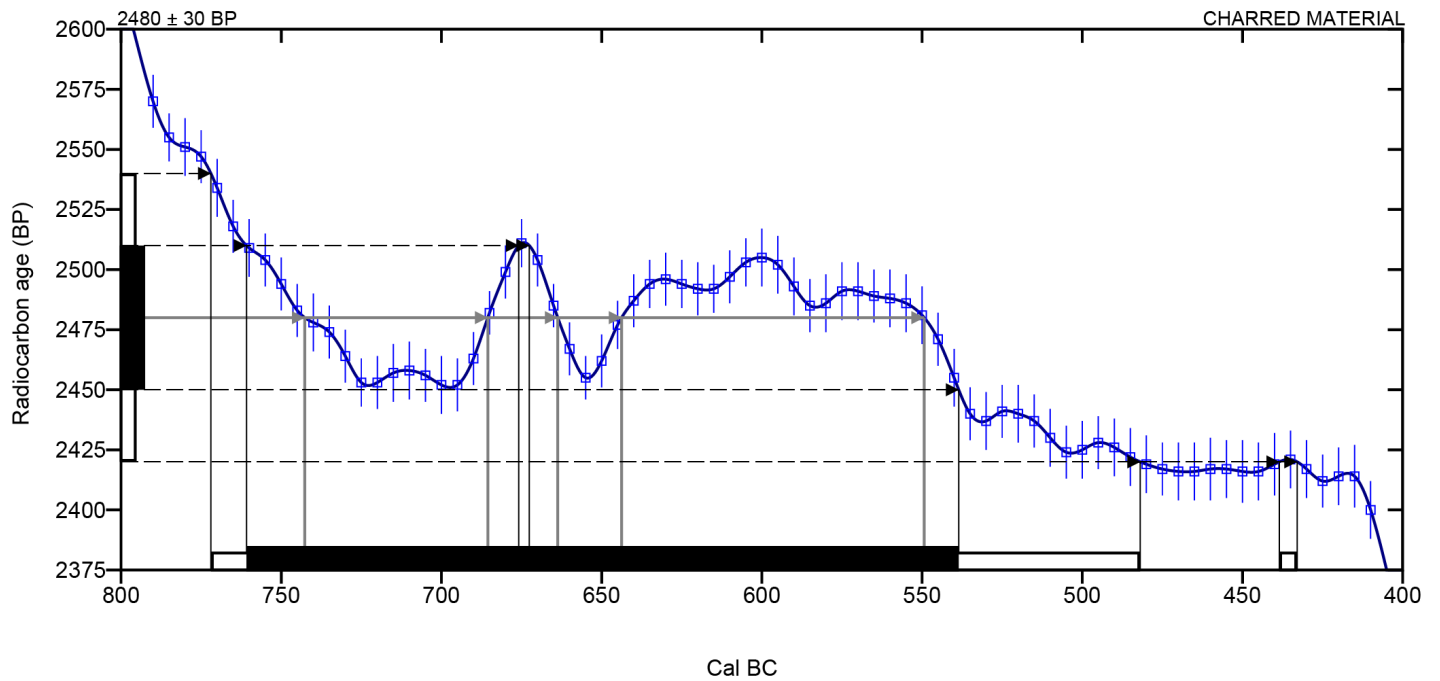


Figure D.2. Calibration curve for sample WS-203 (unit Qfay). Age given in upper left is conventional age (^{14}C yr BP).

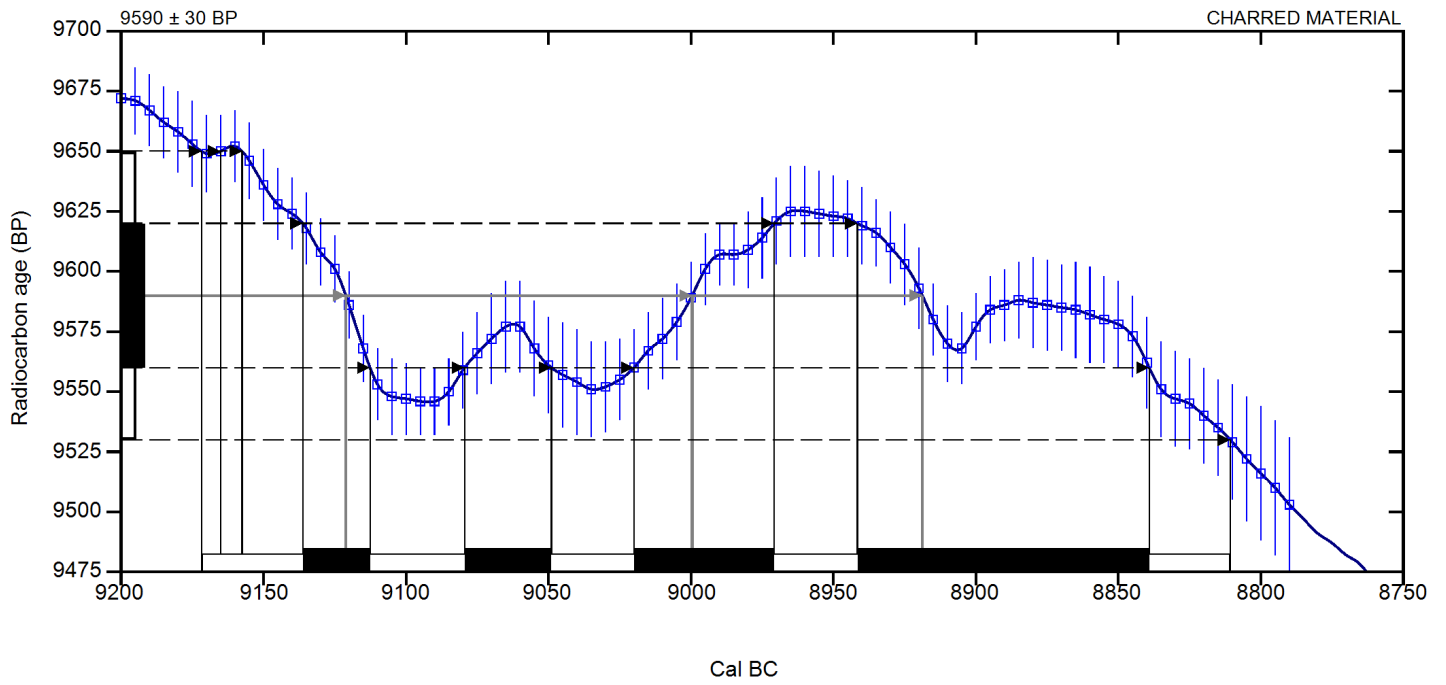


Figure D.3. Calibration curve for sample WS-202D (unit Qfay). Age given in upper left is conventional age (^{14}C yr BP).